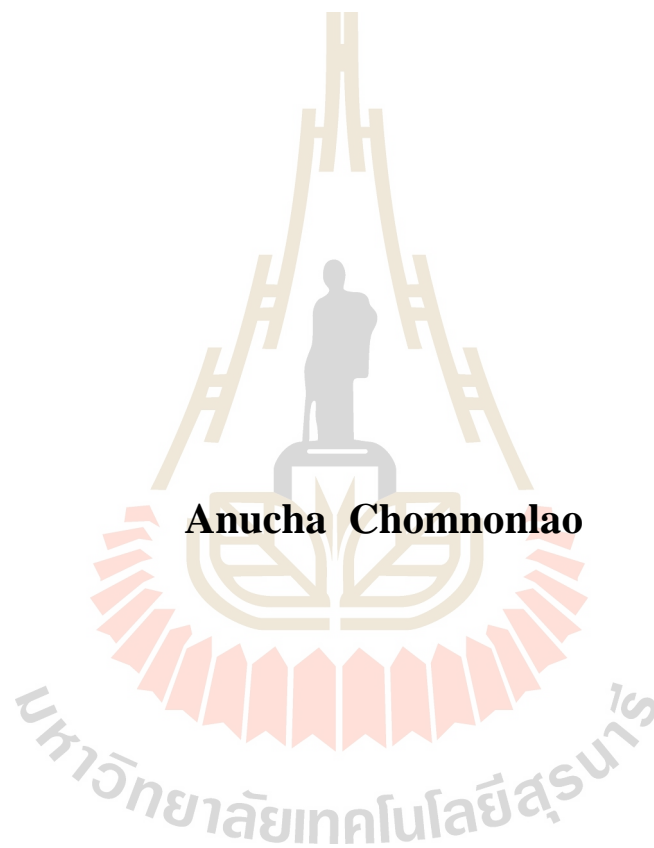


**STRUCTURAL STUDY OF OVARIAN TUBULES AND
OOCYTES IN THE GOLDEN APPLE SNAIL**

(Pomacea canaliculata)



A Thesis Submitted in Partial Fulfillment of the Requirements for the

Degree of Master of Science in Biomedical Science

Suranaree University of Technology

Academic Year 2018

การศึกษาโครงสร้างของท่อรังไข่และไข่ในหอยเชอริ



นายอนุชา ชมโนนลาว

วิทยานิพนธ์นี้เป็นส่วนหนึ่งของการศึกษาตามหลักสูตรปริญญาวิทยาศาสตรมหาบัณฑิต

สาขาวิชาชีวเวชศาสตร์

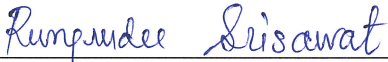
มหาวิทยาลัยเทคโนโลยีสุรนารี

ปีการศึกษา 2561

**STRUCTURAL STUDY OF OVARIAN TUBULES AND OOCYTES IN
THE GOLDEN APPLE SNAIL
(*Pomacea canaliculata*)**

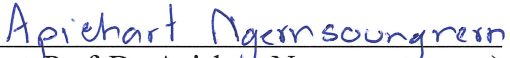
Suranaree University of Technology has approved this thesis submitted in partial fulfillment of the requirements for a Master's Degree.

Thesis Examining Committee



(Asst. Prof. Dr. Rungrodee Srisawat)

Chairperson




(Asst. Prof. Dr. Apichart Ngerngsoungrern)

Member (Thesis Advisor)



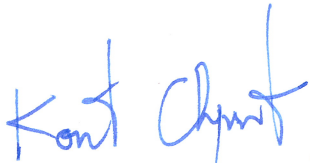
(Asst. Prof. Dr. Piyada Ngerngsoungrern)

Member



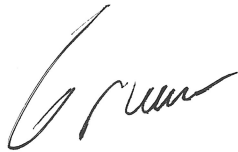
(Asst. Prof. Dr. Naruwan Saowakon)

Member



(Assoc. Prof. Flt. Lt. Dr. Kontorn Chamniprasart)

Vice Rector for Academic Affairs
and Internationalization



(Assoc. Prof. Dr. Worawat Meevasana)

Dean of Institute of Science

อนุชา ชมโนนลาว : การศึกษาโครงสร้างระดับจุลกายวิภาคของท่อรังไข่และไข่ในหอย
เชอร์รี่ (STRUCTURAL STUDY OF OVARIAN TUBULES AND OOCYTES IN THE
GOLDEN APPLE SNAIL (*Pomacea canaliculata*) อาจารย์ที่ปรึกษา : ผู้ช่วยศาสตราจารย์
ดร.อภิชาติ เงินสูงเนิน, 105 หน้า.

โพมาเซีย คานาลิคูลาตา เป็นสัตว์ในไฟลัมมอลลัสกา จัดอยู่ในเป็นคลาส แกสโตรพอด สปี
ชีส์นี้เป็นหอยทากน้ำจืดเพียงหนึ่งเดียวที่อยู่ในรายชื่อ 100 ผู้รุกรานที่เลวร้ายที่สุดทั่วโลก มันทำให้
เกิดความสูญเสียทางเศรษฐกิจทั่วโลกหลายพันล้านดอลลาร์ต่อปี การศึกษาครั้งนี้เป็นครั้งแรก
ในการศึกษาระยะของท่อรังไข่ของ โพมาเซีย คานาลิคูลาตา ท่อรังไข่แบ่งออกเป็นสี่ระยะ ได้แก่
ระยะวางไข่ ระยะเจริญ ระยะก่อนสุกและระยะสุก เนื้อเยื่อสืบพันธุ์ถูกปกคลุมไปด้วยเยื่อบุผิวชนิด
ซิมเปิลคอลลีนาและเซลล์คัดหลังที่กระจายระหว่างเซลล์เยื่อบุผิว ด้านใต้เนื้อเยื่อเกี่ยวพันและเส้นใย
กล้ามเนื้อ โครงสร้างของเซลล์ไข่และเนื้อเยื่อสืบพันธุ์ได้รับการศึกษาเป็นครั้งแรกในสายพันธุ์นี้
โดยใช้กล้องจุลทรรศน์อิเล็กตรอนและเนื้อเยื่อวิทยา พบว่าภายในท่อรังไข่มีการพัฒนาเซลล์ไข่ใน
ระยะต่าง ๆ โดยที่โอโอโกเนียมีการพัฒนามาจากโปรโตเนียและจากนั้นจะพัฒนาไปอีก 3 ระยะ
ได้แก่ พริววิทเทลโลจินิก โอโอไซต์ วิทเทลโลจินิก โอโอไซต์ และโพสวิตเทลโลจินิก โอโอไซต์
ตามลำดับ ภายในเซลล์ไข่พบการกระจายของเม็ดไขมันไซโทพลาสซึม เม็ดไขมันมีแนวโน้มเพิ่มขึ้น
อย่างสอดคล้องกับระยะจำนวนและขนาดของเซลล์ไข่ ในครั้งนี้ได้ศึกษาการเปลี่ยนแปลงของ
องค์ประกอบทางชีวเคมี (โปรตีน กรดนิวคลีอิกและ คาร์โบไฮเดรต) พบว่ามีความแตกต่างของ เอ
ไมด์ วัน ในระยะต้นและระยะปลายของเซลล์ไข่ในระหว่างการพัฒนาของเซลล์ ซึ่งบ่งชี้ว่าโปรตีนมี
การเปลี่ยนแปลงโครงสร้างในระหว่างการพัฒนาของเซลล์ไข่ นอกจากนี้ยังพบว่าภายในแต่ละท่อ
รังไข่มีโอโอไซต์หลายระยะ ซึ่งบ่งชี้ได้ว่าการพัฒนาของท่อรังไข่เป็นแบบ อะซิงโครนัส การ
ค้นพบเหล่านี้เป็นสิ่งสำคัญในการทำความเข้าใจการเจริญพัฒนาทางเพศของหอยสายพันธุ์นี้ ข้อมูล
ที่ได้มีความจำเป็นและเป็นประโยชน์ ซึ่งอาจนำไปสู่การหาวิธีการจัดการที่เหมาะสมในการ
ควบคุมการกระจายพันธุ์ในหอยสายพันธุ์นี้

สาขาวิชาปริคณินก
ปีการศึกษา 2561

ลายมือชื่อนักศึกษา Anucha chomnonlao
ลายมือชื่ออาจารย์ที่ปรึกษา 

ANUCHA CHOMNONLAO : STRUCTURAL STUDY OF OVARIAN
TUBULES AND OOCYTES IN THE GOLDEN APPLE SNAIL (*Pomacea
canaliculata*). THESIS ADVISOR : ASST. PROF. APICHART
NGERNGSOUNGNERN, Ph.D. 105 PP.

EPITHELIUM/ GASTROINTESTINAL TRACT/ IMMUNOHISTOCHEMISTRY/
LEPTIN/ MUCIN

Pomacea canaliculata (Lamarck, 1822) is an animal in phylum Mollusca and is classified into class gastropod. This species is the only freshwater snail listed among the 100 worst invaders worldwide. It causes global economic losses of several billion dollars to aquatic crops. The present study represented for the first time in evaluating the stages of the ovarian tubule of *P. Canaliculata*. The ovarian tubules were classified into four continuous stages that consecutively occurred (spent stage, proliferative stage, premature stage and mature stage). The gonadal tissue was covered with a simple cuboidal epithelium and the secretory cells that scattered between the epithelial cells. The underneath was the connective tissue and muscle fibers. The structures of oocytes and gonadal tissue were studied for the first time in this species, using electron microscopy and histology. The ovarian tubule was found to contain oocytes in various developmental stages. Oogonia derived from protogonia and then underwent three distinct stages of oogenesis to become pre-vitellogenenic oocytes, vitellogenenic oocytes and post-vitellogenenic or mature oocytes, respectively. In the oocytes, lipid droplets were homogenously distributed throughout the cytoplasm. The lipid droplets showed an increasing tendency corresponding to stage as well as numbers and sizes of

oocytes. In the present study, changes of the biochemical components (proteins, nucleic acid, and carbohydrate) were evaluated during the development of the oocytes. It was found the difference of amide I between early stage and late stage of oocyte development suggesting that protein structure was changed by protein modification during oocyte development. In additional, it was found that each ovarian tubule contained various stages of oocytes indicating that the development of ovarian tubule was asynchronously. These findings were an important step in understanding sexual maturation in this species, and could thus contribute essential information for implementing adequate management techniques for management of this invasive species.

School of Preclinic

Academic Year 2018

Student's Signature Ancha chomnonlae

Advisor's Signature Apichart Ngernsoungrern

ACKNOWLEDGEMENTS

I would like to express my sincere thanks to my thesis advisors, Asst. Prof. Dr. Apichart Ngerngsounnern and Asst. Prof. Dr. Piyada Ngerngsounnern for their technical consultation and constant encouragement throughout my work. I am most grateful for their teachings and advices, which has enabled me to attain this thesis successfully. Thank you to my youngest co-laboratory, Miss Piyachart Songwijit who helped me during the period of my work.

In addition, I would like to thank the financial, material and facility supports from the School of Preclinic, Institute of Science, Suranaree University of Technology for supports throughout the course of the thesis.

Finally, I most gratefully acknowledge my family and my friends for all their supports throughout the period of this research.

Anucha Chomnonlao

CONTENTS

	Page
ABSTRACT IN THAI.....	I
ABSTRACT IN ENGLISH	II
ACKNOWLEDGEMENTS.....	IV
CONTENTS.....	V
LIST OF FIGURES	VIII
LIST OF ABBREVIATIONS.....	XI
CHAPTER	
I INTRODUCTION.....	1
1.1 Background/Problem	1
1.2 Research Objectives.....	5
1.3 Research Hypothesis.....	5
1.4 Scope and Limitation of the Study.....	6
II LITERATURE REVIEW.....	7
2.1 Reproductive cycle of Mollusca	7
2.2 Microanatomy of ovarian tubule of Mollusca	11
2.3 Oogenesis of Mollusca.....	15
2.3.1 Protogonia.....	16
2.3.2 Oogonia.....	16
2.3.3 Pre-vitellogenic oocytes.....	17
2.3.4 Vitellogenic oocytes.....	21

CONTENTS (Continued)

	Page
2.3.5 Mature oocytes.....	24
2.4 Biochemical composition changes in developing oocytes.....	25
III MATERIALS AND METHODS	28
3.1 Animal preparation	28
3.2 Stereomicroscopic studied of external morphology of the gonadal tissue ...	28
3.3 Scanning electron microscopic study of external morphology of the gonadal tissues and oocytes	29
3.4 Light microscopic study of the gonadal tissues and oocytes	29
3.5 Transmission electron microscopic study of oocytes	31
3.6 Histochemical study of yolk granules in the oocytes.....	32
3.7 Biochemistry analysis during oocyte development	33
3.7.1 Tissue Preparation.....	33
3.7.2 Synchrotron- Fourier Transform-Infrared Spectroscopy (FTIR) microspectroscopy	33
3.7.3 Spectral data analysis	34
3.8 The relationship between ovarian tubule stages and oocyte stages	34
3.8.1 Animal preparation	34
3.8.2 Histological study of oocytes.....	35
IV RESULTS	37
4.1 Stereomicroscopic study of external morphology of the gonadal tissue	37

CONTENTS (Continued)

	Page
4.2 Scanning electron microscopic study of external morphology of the gonadal tissue.....	38
4.3 Light microscopic study of the gonadal tissue.....	41
4.4 Light microscopic study of the oocytes	45
4.5 Scanning electron microscopic study of oocytes	47
4.6 Transmission electron microscopic study of oocytes	49
4.7 Presence of yolk granules in the oocytes	58
4.8 Biochemistry analysis during oocyte development	60
4.9 The relationship between ovarian tubule stages and oocyte stages	65
V DISCUSSION AND CONCLUSION	70
5.1 External morphology and histology of ovarian tubules.....	70
5.2 Histology and ultrastructure of oocytes	72
5.3 Development of oocytes	73
5.4 The relationship between ovarian tubule stages and oocyte stages	75
REFERENCES	78
APPENDICES	95
APPENDIX A THE PREPARATIONS OF REAGENTS	96
APPENDIX B ROCEEDING PRESENTATION	101
CURRICULUM VITAE.....	105

LIST OF FIGURES

Figure	Page
1.1 The external morphology of male.....	4
1.2 The shell of adult female <i>P. canaliculata</i>	4
2.1 Schematic drawing representation of oogenesis in <i>N. margaritacea</i>	8
2.2 Schematic drawing of whole juvenile showing developing ovarian tubule.	10
2.3 Photographs showing different oogenesis stages of <i>N. margaritacea</i>	13
2.4 Schematic representation of oogenesis in <i>A. maura</i>	14
2.5 Histology of ovarian tubule (ot) located next to midgut gland (mgg) and haemocoelic spaces (hs).....	14
2.6 Oogonia (Oo) located in the acinus wall and oogonia next to a pre-vitellogenic oocyte (Pvo) with a distinct nucleus.....	19
2.7 Photographs showing the pre-vitellogenic oocytes in <i>A. maura</i>	20
2.8 Ultrastructure of oogonium and pre-vitellogenic oocyte of <i>Haliotis varia</i>	20
2.9 Ultrastructure of vitellogenic oocyte of <i>H. varia</i>	23
2.10 Photographs showing ultrastructure of late-vitellogenic oocyte of <i>H. varia</i>	23
2.11 Photographs showing cytoplasm of mature oocytes of <i>H. aspersa</i>	25
2.12 Total absorbance cartogram of oocyte, reconstructed by integrating the area between 1,800 and 1,000 cm^{-1}	27
3.1 The snails were allowed to mate and the couples were isolated and housed in separate containers.....	35

LIST OF FIGURES (Continued)

Figure	Page
4.1 Photographs showing the gross morphology of gonadal tissue.....	39
4.2 Photographs showing the gross morphology of gonadal tissue at different stages of development in <i>P. canaliculata</i> ..	40
4.3 Photographs showing external morphology of the digestive gland and the gonadol tissue.....	41
4.4 .Photographs showing cross section of the ovarian tubules of <i>P. Canaliculata</i> stained with Masson's Trichrome.	43
4.5 Photographs showing ovarian tubules containing difference oocyte stages.....	44
4.6 Photographs showing transverse sections through the ovarian tubules.....	46
4.7 Photographs showing scanning electron microscopy of the various stages of development oocytes within ovarian tubules.	48
4.8 Photographs showing transmission electron micrograph of pre-vitellogenic oocytes (PvitO) and oogonia (Oo) of <i>P. Canaliculi</i>	51
4.9 Transmission electron micrographs of difference stages oocytes.....	55
4.10 Transmission electron micrograph of mature oocyte encompassing lipid granules components.....	56
4.11 Transmission electron microscope showing the lipid granules (LG) in the oocyte.....	57
4.12 Light micrographs of Sudan black stained sections of ovarian tubules.....	59
4.13 Numbes of lipid granules in different oocyte stages.....	60

LIST OF FIGURES (Continued)

Figure	Page
4.14 Functional group area maps obtained under the spectral regions ranged from 1,700-1,500 cm^{-1} of pre-vitellogenic, vitellogenic, and mature oocytes. ..	62
4.15 Infrared spectra from previtellogenic oocyte	63
4.15 Infrared spectra from previtellogenic oocyte	63
4.16 Average original infrared spectra of amide I, amide II, carbohydrate, and nucleic acid.	63
4.17 Second derivative spectra between 1,700-1620 cm^{-1} (amide I).....	64
4.18 Curve-fitting on amide I from pre-vitellogenic oocyte (PvitO), vitellogenic oocyte (VitO), and mature oocyte (MatO).	64
4.19 PCA analyzed from the spectra region between 1800-900 cm^{-1} of pre-vitellogenic oocyte (PvitO), vitellogenic oocyte (VitO), and mature oocyte (MatO).	65
4.20 Photographs showing comparison between the histology of oocytes and external morphology of gonadal tissue.....	68
4.21 Percentage distributions of oocyte stages in the ovarian tubule after spawning.	69

LIST OF ABBREVIATIONS

μg	=	Microgram
μm	=	Micrometer
$^{\circ}\text{C}$	=	Degree Celsius
CO_2	=	Carbon dioxide
cm	=	Centimeter
cm^{-1}	=	Centimeter to minus one
CPD	=	Critical point dried
DI	=	Distilled water
H&E	=	Hematoxylin and Eosin
hr	=	Hour
M	=	Molar
ml	=	Milliliter
Oo	=	Oogonia
Pr	=	Protogonia
PviyO	=	Pre-vitellogenic oocyte
VitO	=	Vitellogenic oocyte
MatO	=	Mature oocyte
mm	=	Millimeter
min	=	Minute
nm	=	Nanometer

LIST OF ABBREVIATIONS (Continued)

OsO ₄	=	Osmium tetroxide
PBS	=	Phosphate buffered saline
pH	=	Potential of hydrogen ion
SD	=	Standard Definition
SEM	=	Scanning Electron Microscope
TEM	=	Transmission Electron Microscopy
LM	=	Light Microscopy
PCA	=	Principal component analysis
FTIR	=	Fourier Transform-Infrared

CHAPTER I

INTRODUCTION

1.1 Background/Problem

Pomacea canaliculata (Lamarck, 1822) belongs to phylum Mollusca and is classified into class gastropod. This class is the largest group of mollusca which is divided into 2 subclasses, prosobranchia and opisthobranchia (Bieler, 1992). *P. canaliculata* has been classified into subclass prosobranchia (Hayes, 2012). The common name of *P. canaliculata* is the golden apple snail. The golden apple snails are the herbivores. They consume varieties of food (rice seedlings, taro, duck weed, water hyacinth, algae, and other succulent leafy plants). They also prefer young with soft plants, rooted plants living at the soil surface. It means that the snails are able to eat almost everything in the environment that are surround them. The snails destroy the ecology system, because they can eat eggs and juveniles of other snail species. They are able to detect food at a distance using chemical cues. This snail has commonly been found in Central and South America. In the early 1980's, the golden apple snails were introduced into East Asia for the starting of an escargot industry. Instead of becoming a useful human food resource, they escaped to rice fields and became serious rice eating pests in many countries. They have rapidly spreaded out to South Korea, Japan, and China (including Hong Kong). After that, they also rapidly spreaded out to many countries in Southeast Asia (Indonesia, Thailand, Cambodia, Laos, Malaysia,

Myanmar, Philippines, Vietnam and Singapore). This information reveals that the snails invade and live in all environments (Rawlings et al., 2007). The external morphology of the shell of adult apple snail's shell is globes and relatively heavy (especially in older snails). The shell of the snail consists of 5 to 6 whorls. Each whorl is separated by a deep and indented suture. Thus, the name of this species is called *P. canaliculata* which means channel. The shell opening or aperture is large and oval to round shape. The external morphology of the apertures can be used to classify sex of the snail. Male snails have rounder apertures than those of females. Generally, the umbilicus of male snails are larger and deeper than those of females (Figure 1.1). However, the overall shell shape of *P. canaliculata* is similar to the external morphology of *P. lineata*, except for the deeper sutures and more globes shape. The sizes of mature golden apple snail are average vary from 40 to 60 mm in width and 45 to 75 mm in high, depending on the environmental conditions, such as food, temperature, and quality of water. The colors of the shell in cultivated snail are separated completely between yellow and green, whereas wild snail is usually brown in color with or without dark spiral bands (Figure 1.2). The shell growth of this specie occurs mainly in spring and summer, while it stagnates in fall and winter. The dimorphism appears to be slight in *P.canaliculata*, but dramatic in other species of golden apple snails (Cazzaniga, 1990; Estebenet and Cazzaniga, 1998).

Recently years, ovarian morphology and gamete ultrastructure have been increasingly evaluated to resolve systematic and phylogenetic questions in the Metazoa (Eckelbarger and Watling, 1995; Jamieson et al., 1995). There is currently widespread interest in gastropod evolution and some workers see an urgent need for new morphological studies to aid in phylogenetic analyses (Ponder and Linberg, 1996). The

goal of the present study is to provide the first detailed ultrastructural description of the ovary and oogenesis in the *P. canaliculata* and provide further comparison to other molluscs.

In gastropods, the developing oocytes become surrounded by a number of follicle cells. In the younger oocyte stages, these follicle cells are closely apposed to the oocytes. Eventually a follicular cavity or cleft is formed between the follicle cells and the oocyte. Various functions of these follicular cells have been described, e.g. transportation of the oocyte (Barth and Jansen, 1962; Starke, 1971), determination of cortical morphogenetic fields of the oocyte (Raven, 1963), phagocytosis (Recourt, 1961; Barth and Jansen, 1963; Bottke, 1972) and nutritional support to of the oocytes (Taylor and Anderson, 1959; Coggeshall, 1970).

Various cytoplasmic constituents have been proposed as being involved in the formation of the yolk granules in gastropods, e.g. the mitochondria, the endoplasmic reticulum and the Golgi apparatus (Ubbels, 1968; Terakado, 1974). The most comprehensive studies on the functions of yolk granules have been carried out on *Lymnaea stagnalis*. Two types of yolk granules have been distinguished in eggs after oviposition; they were supposed to be involved in the formation of membranes and in the digestion of perivitelline fluid, respectively (Bluemink, 1967; Wal, 1974).

In addition to these, other possible functions of the yolk granules may be considered, e.g. hormone production, involvement in the ovulation process. In the present study, some aspects of yolk granule and yolk formation and the role of the follicle cells were investigated, by means of histochemical and electron microscop techniques.

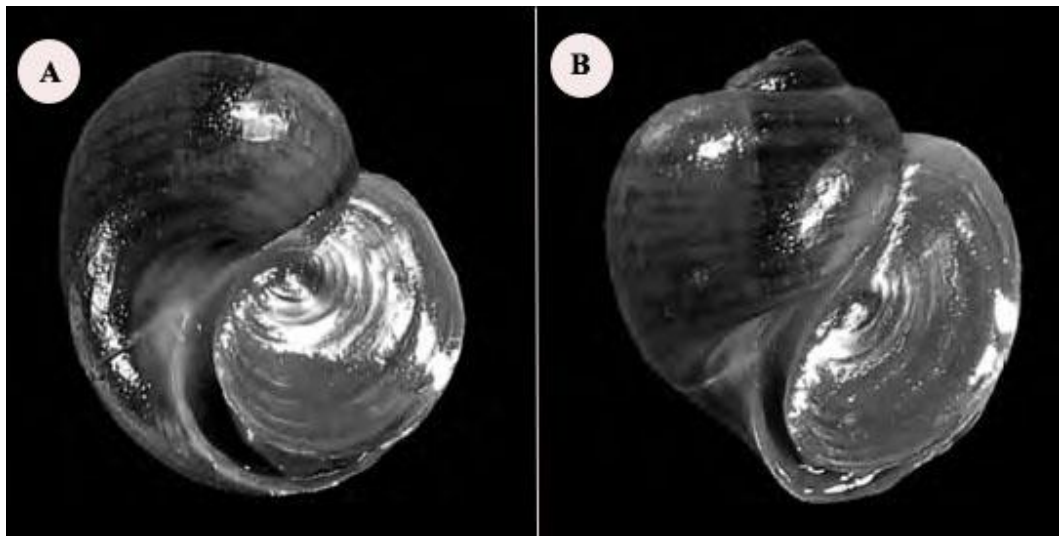


Figure 1.1 The external morphology of male (A) and female (B) *P. canaliculata* (Gamarra- Luques et al., 2013).



Figure 1.2 The shell of adult female *P. canaliculata* is brown in color. The operculum is oval in shape, and has deep umbilicus. Scale bar =1 cm.

1.2 Research Objectives

The purposes of this study are as follows:

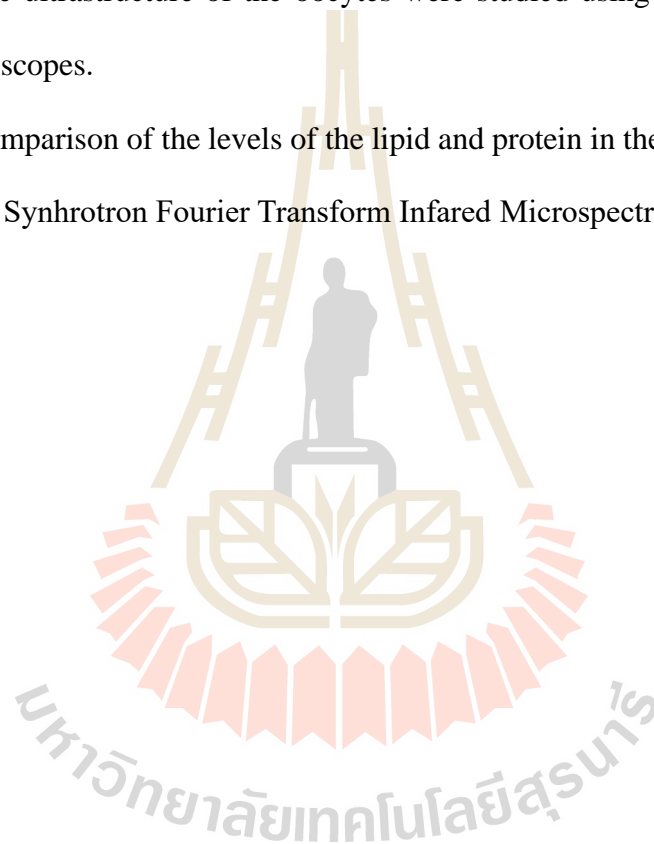
- 1) To classify the ovarian tubule stages using stereo and light microscopes.
- 2) To investigate the structure of ovarian tubules using light and scanning electron microscope.
- 3) To classify stages of oocytes based on morphology using scanning and transmission electron microscopes.
- 4) To investigate biochemical components during oocyte development by Synchrotron Fourier Transform Infrared Microspectroscopy.
- 5) To investigate relationship between ovarian tubule stages and oocyte stages.

1.3 Research Hypothesis

- 1) The structure of ovarian tubules and oocytes of *P. canaliculated* can be classify using light and electron microscopes.
- 2) The stages of oocytes can be classify by light and electron microscopes.
- 3) Synchrotron Fourier Transform Infrared Microspectroscopy can be used to determine the biochemical composition changes during development of oocytes.

1.4 Scope and Limitation of the Study

- 1) This research focused on microstructure and ultrastructure of the ovarian tubules and the oocyte stages in *P. canaliculata*.
- 2) The external and internal morphology of the ovarian tubules were investigated using light and scanning electron microscopes.
- 3) The ultrastructure of the oocytes were studied using transmission electron microscopes.
- 4) Comparison of the levels of the lipid and protein in the oocytes were studied using Synhrotron Fourier Transform Infared Microspectroscopy.



CHAPTER II

LITERATURE REVIEW

2.1 Reproductive cycle of Mollusca

The reproductive cycle of an *Alvan ia mediolittoralis* reproduces throughout the year with two spawning peaks, one during early spring and the other in late autumn. Three stages of the oocytes development were distinguished during oogenesis including (1) pre-vitellogenic oocytes (small, rounded cells, with strong basophilic cytoplasm; (2) vitellogenic oocytes (larger than the previous stage, irregular in shape, and lightly basophilic cytoplasm with slight granulations; (3) maturing oocytes (round in shape with eosinophilic and granular cytoplasm) (Rodrigues and Medeiros, 2005; Curdia et al., 2005. In *Neotrigonia margaritacea*, the ovary was found only in the summer season. It contained oocytes in various developmental stages (Glavinic et al., 2012). In this species, the first stage of the oocytes started from oogonia that derived from protogonia. The oocytes can be divided into three different developmental stages of oogenesis (pre-vitellogenesis oocyte, vitellogenesis oocyte and mature oocytes) (Figure 2.1).

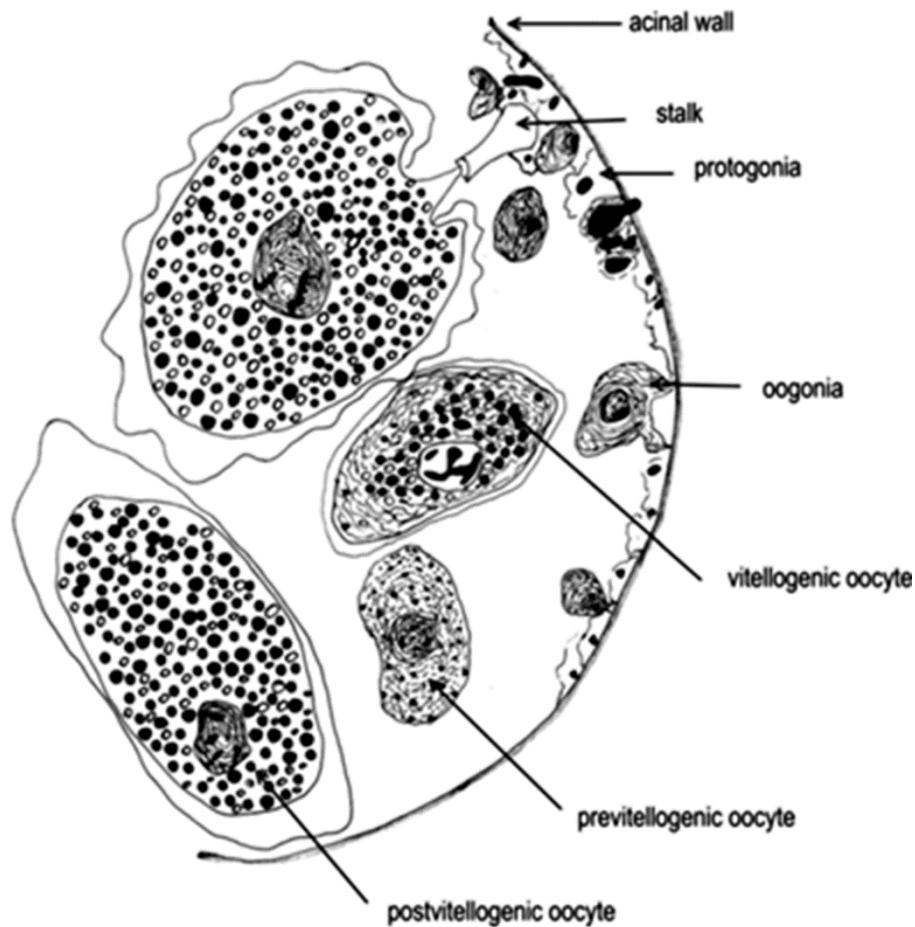


Figure 2.1 Schematic drawing representation of oogenesis in *N. margaritacea*. The various stages of oogenesis were protogonia, oogonia, pre-vitellogenic, vitellogenic and post-vitellogenic oocytes (Glavinic et al., 2012).

Pomacea canaliculata (Lamarck, 1822) is a freshwater snail which is a native species in South America. It has invaded Asia, North America and some Pacific islands (Cowie, 2002; Rawlings et al., 2007; Hayes et al., 2008) during the last three decades. This species is the only freshwater snail listed among the 100 worst invaders worldwide (Lowe et al., 2000; Dreon et al., 2014). It causes global economic losses of

several billion dollars to aquatic crops (Joshi and Sebastian, 2006). The gross anatomy of ovarian tubule reveals that the gonad possesses abundant mature gametes in ovarian tubule and many stages of oocytes are also found (Figure 2.2). *P. canaliculata* females deposit egg masses above the water line. Each egg mass contains 100-300 eggs (Estebenet and Cazzaniga, 1993; Albrecht et al., 1996; Estoy et al., 2002; Martin and Estebenet, 2002). In the reproductive season, a mature female *P. canaliculata* deposits 2-3 egg clusters per week, each one contains 100-300 bright-reddish eggs (Albrecht, et al., 1996; Estoy et al., 2002; Tamburi and Martin, 2011). The egg color is mainly due to ovorubin, a carotene glycoprotein present in the perivitelline fluid which is the main energy source for developing embryos (Heras et al., 2007; Heras et al., 1998). The egg contains perivitellin protein 2 that serves as a deterrent to predation (Heras et al., 2008; Dreon et al., 2010). The golden apple snails live up to 4 years depending on food and many factors. Their reproductive maturity can be reached within 3 months to 2 years depending on ambient temperature regime (Rawlings et al., 2007). The female reproductive system of the golden apple snails is dioeciously and they have internal fertilization with a very high percentage of fertilization rate. It means that the snails serve as the most successful reproduction within mollusk species. In temperate climates, the egg-laying period of this species extends from early spring to early fall, whereas the reproduction of in tropical areas is continuous production. Every 12-15 days, females lay bright pink clusters of eggs on substrates above the water. The snails live very short time to reach maturity which is usually 60-85 days after hatching. A female can produce up to 15,000 off springs per year. Eggs are laid on emergent structures, because the eggs require air exposure for the developing of embryos. Exposure to water decreases hatching efficiency of the embryo (Hayes et al., 2012)

Animal eggs with high nutritional value would be expected to be subject to intense predation (Christeller, 2005; Kamler, 2005). The eggs of *P. canaliculata* are filled with large amounts of polysaccharides and proteins, yet only one predator has been reported worldwide, the fire ant *Solenopsis geminata* (Yusa, 2001). Eggs of *P. canaliculata* must also be somehow protected against the predators. Many studies have been suggested that the proteins in the perivitelline fluid secreted by the albumen gland may provide defense mechanism against environmental factors and predators (Dreon et al., 2004; Heras et al., 2008). *P. canaliculata* females lay fewer eggs when they are exposed to very low food availability, but the weight of individual eggs did not change (Heras et al., 2007). Any reduction in food availability would reduce population growth through a delay in female maturity (Estoy et al., 2002; Tamburi and Martin, 2009).

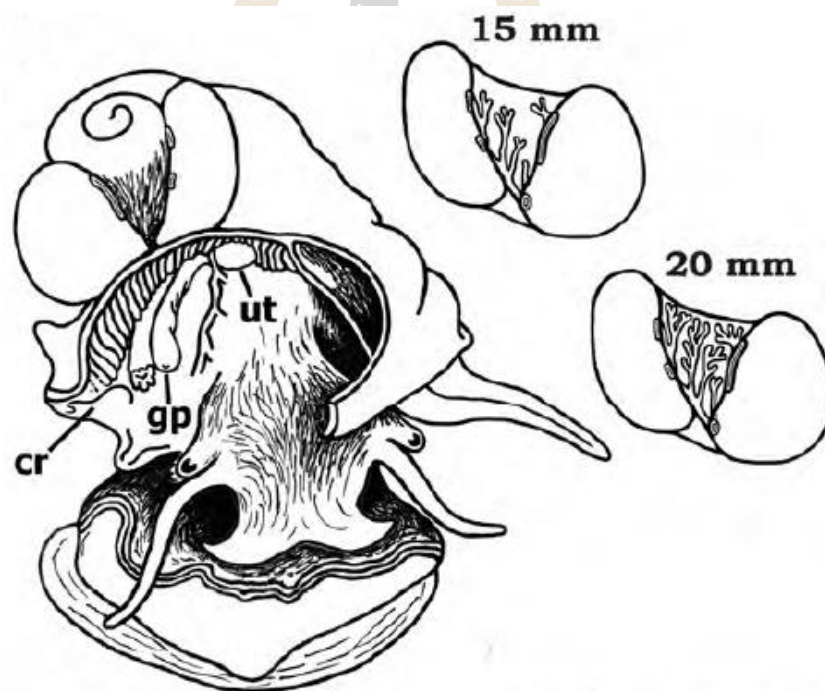


Figure 2.2 Schematic drawing of whole juvenile showing developing ovarian tubule with genital papilla (gp), vagina and uterus (ut), and copulatory rudiment (cr) (Gamarra-Luques et al., 2013).

2.2 Microanatomy of ovarian tubule of Mollusca

The developments of the oocytes of mollusk took place within acini that make up the female gonad. Each acinus was surrounded by connective tissue with haemocoelic sinus and intermittent myoepithelial cells (Eckelbarger and Davis, 1996; Al-Mohanna et al., 2003). The gonad of *N. margaritacea* was found in the viscera above the foot and ventral to the stomach and contained developing oocytes during oogenesis. The ovary consisted of a series of highly branched and globulated clusters of acini that surrounded by a thin acinal wall (Glavinic et al., 2012). In this species, the gonad tissue contained all developmental stages of oocytes including protogonia, oogonia, pre-vitellogenic oocyte, vitellogenic oocyte and post-vitellogenic (mature) oocyte (Figure 2.3).

In addition, the ovary of *Atrina maura* consisted of several clusters of highly branched globular acini surrounded by a thin acinar wall. The ovarian maturation process of *A. maura* was asynchronous, as oocytes at different developmental stages can be found simultaneously. In *A. maura*, oocytes developed from oogonia and then underwent three distinct stages of oogenesis: pre-vitellogenesis, vitellogenesis and post-vitellogenesis (mature oocytes). During oogenesis, each acinus contained oocytes in different stages of development. Oogenesis in mollusk has been classified as either follicular or solitary (Glavinic et al., 2012). The least common modality was follicular oogenesis, in which follicular cells were completely surrounded oocytes throughout the development process. This has been reported in only a few species (Ituarte, 2009). In solitary oogenesis, developing oocytes were completely surrounded by follicular cells, and these occurred only during certain development stages (De Gaulejac et al., 1995). Developing oocytes (oogonia and pre-vitellogenic stages) were in close contact

with the follicular cells, whereas post-vitellogenic (mature) oocytes were free in the acinar lumen (Camacho-Mondragón et al., 2015) (Figure 2.4). The microanatomy of the gonad tissue had been studied in patella limpet, including *Patella barbara*, *Patella argenvillei*, *Patella granularis*, *Patella oculus*, *Patella miniata*, and *Helcion pectunculus*. The ovarian tubule wall was 50-100 µm in thickness. The structure of ovarian tubule consisted of smooth muscle bands in outer layer, connective tissue in middle layer, and anastomosing of fenestrated cells in an inner layer. The ovarian tubule was subdivided into numerous compartments by connective tissue septum, called trabeculae. The trabeculae extended radially from the inner surface of the ovarian tubule to the lumen. The function of this septum was to provide the structural support to the germinal epithelium. The trabecular wall consisted of three layers including 1) an outer layer of squamous epithelial cells, 2) middle bands of smooth muscle cells, and 3) connective tissue (Hodgson and Eckelbarger, 2000). In *Chlamys (Azumapecten) farreri farreri*, qualitative histologic analysis of the ovarian tubule revealed that the ovarian tubule stages were classified into five successive stages: early active stage, late active stage, ripe stage, partially spawned stage, and spent stage (Je-Cheon et al., 2014). In the Chinese pen-shell bivalve, *A. Maura*, four reproductive stages of ovarian tubule were recognized based on oocyte sizes and cytological characteristics of the gonads including early gametogenesis, growing, mature, and degenerating (Enriquez-Diaz et al., 2003). In *P. canaliculata*, microanatomy of ovarian tubule was studied. It was showed that the gonad tissue possessed abundant mature gametes in ovarian tubule and many stages of oocytes were also found. The oogenesis occurs directly on the basal membrane and the final stages of the oocytes locate within the lumen (Figure 2.5) (Gamarra-Luques et al., 2013).

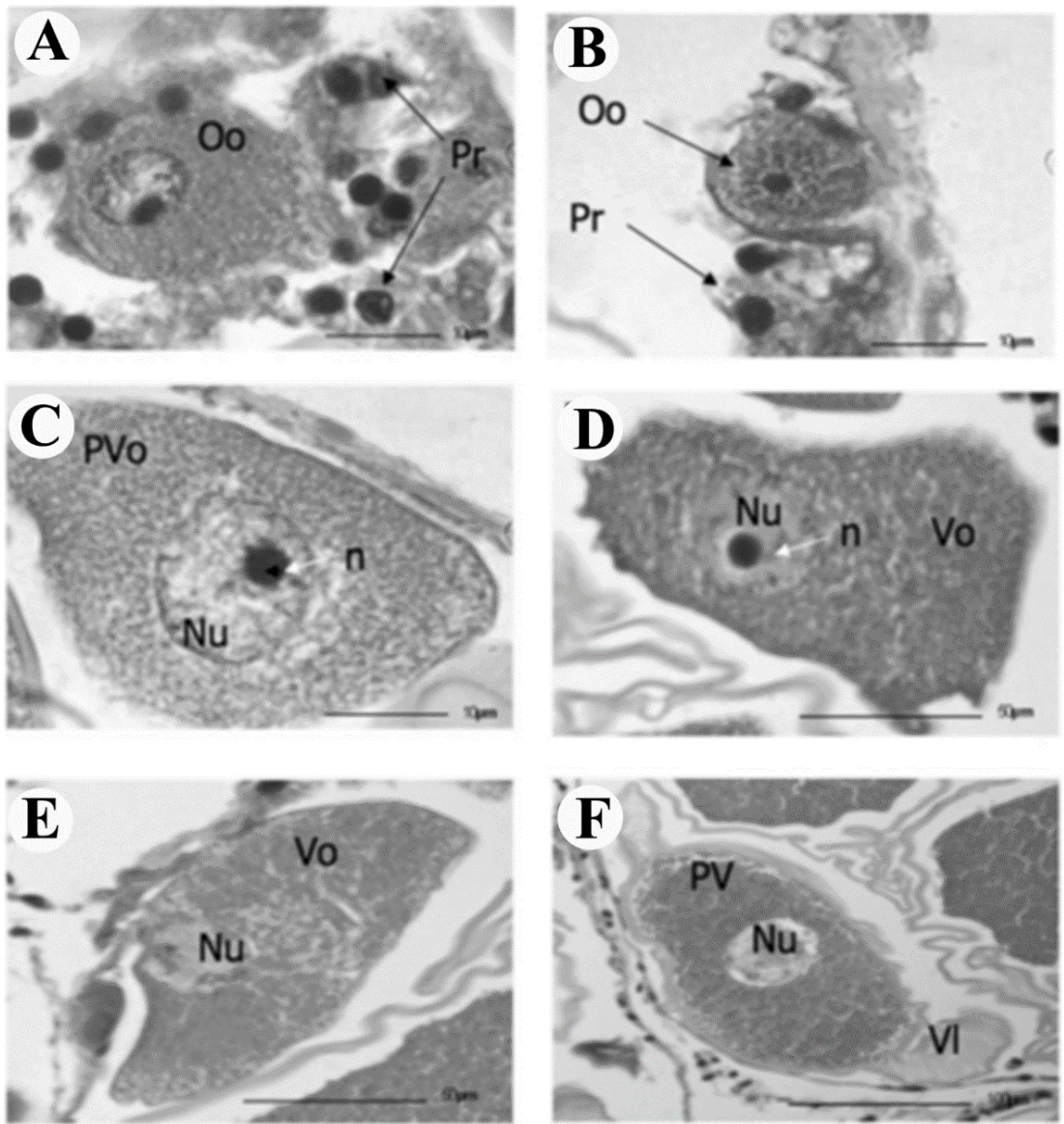


Figure 2.3 Photographs showing different oogenesis stages of *N. margaritacea*; **(A)** protogonia (Pr) located closely to the acinal wall; **(B)** oogonia (Oo) showing a distinct nucleus; **(C)** pre-vitellogenic oocytes (PVo) with nucleus (Nu) and distinct nucleolus (n); **(D and E)** vitellogenic oocytes (Vo); and **(F)** post-vitellogenic oocytes (PV) with visible vitelline layer (VI) (Glavinic et al., 2012).

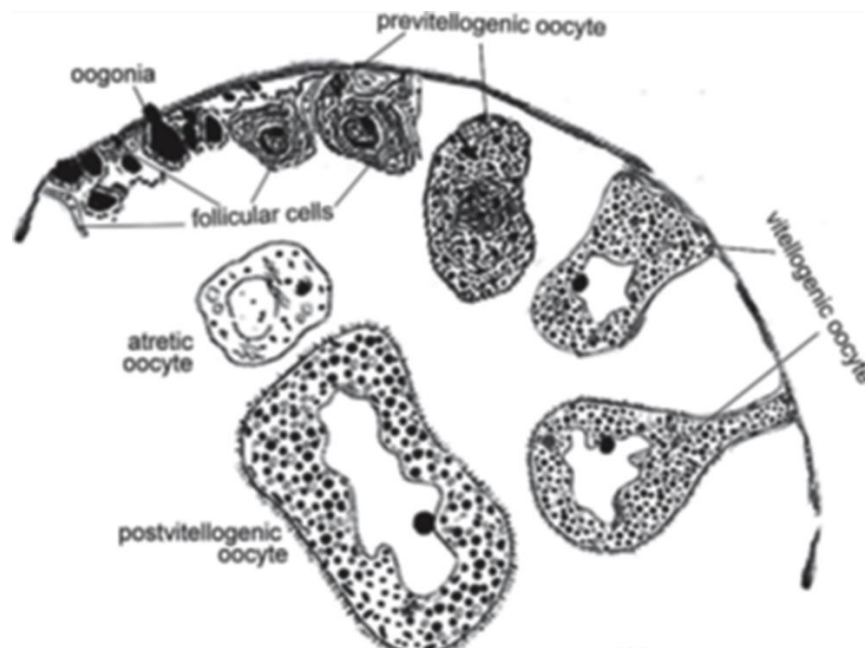


Figure 2.4 Schematic representation of oogenesis in *A. maura*. The stages of oogenesis were oogonia and pre-vitellogenic, vitellogenic and post-vitellogenic oocytes (Camacho-Mondragón et al., 2015).

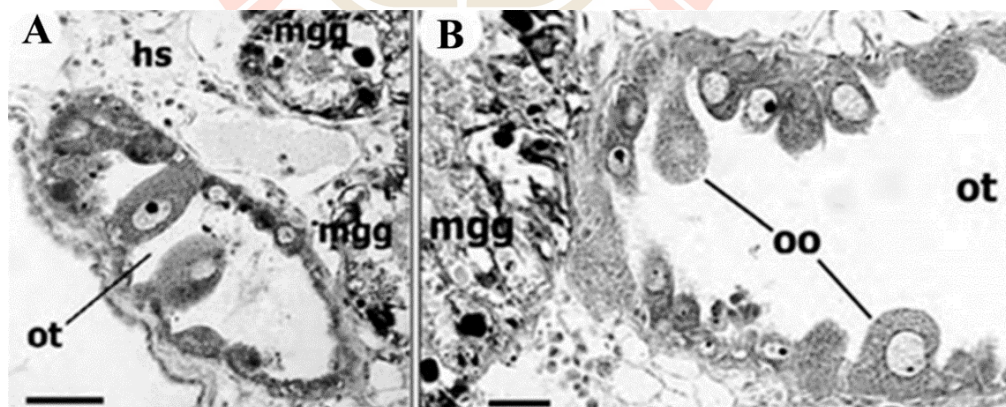


Figure 2.5 (A) Gonads of adult *P. canaliculata*. Histology of ovarian tubule (ot) located next to midgut gland (mgg) and haemocoelic spaces (hs) **(B)** Ovarian tubule contained large lumen and many stages of oocytes (oo). Scale bars = 50 μm (Gamarra-Luques et al., 2013).

2.3 Oogenesis of Mollusca

The oogenesis in bivalves was classified into solitary or follicular types. Solitary oogenesis was the stages that the developing oocyte was not completely surrounded by follicle cells (Ituarte, 2009). The follicle cells were only associated with developing oocyte during early stages of oogenesis (Woods, 1931; Okada, 1935; Ituarte, 1997). This has been reported in freshwater species *Sphaerium striatinum*, *Musculium heterodon* and *Eupera platensis*. In marine bivalves, solitary oogenesis was reported based on the presence of follicle cells during early and middle stages of oogenesis in Ostreidae (Eckelbarger and Davis, 1996) and in the middle and advanced stages of oogenesis in Mytilidae (Pipe, 1987), Pectinidae (Dorange and Le Pennec, 1989) and Pinnidae (De Gaulejac et al., 1995). The truly follicular type of oogenesis was so far been reported for *Pseudokellya Pelseener*, 1903 (Zelaya and Ituarte, 2004) and *Gaimardia trapesina* (Ituarte, 2009) which follicular cells completely surrounded the oocytes during all stages of oogenesis.

In various studied, oogenesis in mollusk has largely been classified into solitary or follicular types. In solitary oogenesis, the developing oocytes was not completely surrounded by follicular cells (Ituarte, 2009). The gamete development in siphonariids species (*Siphonaria serrata* and *Siphonaria capensis*) occurred within acinus where different stages of oocyte were found (Hodgson, 1999). In these species, oocytes were divided into 4 stages including 1) pre-vitellogenic, 2) early vitellogenic, 3) late vitellogenic and 4) mature oocytes (Figure 2.5). Pre-vitellogenic oocytes were characterized by the cytoplasmic area which was smaller than the nuclear area. Moreover, more than one nuclei were found in this oocyte stage. Early vitellogenic oocytes were characterized by a large germinal vesicle in the nucleus. Late vitellogenic

oocytes showed eosinophilia staining in the cytoplasm. Mature oocytes were detached themselves from the acinar wall and moved to the lumen (Pal and Hodgson, 2002). In *Helix aspersa*, the development of the female germ cells was divided into six stages including, oogonia, young oocytes, premeiotic stage, pre-vitellogenic stage, first vitellogenic stage and second vitellogenic stage based on morphological, cytochemical, and ultrastructural criteria (Griond and Bolzoni-Sungur, 1986).

In addition, the ultrastructural features of oogenesis were examined in Mollusca. Based on the ultrastructure, the female germ cells were subdivided into five stages, including 1) protogonia, 2) oogonia, 3) pre-vitellogenic oocyte, 4) vitellogenic oocyte, and 5) mature oocyte (Najmudeen, 2008; Glavinic et al., 2012; Camacho-Mondragon et al., 2015).

2.3.1 Protogonia

Germ cells (protogonia) of *N. margaritacea* were located along the internal walls of the acini. They were irregular in shape and had a large irregularly shaped nuclei in comparison to the total cell sizes. They were between 3 and 6 μm in size. By conducting TEM, some mitochondria and golgi apparatus were visible (Glavinic et al., 2012).

2.3.2 Oogonia

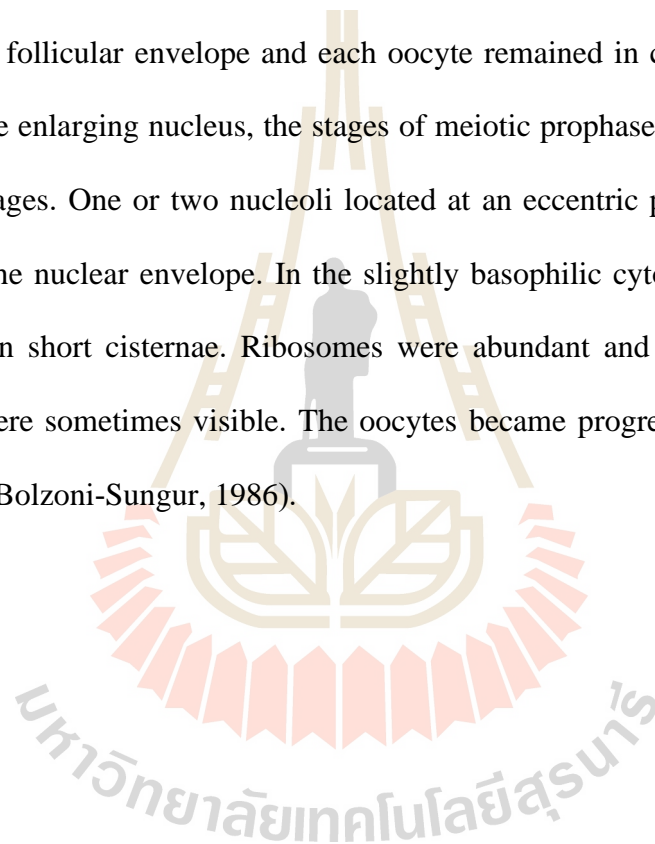
Oogonia of *N. margaritacea* were present in the wall of acini, one or two cell layers into the lumen. Oogonia were from 6 to 10 μm in sizes. Routine staining (Hematoxylin and Eosin) showed a basophilic nucleus and lighter basophilic cytoplasm (Glavinic et al., 2012). In *A. maura*, oogonia occurred as one- or two-cell layers that covered the inner acinus wall. Oogonia were round or elongated and were between 6 and 10 μm in diameter (Camacho-Mondragón et al., 2015). In this species, oogonia

showed a high nucleus-cytoplasm ratio and the round and large nuclei was more basophilic than the cytoplasm containing numerous spherical mitochondria. By conducting TEM, it was observed that oogonia of *N. margaritacea* often had a large nucleus in which chromatin was reticular and marginal (Figure 2.6). Some membrane-bound cortical granules, and mitochondria and Golgi body were visible within plasma membranes. TEM revealed that oogonia of *A. maura* frequently had a large nucleus with reticular, marginally located chromatin and a single nucleolus. Numerous ribosomes, Golgi apparatus, some cisternae of the rough endoplasmic reticulum, lipid droplets and dense aggregates were also presented in the cytoplasm.

2.3.3 Pre-vitellogenic oocytes

Pre-vitellogenic oocytes of *A. maura* were able to reach up to 30 μm in diameter, with irregular edges and a nucleolus which was 5 μm in diameter (Figure 2.7). In this species, pre-vitellogenic oocytes had a basophilic nucleus and a slightly eosinophilic cytoplasm (Camacho-Mondragon et al., 2015). In petella limpets, sizes of pre-vitellogenic oocytes was the smallest (about 10 μm in diameter). This stage of oocytes was observed within the wall of the trabecular and just beneath the epithelial cells (Hodgson and Eckelbarger, 2000). The ultrastructure showed small nucleus with a single nucleolus. The cytoplasm consisted of mitochondria, electron-dense granules, and lipid droplets. During development, the oocytes still attached to the connective tissue of trabecular (Hodgson and Eckelbarger, 2000). The pre-vitellogenic oocytes were elongated in shape. This stage had a large nucleus (12 μm in diameter) and a small volume of cytoplasm. As they enlarged, the oocytes moved away from the germinal epithelium towards the digestive gland but remained attached by stalks. Because of this oocyte stage had a lot of protein synthesis, so that the cytoplasm became strongly

basophilic. Their nuclei contained chromatin materials and prominent electron dense nucleolus (Figure 2.8). The cytoplasm of the developing oocytes contained many ribosomes, mitochondria, Golgi bodies, as well as rough endoplasmic reticulum indicating that they were in active stage of protein synthesis (Najmudeen, 2008). In *H. aspersa*, the pre-vitellogenic oocytes might still be adjacent but neighboring epithelial cells isolated them from each other and also from the acinar lumen. They gradually constituted a follicular envelope and each oocyte remained in contact with the basal lamina. In the enlarging nucleus, the stages of meiotic prophase were visible until the pachytene stages. One or two nucleoli located at an eccentric position and might be adjacent to the nuclear envelope. In the slightly basophilic cytoplasm, the RER was fragmented in short cisternae. Ribosomes were abundant and a few heterogeneous inclusions were sometimes visible. The oocytes became progressively oval in shape (Griond and Bolzoni-Sungur, 1986).



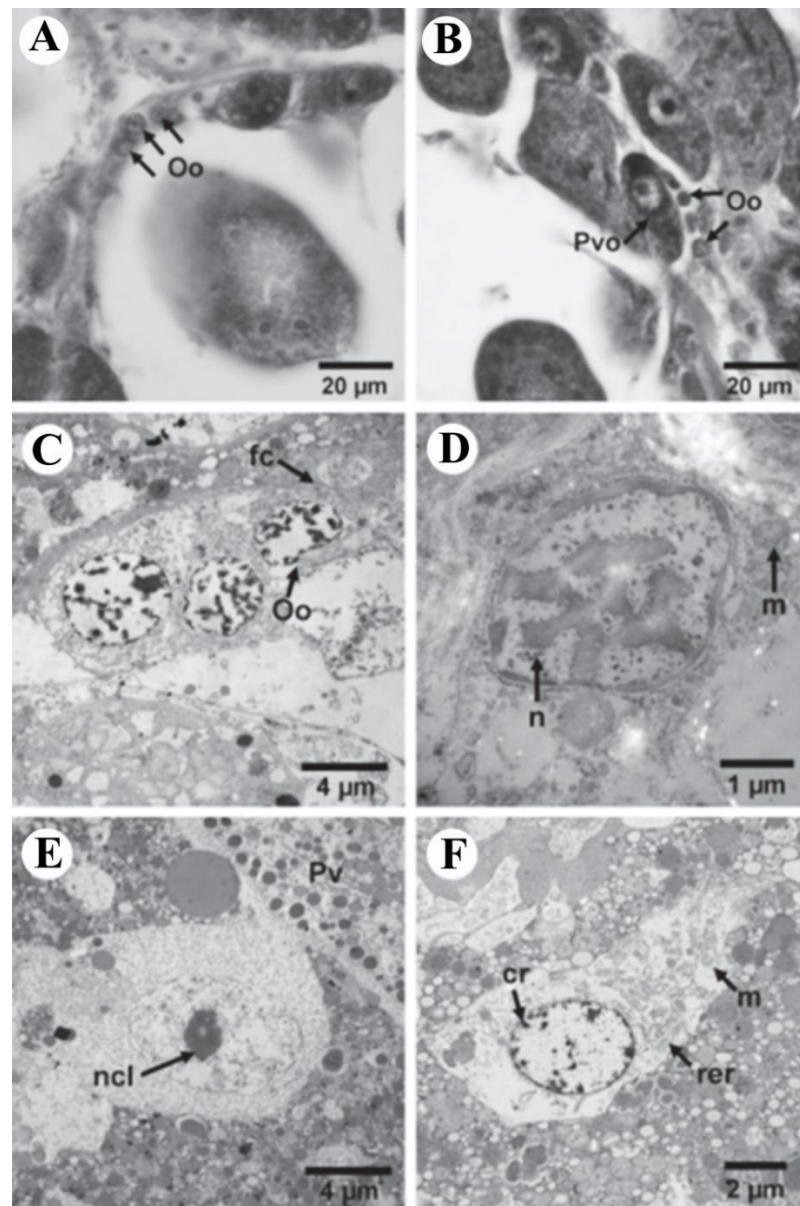


Figure 2.6 (A) Oogonia (Oo) located in the acinus wall; (B) Oogonia next to a pre-vitellogenic oocyte (Pvo) with a distinct nucleus; (C) Oogonia in contact with a follicular cell (fc); (D) High magnification of an oogonia showing the nucleus (n) and mitochondria (m); (E) Oogonia showing the nucleolus (ncl) next to a post-vitellogenic oocyte (Pv); (F) Oogonia with chromatin (cr) on the periphery of the nucleus and a large number of organelles in the cytoplasm, including mitochondria (m) and rough endoplasmic reticulum (rer) (Camacho-Mondragon et al., 2015).

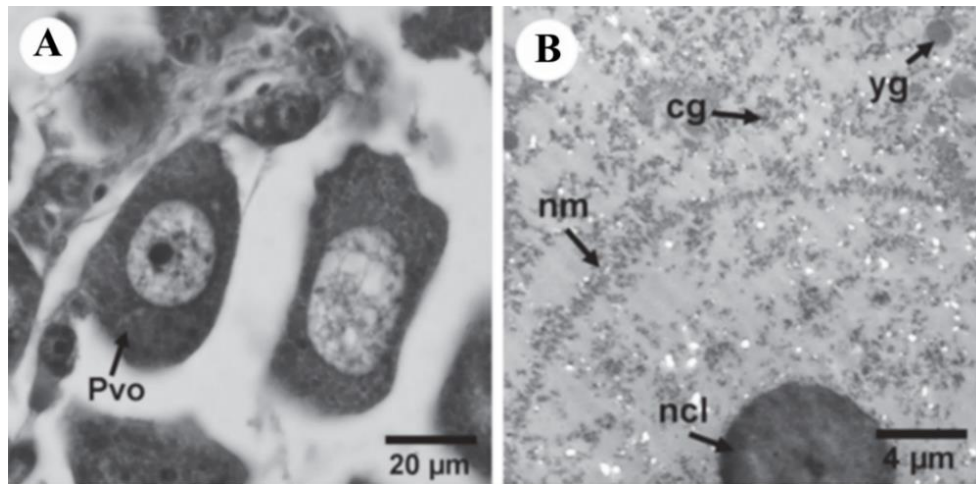


Figure 2.7 Photographs showing the pre-vitellogenic oocytes in *A. maura*. **(A)** Pre-vitellogenic oocyte (Pvo) in the acinus wall; **(B)** Pre-vitellogenic oocyte with a well-defined nuclear membrane (nm) and nucleolus (ncl); numerous cortical (cg) and some yolk granules (yg) were observed in the cytoplasm. (Camacho-Mondragon et al., 2015)

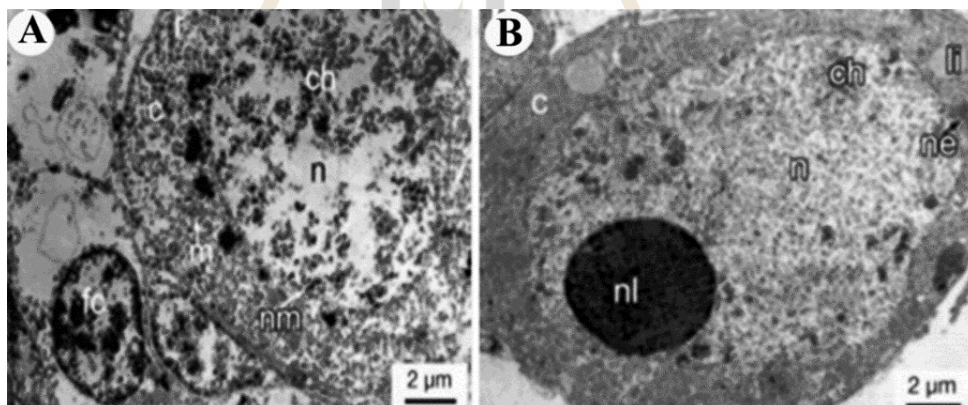


Figure 2.8 **(A)** Ultrastructure of oogonium and pre-vitellogenic oocyte of *Haliotis varia*. The oogonium showed very large nucleus containing chromatin bodies (ch), follicle cells (fc) and a nuclear membrane (nm). The cytoplasm (c) contained numerous ribosomes (r) and mitochondria (m). **(B)** Early vitellogenic oocyte showed an enlarged clear nucleus and darkly stained nucleolus (nl), nuclear emissions (ne) and lipid droplets (li) in the cytoplasm (Najmudeen, 2008).

2.3.4 Vitellogenic oocytes

In *N. margaritacea*, vitellogenic oocytes were larger (100 μm in diameter) and continued to grow by accumulation of yolk granules. They were found in the lumen of acinus. The point of attachment to the acinal wall was visible and was referred to here as a stalk. Microvilli appeared for the first time at this stage. The nucleus was round and 50 μm in diameter with a nucleolus of 10 μm in diameter. Numerous mitochondria, Golgi apparatus and endoplasmic reticulum were visible. By conducting TEM, membrane-bound yolk granules were 1-5 μm in diameter, while lipid granules were smaller (1 μm in diameter) and dense in consistency (Glavinic et al., 2012). In *A. Maura*, oocytes entering the vitellogenesis stage continued to grow while migrating into the acinar lumen by accumulation of yolk granules in the cytoplasm and reach diameters \sim 40 μm . The junction with the acinus wall, known as the stem, displayed numerous clustered mitochondria. The nucleus of vitellogenic oocyte was round and often displayed several dense accumulations near the nuclear membrane; only one nucleolus was present. Microvilli appeared for the first time in the final vitellogenesis stage; cytoplasmic organelles proliferated and numerous whorls of rough endoplasmic reticulum (rER) were apparent throughout the cytoplasm. In *H. varia*, early vitellogenic oocytes were enlarged compared to the previous stage (about 50 μm in diameter). This indicated that the vitellogenesis occurred within the cytoplasm. Moreover, ultrastructure of the oocytes showed electron dense, round, lipid droplets in the cytoplasm. The nuclei of early vitellogenic oocytes were clear and round in shape (Figure 2.9). Large numbers of ribosome-studded, as well as smooth, membrane-bound vesicles were also presented in the cytoplasm (Najmudeen, 2008). In *Helix aspersa*, this oocyte stage was characterized by a considerable increase in size and

nuclear volume. The oocyte was generally oriented parallel to the acinar wall. The cytoplasm lost the basophilia. The number of mitochondria as well as the rER formed flattened cisternae (Figure 2.10). The lipid droplets occurred in clusters and usually located at both extremities of the cell (Griond and Bolzoni-Sungur, 1986).

The late vitellogenic oocytes of *H. varia* were 80 to 120 μm in diameters (Najmudeen, 2008). The oocytes attached to the trabeculae in the ovarian lumen. Darkly stained protein yolk granules and lipid droplets also found within the cytoplasm. In the nucleus, the nucleolus showed a dark, round, electron-dense body. In *H. aspersa*, the cytoplasm of late vitellogenic oocytes was filled with clear vesicles which probably originated from the rER because their surface beared some ribosomes. Elongated mitochondria with a dense matrix and few cristae were numerous, especially at the extremities of the oocyte. Prominent saucer-shaped dictyosomes pinched off a multitude of vesicles. Some lysosomes, multivesicular bodies and the first yolk granules appeared. These were spherical with a homogeneous, electron dense content (Griond and Bolzoni-Sungur, 1986).

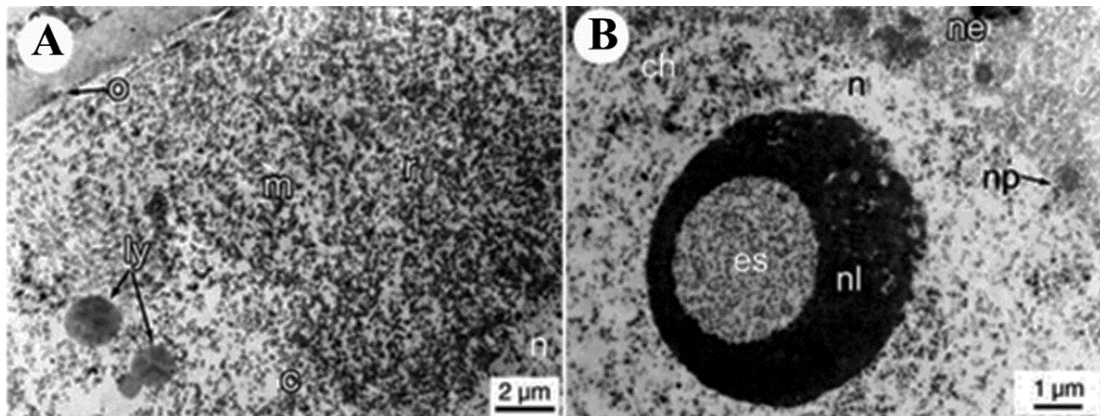


Figure 2.9 (A) Ultrastructure of vitellogenic oocyte of *H. varia*. Cytoplasm of early vitellogenic oocyte contained lipid yolk bodies (ly), mitochondria (m), ribosomes (r) and a well-defined oolemma (o). (B) This stage of oocyte increased in cytoplasmic area and electron lucent space (es) in the nucleolus (nl) (Najmudeen, 2008).

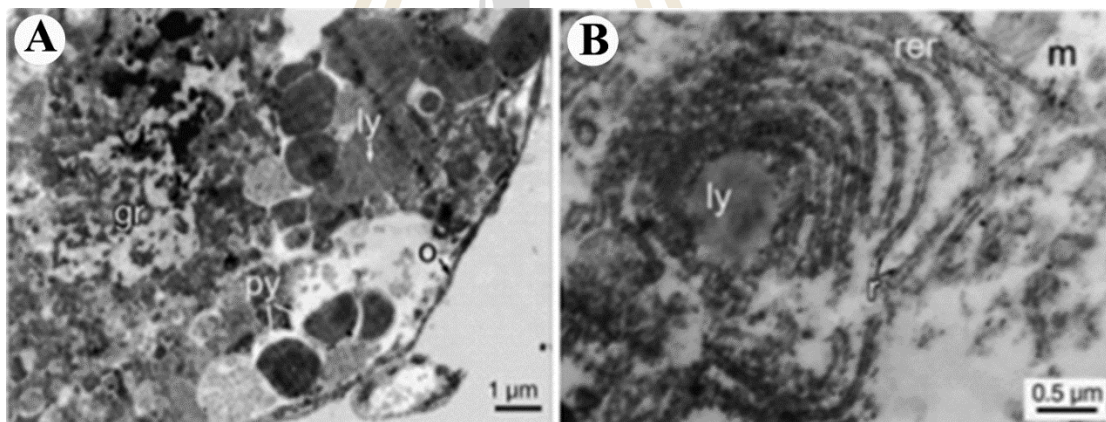


Figure 2.10 Photographs showing ultrastructure of late-vitellogenic oocyte of *H. varia*. (A and B) This stage of oocyte contained lipid yolk (ly), protein yolk (py), granular materials (gr), mitochondria (m), and rough endoplasmic reticulum (rer). (Najmudeen, 2008).

2.3.5 Mature oocytes

In *N. margaritacea*, post-vitellogenic (mature) oocytes ranged in size from 200-284 μm . The cytoplasm of mature oocyte contained numerous lipid droplets and protein yolk granules. This stage was the largest oocyte. The oocytes at this stage were located in the center of the acinus lumen but still connected to the wall of acini by a stalk. The cytoplasm was extremely eosinophilic (Glavinic et al., 2012). By conducting TEM, the nucleus was homogeneous and the nucleolus appeared dense. Mitochondria and rough endoplasmic reticulum appeared through the ooplasm. In *H. varia*, the diameter oocyte was about 170 μm in diameter. The oocytes became detach from the trabeculae and were tightly packed in the ovarian lumen. The nucleus was very large and less electron dense with a dark nucleolus. In the cytoplasm, the membrane-bound vesicles were found in mature oocytes (Figure 2.11). They occupied beneath the cytoplasmic membrane of the mature oocytes (Najmudeen, 2008). The mature oocytes were characterized by the presence of numerous vitellogenic inclusion bodies in the cytoplasm. In the nucleolus, nucleolus-like bodies and fibrillar spheres were enlarged. They appeared close to the nuclear envelope or were connected with rER. In light microscopy sections, they formed a group of rods between the nuclear and the plasma membranes next to the acinar lumen. Outside this area, the cytoplasm was crowded with various organelles and inclusions, as well as dark elongated mitochondria, lipid droplets, and clear vesicles (Griond and Bolzoni-Sungur, 1986). In *A. Maura*, mature oocytes reached up to 80 μm in diameter. They contained numerous yolk and lipid granules. The nucleus was homogeneous, and the nucleolus, generally located in a marginal position, but sometimes to the center of the nucleoplasm and appeared appears

dense. At this stage, microvilli were quite visible and completely surrounded the oocytes (Camacho-Mondragon et al., 2015).

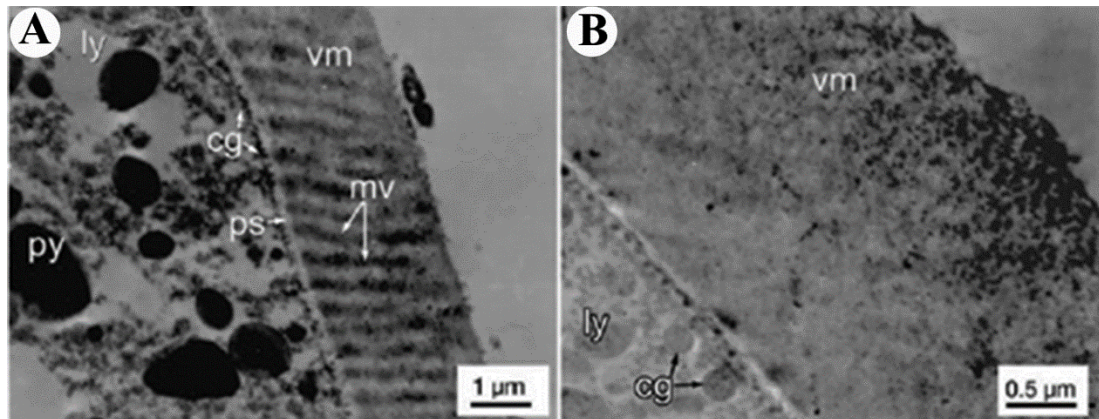


Figure 2.11 (A and B) Photographs showing cytoplasm of mature oocytes of *H. aspersa* containing numerous lipid yolk (ly) and protein yolk (py) bodies and cortical granules (cg). Perivitelline space (ps) was presented the vitelline envelope (vm). Numerous microvilli (mv) were surrounded the mature oocyte. (Najmudeen, 2008).

2.4 Biochemical composition changes in developing oocytes

Investigation of changes of biochemistry components during oocyte development can be performed using many classical techniques, such as electrophoresis and Western blotting. However, one disadvantage of these techniques is time consuming. At present, infrared spectroscopy is another technique that can be used to determine chemical compositions and architectures of biochemical molecules in cells. This technique can be used to investigate protein structure, protein folding, unfolding and misfolding (Dyer et al., 1998; Gilmanishin et al., 1997). Fourier Transform-Infrared (FTIR) microspectroscopy is believed to be a reliable tool which exhibits excellent results in investigations of biochemical compositions and organizations (Figure 2.12). This

powerful tool allowed us to obtain information in non-invasive way by generating unique spectral signal that sensitive to the chemical compositions and architectures of molecules (Mazzeo et al., 2016; Sinclair and Singh, 2007). Other advantages of the FTIR microspectroscopy are known, for example, FTIR microspectroscopy consumes short time for sample preparation and data analysis (Mazzeo et al., 2016). Nowadays, high resolution of FTIR imaging can be improved by replacement of conventional infrared light source with synchrotron light source. The synchrotron light is much brighter than infrared source for about 100-1,000 times (Wood et al., 2008). However, FTIR spectroscopy is also becoming accepted as an increasingly useful tool for the structural analysis of peptides and proteins. (Torii et al., 1998; Venyaminov and Kalnin, 1990; Arrondo and Goni, 1999). There are a number of advantages that make infrared spectroscopy an attractive tool for studying of proteins. Probably the most important advantage is that the spectra of proteins can be obtained in a wide range of environments. Measurements can be performed on solids such as powders or films, in aqueous solutions, in organic solvents and in detergent micelles as well as in phospholipid membranes (Besset, 1975; Byler and Susi, 1986; Arrondo and Goni, 1999; Grdadolnik and Marechal, 2001). Information on the secondary structure of proteins can be derived from analysis of the intensity of the amide I band. Therefore, most methods used to determine the secondary structure of peptides and proteins concentrate on an analysis of the amide I band, located between 1700 cm^{-1} and 1600 cm^{-1} . The amide I band is composed mainly (around 80%) of the C=O stretching vibration of the peptidic bond. The band can be analysed by comparison with a calibration set of spectra from proteins with known structures using factor analysis or by decomposing the amide I band into its constituents via spectral decomposition,

derivative spectroscopy (Susi and Byler, 1983; Grdadolnik and Marechal, 2003). Fourier deconvolution or a band fitting algorithm (Venjaminov and Kalnin, 1990; Byler and Susi, 1985). All mentioned methods are based on examination of the structure of the amide I band and the results of the analysis crucially depend on the shape of amide I band.

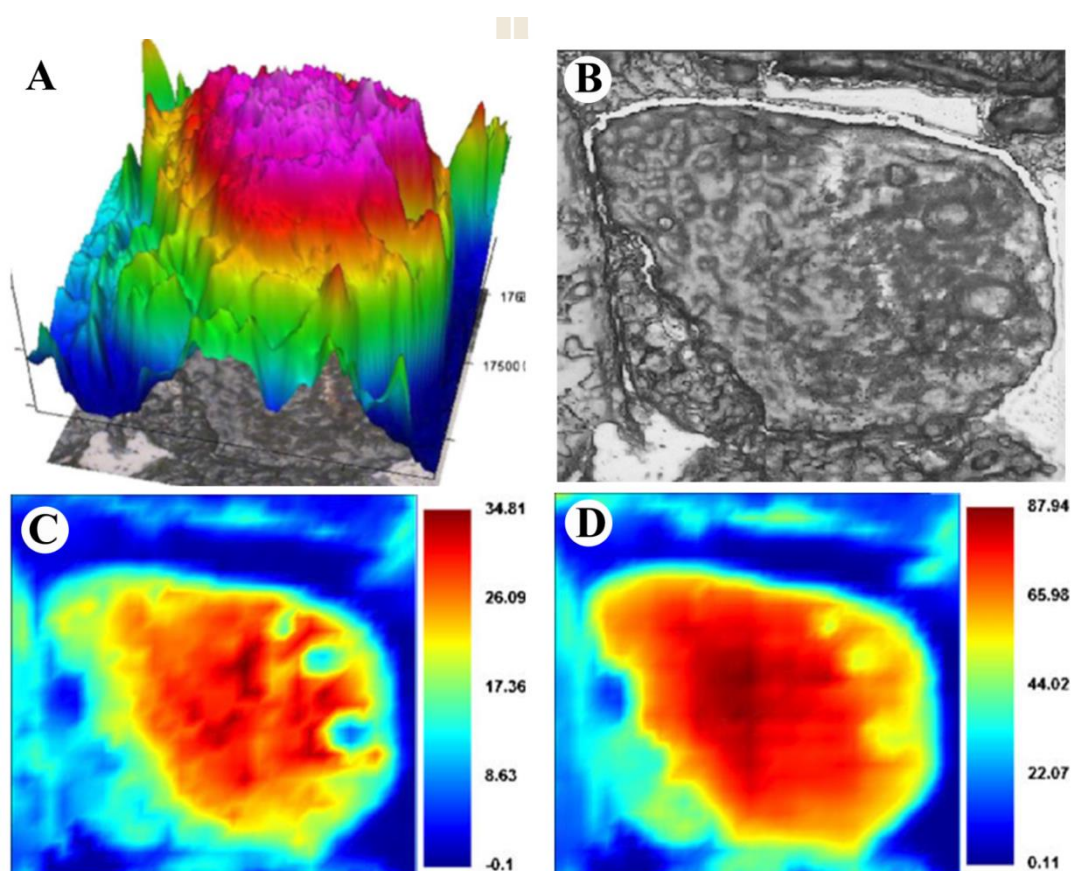


Figure 2.12 (A and B) Total absorbance cartogram of oocyte, reconstructed by integrating the area between 1,800 and 1,000 cm^{-1} together with the corresponding photomicrograph; (C) chemical maps of the integrated areas under the CH₂ and CH₃ stretching regions (3,100-2,800 cm^{-1}), (D) the amide I band (1,720-1,580 cm^{-1}) (Mazzeo et al., 2016; Sinclair and Singh, 2007).

CHAPTER III

MATERIALS AND METHODS

3.1 Animal preparation

Male and female snails were collected from rice fields in Chum Phuang subdistrict, Nakhon Ratchasima province, Thailand in April 2014. To ensure maturity, sizes of operculum were measured and only adult snails with operculum sizes more than 4 cm were used in the experiments. The snails were kept under a normal day/ light cycle (12/12 h) and the temperatures were ranged between 25-28°C They were acclimatized under the natural light–dark cycle for 2 weeks before the experiments. They were housed in soil-made containers filling with de-chlorinating water. The snails were fed daily with morning glories and commercial pelletized food.

3.2 Stereomicroscopic studied of external morphology of the gonadal tissue

The external morphology of the ovarian tubule was examined using stereomicroscope. The snail's shell was cracked with bone cutting scissors and gently removed. In order to classify the stages of the ovarian tubule from the external morphology, photographs of the ovarian tubules were captured with digital camera that connected with stereomicroscope. The conditions used to classify the stages of

development of the ovarian tubules were the sizes of the ovarian tubule and the quantity of the adipose tissue that surrounded them.

3.3 Scanning electron microscopic study of external morphology of the gonadal tissues and oocytes

Scanning electron microscope (SEM) was used to observe the external morphology of the oocytes in the ovarian tubule. The gonadal tissues were dissected from the digestive gland and cut into small pieces. After that, the pieces of the gonadal tissues were fixed in 4% paraformaldehyde and 2% glutaraldehyde in 0.1M PBS (pH 7.4), at 4°C, for 60 min. The specimens were then washed with three changes of 0.1M PBS, pH 7.4 (10 min, each). The lipid component in the tissues was preserved by post-fixation with 1% osmium tetroxide (OsO_4) in 0.1M PBS, pH 7.4, for 60 min. After that, the specimens were dehydrated in an increasing concentration of ethanol (50%, 70%, 80%, 90%, 95% and 100%), 15 min, twice, each at 4°C. The specimens were critical point dried (CPD) and then mounted on stubs. Finally, the tissues were sputter-coated with gold. The external morphology of ovarian tubules and oocyte stages were observed under a JSM-6010LV scanning electron microscope operating at 10 kV.

3.4 Light microscopic study of the gonadal tissues and oocytes

For histological observation, the gonadal tissues were dissected from the snail and then fixed in Bouin's fixative (Bio-optica) at room temperature with gentle shaking for overnight. The gonadal tissues were then washed several times with 70% ethanol to remove the excess of fixative. After that, the gonadal tissues were dehydrated in graded

ethanol series; 50%, 70%, 80%, 90%, 95% and 100%, (60 min in each step and twice) at room temperature. The gonadal tissues were then cleared with two changes of xylene (60 min, each) at room temperature followed by immersing in liquid paraffin using tissue processor (BIO-OPTICA CD1000). The gonadal tissues were embedded in paraffin wax. Serial paraffin sections were cut using a rotary microtome (Microm HM 325), at 5 μm thick, subsequently floated on a 0.1% gelatin solution, and mounted on clean glass slides.

The paraffin sections were deparaffinized with xylene (5 min, 3 times) at room temperature. The tissue sections were rehydrated in a graded series of ethanol (100%, 95%, 90%, 80% and 70%) with two final changes of distill water (15 min, each at room temperature). Then, the tissue sections were stained with Mayer's hematoxylin for 3 min and Eosin for 1 min at room temperature (Bio-optica). In order to stain the connective tissue and muscular tissue in the gonadal tissue, the specimens were stained with Masson's trichrome staining kit as described by manufacturer. Thereafter, the tissue sections were dehydrated in a graded series of ethanol (100%, 95%, 90%, 80% and 70%) and then mounted with per mount. The stained sections were viewed under a Nikon E600 light microscope. Photographs were captured with Olympus DP72 digital camera (Japan). In order to measure diameters of oocyte, five sections of Mayer's hematoxylin and Eosin staining were selected for the determination of their diameters. Each section was photographed for ten microscopic fields (a microscopic field area equaled 0.12 mm^2). The measurements were conducted from the widest diameter of the oocyte that pass through the nucleus. The data was analyzed using a computerized image analysis program (Cell^D software). Differences among sizes of stages of the oocytes were statistically analysis using one-way analysis of variance (ANOVA)

followed by a Turkey post hoc multiple comparisons. A probability value of less than 0.05 ($P < 0.05$) was used to indicate a significant difference.

3.5 Transmission electron microscopic study of oocytes

The gonadal tissues were removed and fixed in 4% paraformaldehyde and 2% glutaraldehyde in 0.1 M PBS, pH 7.2 at 4°C for 30 min. Afterwards, the fixed tissues were sliced into small pieces (about 1x1 mm) and immersed in the same fixative for overnight at 4°C with gentle shaking. The specimens were then post-fixed with 1% osmium tetroxide (OsO_4) in 0.1M PBS for 60 min at 4°C, following by dehydration in an increasing concentration of cold ethanol (50%, 70%, 80%, 90%, 95% and 100%). After dehydration, the tissues were infiltrated with propylene oxide for 60 min at room temperature. Thereafter, the specimens were infiltrated with propylene oxide and Araldite 502 (Electron Microscopic Science, Hatfield, PA) at ratio 2:1 and 1:1 for 60 min, each at room temperature. After that, the tissues were infiltrated with propylene oxide and Araldite 502 at ratio 1:2 for overnight at room temperature. The propylene oxide was evaporated at least 6 hours in fume hood and then the specimens were infiltrated with pure Araldite 502 for 60 min at room temperature. The specimens were embedded with pure Araldite 502 and incubated at 37°C for 2 days and changed the temperature was changes to 48°C for 2 days. Finally, the specimens were incubated at 60°C until the resin was completely polymerized.

To describe the morphology and histology of the oocytes, semi-thin sections were cut with glass knight at 200 nm thick and placed on a drop of distilled water on acetone cleaned glass slides. The sections were dried for 5 min at 50-60°C, and then cooled down at room temperature. After that, the semi-thin sections were stained with toluidine

blue for 1-2 min at 50-60°C. The excess methylene blue was washed with distilled water for several times. The slides were then mounted with resinous medium.

Ultrathin sections were cut with a diamond knight at 50-70 nm thick using a RMC/MTX75500 ultra-microtome. Ultrathin sections were placed on 200-mesh copper grids, counter-stained with uranyl acetate and lead citrate, and viewed under a (FEI-Tecnai g220S-Twin) transmission electron microscope operating at 100 kV.

3.6 Histochemical study of yolk granules in the oocytes

The snail's shells were cracked with bone cutting scissors and gently removed. The gonadal tissues were cut and separated from the digestive gland. The specimens were immediately fixed for overnight in freshly prepared 4% paraformaldehyde in 0.1M PBS (pH 7.4) with gently shaking in a refrigerator. In order to wash the excess fixative, the gonadal tissues were intensively washed and shaken with cold PBS (0.1M, pH 7.4) for 30 min. To prevent the crystal ice in the tissue, the specimens were immersed in 10% sucrose in cold PBS (0.1M, pH 7.4) for 30 min, followed by immersing in 30% in sucrose in cold PBS (0.1M, pH 7.4), with gentle shaking at 4°C for overnight. The tissues were embedded in optimal cutting temperature compound (OCT compound) (Miles Laboratory) and immediately frozen in liquid nitrogen. The cryosections were cut at 10 µm thickness and picked up on poly-L-lysine coated slides. The cryosections were kept in -20°C until used for histochemistry staining.

In order to detect the lipid granules in the oocytes, the cryosections were stained with Sudan Black for 7 min, and immersed in 85% propylene glycol for 3 min. After that, the tissues were rinsed with distilled water, and stained with nuclear fast red for 3 min. The cryosections were washed with tap water and rinsed with distilled water.

Finally, the cryosections were mounted with mounting medium. At least 20 oocytes from each stage were selected for the determination of their lipid yolks. Differences among numbers of lipid yolk in each stage of oocytes were statistically analysis using one-way analysis of variance (ANOVA) followed by a Turkey post hoc multiple comparisons. A probability value of less than 0.05 ($P < 0.05$) was used to indicate a significant difference.

3.7 Biochemistry analysis during oocyte development

3.7.1 Tissue Preparation

The gonadal tissues were cut into small pieces and immersed in 10% neutral buffered formalin for overnight at 4°C (Sigma, Saint Louis, Missouri, USA). The tissues were processed for embedding in Leica Microsystems Surgipath Paraplast Tissue Embedding Medium (Leica Microsystems, St. Louis, Missouri, USA). The gonadal tissues were subsequently sectioned with Rotary Microtome HM 355S (MICROM, Germany) at 5 µm thickness. The tissue sections were finally placed on barium fluoride optical windows (Spectral Systems, Hopewell Junction, New York, USA).

3.7.2 Synchrotron- Fourier Transform-Infrared Spectroscopy (FTIR) microspectroscopy

Stages of oocyte (pre-vitellogenic, vitellogenic, and mature oocytes) in the ovarian tubule were investigated for amide I, amide II, nucleic acid, and carbohydrate using Synchrotron-FTIR microspectroscopy. The spectra were generated from Vertex 70 spectrometer that equipped with Hyperion 2000 microscope (Bruker Optics Ltd,

Ettlingen, Germany). Range of the spectrum was collected from 1,800 to 900 cm^{-1} with a cooled Mercury Cadmium Telluride (MCT) detector (Bruker Optics Ltd, Ettlingen, Germany). The diaphragm aperture of the microscope was set at 10 x 10 μm in order to get the excellent signal to noise ration and high resolution. Images were acquired in transmission mode (OPUS 7.2, Bruker software package).

3.7.3 Spectral data analysis

Each image was analyzed for intensity of the infrared absorption using OPUS 7.2 software package. Integral areas under ranges of spectra of 1700-1500 cm^{-1} , 1300-1200 cm^{-1} and 1200-900 cm^{-1} represented protein (amide I and amide II), nucleic acid and carbohydrate, respectively. Original spectrum (1,800 to 900 cm^{-1}) was analyzed using Savitsky-Golay method (3rd grade polynomial, 13 smoothing points). Second derivatives were then generated using Unscrambler X 10.0 software. The second derivatives were subsequently observed the correct position and absorbance intensity of the spectra. Curve-fitting and principal component analysis (PCA) were also generated.

3.8 The relationship between ovarian tubule stages and oocyte stages

3.8.1 Animal preparation

Male and female snails were collected from rice fields in Nakhon Ratchasima province, Thailand. To ensure maturity, the sizes of operculum were measured and only adult snails with operculum sizes more than 4 cm were used in the experiments. To allow natural mating, they were housed in soil-made containers filling with de-

chlorinating water in the ratio of 8:1 (female: male). The snails were fed daily with morning glories and commercial pelletized food. They were acclimatized for at least 2 weeks prior to experiments. Thirty snails were divided into six groups (5 snails/group). The snails were allowed to mate and the couples were isolated and housed in separate container. After that, the female snails were sacrificed at every 5 day after mating (group 1: day 0; group 2: day 5; group 3: day 10; group 4: day 15; group 5: day 20; and group 6: day 25) (Figure 3.1).

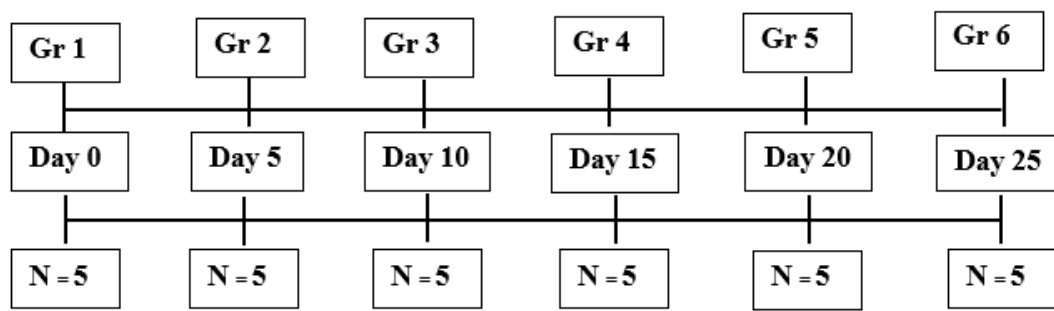


Figure 3.1 The snails were allowed to mate and the couples were isolated and housed in separate containers.

3.8.2 Histological study of oocytes

For histological observation, the gonadal tissues were dissected and then immediately fixed in Bouin's fixative (Bio-optica) for overnight. After washing of the excess fixative, the gonadal tissues were dehydrated in graded ethanol series; 50%, 70%, 80%, 90%, 95% and 100% at room temperature. Afterward, the gonadal tissues were processed for routinely embedding. Serial paraffin sections were cut using a rotary microtome (Microm HM 325), at 5 μm thickness, subsequently floated on a 0.1% gelatin solution, and mounted on clean glass slides.

The paraffin sections were deparaffinized with xylene (5 min, 3 times) at room temperature. The tissue sections were rehydrated in a graded series of ethanol (100%, 95%, 90%, 80% and 70%) with two final changes of distill water (15 min, twice, at room temperature). Then, the tissue sections were stained with Mayer's hematoxylin and Eosin (Bio-optica). Ten photographs of the ovarian tubules were taken from each snail on each day. In each photograph, the numbers of each oocyte stage were counted using a computerized image analysis. The data was expressed as mean \pm S.D.

Differences among numbers of the oocyte stages in each day of ovarian tubules were statistically analysis using one-way analysis of variance (ANOVA) followed by a Turkey post hoc multiple comparisons. A probability value of less than 0.05 ($P < 0.05$) was used to indicate a significant difference.

Numbers of the oocytes were counted from 10 sections of ovarian tubules at day 0, 5, 10, 15, 20 and 25 post-spawning. From each section, 10 microscopic fields (each field equaled 0.12 mm²) were photographed. Percentages of the oocyte stages were than calculated as described below.

$$\text{Percentages of oocyte stages} = \frac{\text{Numbers of each oocyte stage}}{\text{Total number of all oocyte stages}} \times 100$$

Percentages of oocyte stages at different days post-spawning were compared using one-way analysis of variance (ANOVA) followed by a Turkey post hoc multiple comparisons. A probability value of less than 0.05 ($P < 0.05$) was used to indicate a significant differen

CHAPTER IV

RESULTS

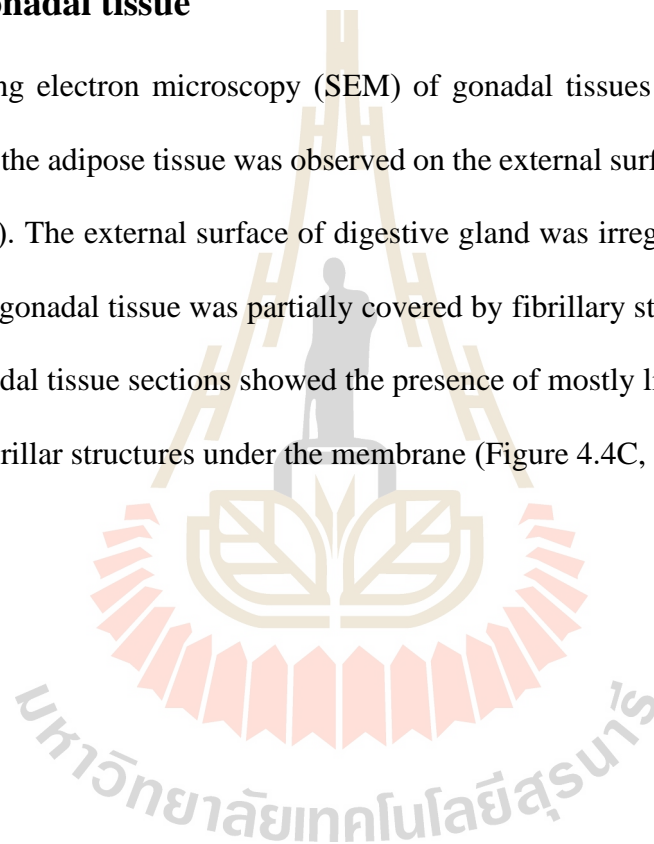
4.1 Stereomicroscopic study of external morphology of the gonadal tissue

In *P. canaliculata*, ovarian development was classified based on the size, color and texture of the adipose tissue. The present study is first time in evaluating the stages of the ovarian tubule in *P. Canaliculata*. The gonadal tissue was located within the digestive gland which was compacted by the fibrous connective tissue and muscle fibers. The ovarian tubule appeared as a tubular branch structure, pale-dark yellow in color, and variable in size depending on the stage of maturity of the individual. The ovarian tubule was situated on the dorsal side of the digestive gland (Figure 4.1). As gonadal tissue maturation progressed, the color of the ovarian tubule was pale yellow and it was surrounded with white granule of the adipose tissue. These features allowed the recognizing and describing of the stages of the ovarian tubule. In this study, the gonadal tissues were classified into four continuous stages (stage I-IV) that consecutively occurred. In stage I (spent stage), gonadal tissue was thin strand-like structure, very small in size, transparent, with no apparent fatty tissue formation (Figure 4.2A). In stage II (proliferative stage), adipose tissue was slightly larger, transparent, and more elongated than that of the pre-vitellogenic stage (Figure 4.2B). In stage III

(premature stage), adipose tissue was further thickened and became grey to yellow in color (Figure 4.2C). Finally, In stage IV (mature stage), adipose tissue was characterized by greyish white in color (Figure 4.2D).

4.2 Scanning electron microscopic study of external morphology of the gonadal tissue

Scanning electron microscopy (SEM) of gonadal tissues from *P. canaliculata* revealed that the adipose tissue was observed on the external surface of digestive gland (Figure 4.3A). The external surface of digestive gland was irregular (Figure 4.3B). In addition, the gonadal tissue was partially covered by fibrillary structures (Figure 4.3C, D). The gonadal tissue sections showed the presence of mostly lipid granules of varies sizes with fibrillar structures under the membrane (Figure 4.4C, D).



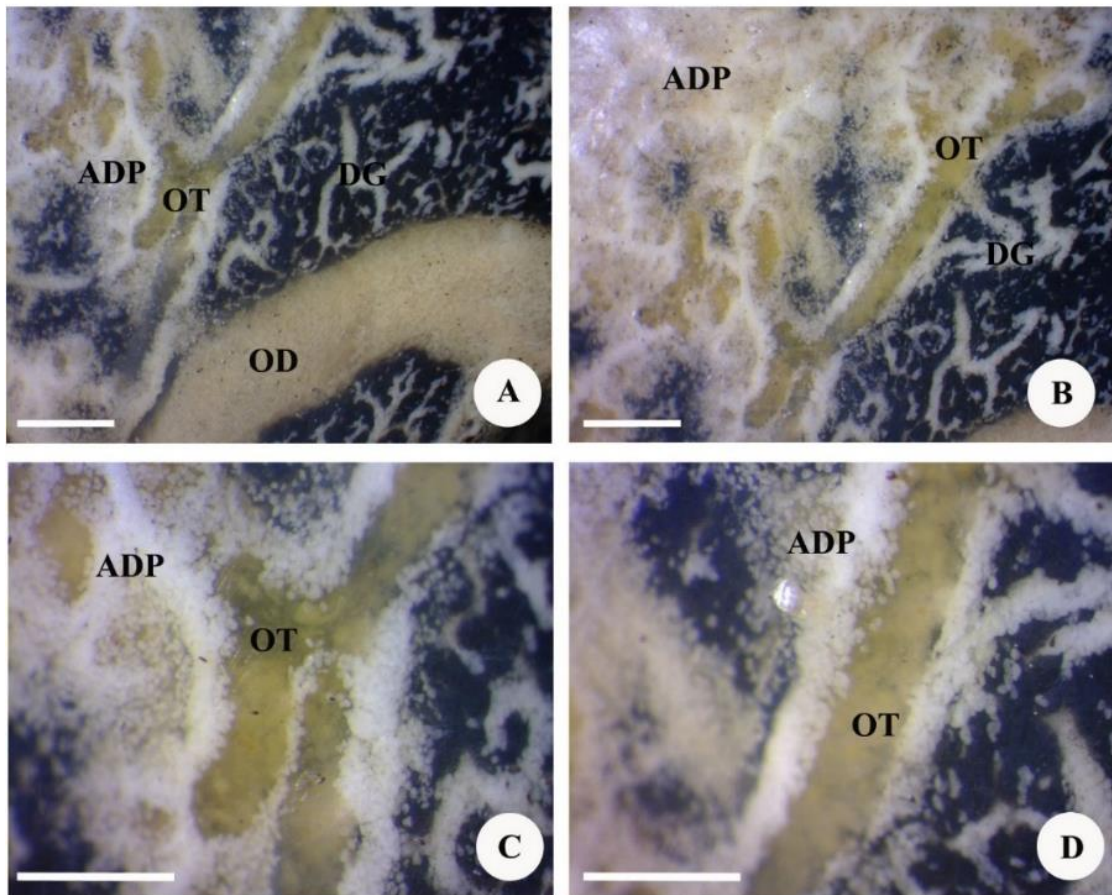


Figure 4.1 Photographs showing the gross morphology of gonadal tissue. (A and B) Digestive gland (DG) was covered with granules of adipose tissue (ADP). The ovarian tubules (OT) and ovary duct (OD) was situated on the dorsal side of the digestive gland (B and D) Digestive gland and gonadal tissue were observed from the external morphology. Scale bar: A, B =3 mm; C, D = 4 mm.

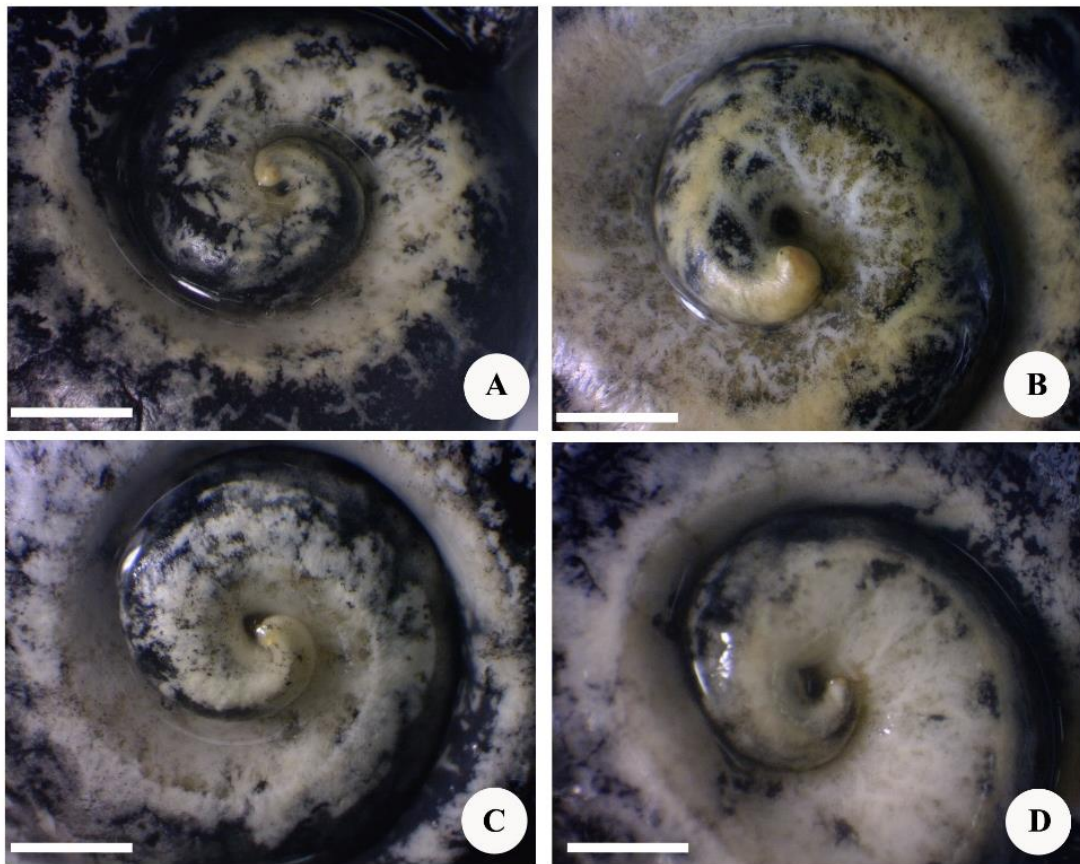


Figure 4.2 Photographs showing the gross morphology of gonadal tissue at different stages of development in *P. canaliculata*. **(A)** Stage I (spent stage). **(B)** Stage II (proliferative stage). **(C)** Stage III (premature stage). **(D)** Stage IV (mature stage). Note the variation in sizes and colors of the ovarian tubule during different stages of the development. Scale bars: A-D = 1 cm.

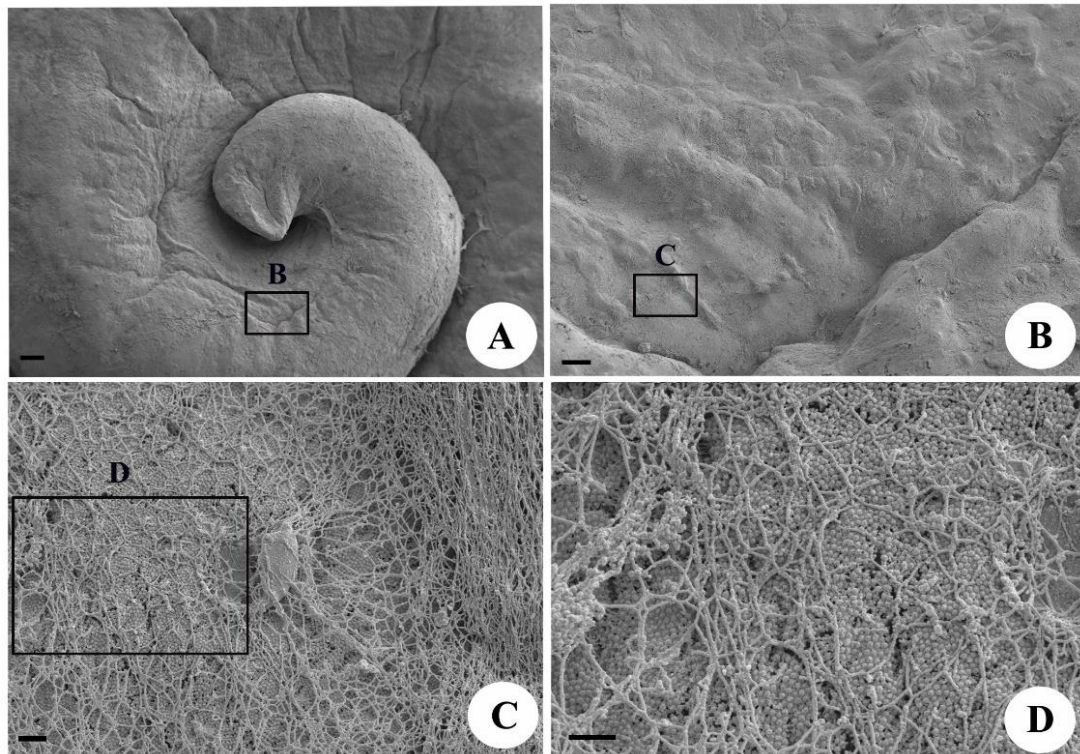


Figure 4.3 Photographs showing external morphology of the digestive gland and the gonadol tissue. **(A and B)** Scanning electron microscopy showed the surface of the digestive gland. **(C)** The external surface of gonadal tissue was covered with numerous of connective tissue network. **(D)** Numerous small granules of the adipose tissue were found under the connective tissue network. Scale bars: A = 200 μm ; B = 30 μm ; C = 1 μm ; D = 1 μm .

4.3 Light microscopic study of the gonadal tissue

The morphology and the stages of oogenesis have been investigated firstly in the present study. The gonadal tissue was covered with a simple cuboidal epithelium and underlain by connective tissue and muscle fibers. Mucin-like coating cells (secretory cells) appeared on the surface of apical epithelial cells. Secretory cells were found

scattered between the epithelial cells (Figure 4.4). The ovarian tubules composed of many tubules that connected with the ovary duct. The ovarian tubules were lobules in structure and situated in the digestive gland on the dorsal side of the coil. It consisted of tightly clustered, grape-like acini, each of which contained oocytes in all stages of oogenesis. The ovarian tubule consisted of several clusters of highly branched tubules surrounded by a thin muscular wall. During oogenesis, each tubule contained oocytes in different stages of development. Under viewing in transverse sections, each ovarian tubule was packed with oocytes ranging from the smallest to the largest, in the central lumen. Developing oocytes were in close contact with the follicular cells, whereas some mature oocytes were free in the tubular lumen. Most of the mature oocytes were also adhered to the epithelium cells, whereas some of them were detached from the epithelium and were floated in the lumens of the ovarian tubules. In this study, the gonadal tissue contained all developmental stages of oocytes including protogonia, oogonia, pre-vitellogenic, vitellogenic and mature oocyte. An association of follicular cells to the developing oocytes was only observed during early stages of oogenesis, which few follicular cells were observed in close proximity to protogonia and oogonia. Mature oocytes were characterized by a dramatically largest in diameter and spherical shape. As oocytes increased in diameter, they aggregated in the center of the lumen. Lumen of the mature ovarian tubules were filled with large oocytes, and no follicular cells were associated with the oocytes which underwent middle or late stages of oogenesis (Figure 4.5).

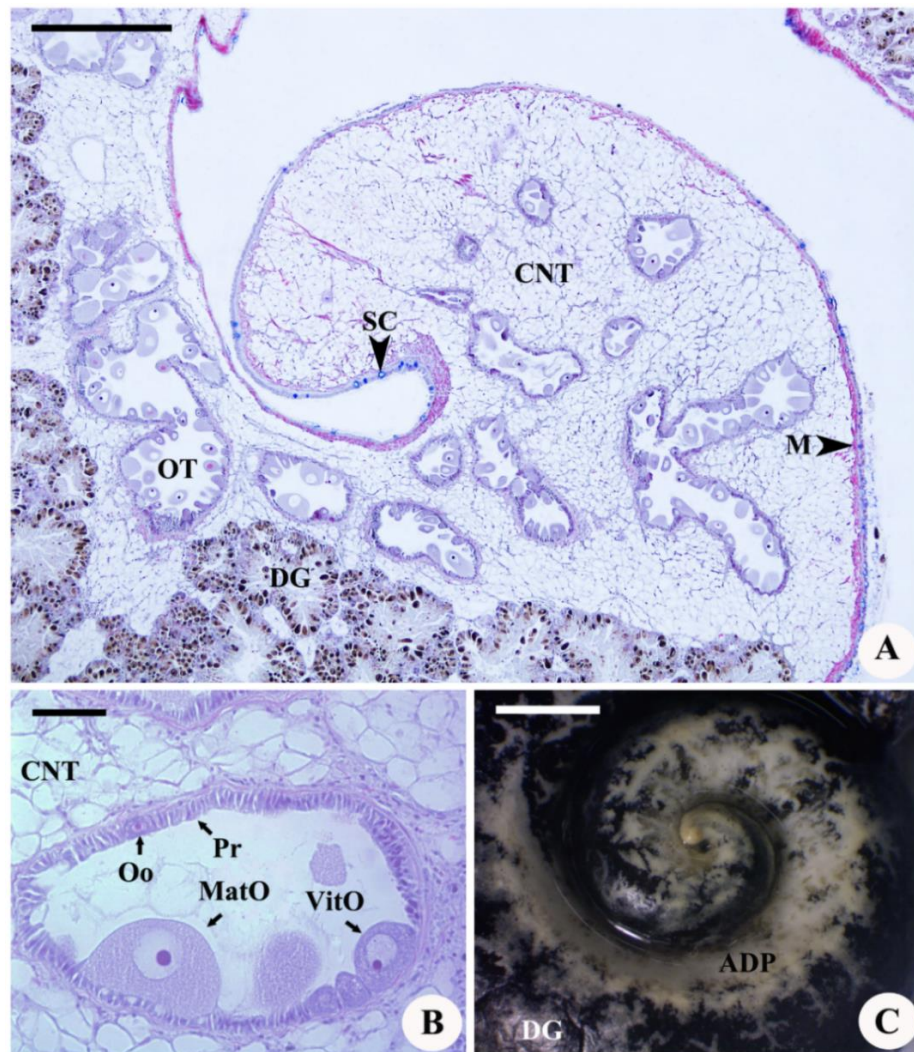


Figure 4.4 Photographs showing cross section of the ovarian tubules of *P. Canaliculata* stained with Masson's Trichrome. **(A)** Showing the ovarian tubules (OT) surrounded by connective tissue (CNT), digestive gland (DG) and muscular tissue (M). The ovarian tubule contained oogonia (Oo), protogonia (Pr), pre-vitellogenic oocytes (PvitO), vitellogenic oocytes (VitO) and mature oocytes (MatO). The secretory cells (SC) were presented outside the digestive gland. **(B)** The lumen of ovarian tubule showed various stages of oocyte. **(C)** The ovarian tubule which was embedded within the digestive gland (DG) and adipose tissue (ADP). Scale bars: A = 2000 μm ; B = 200 μm ; C = 1 cm

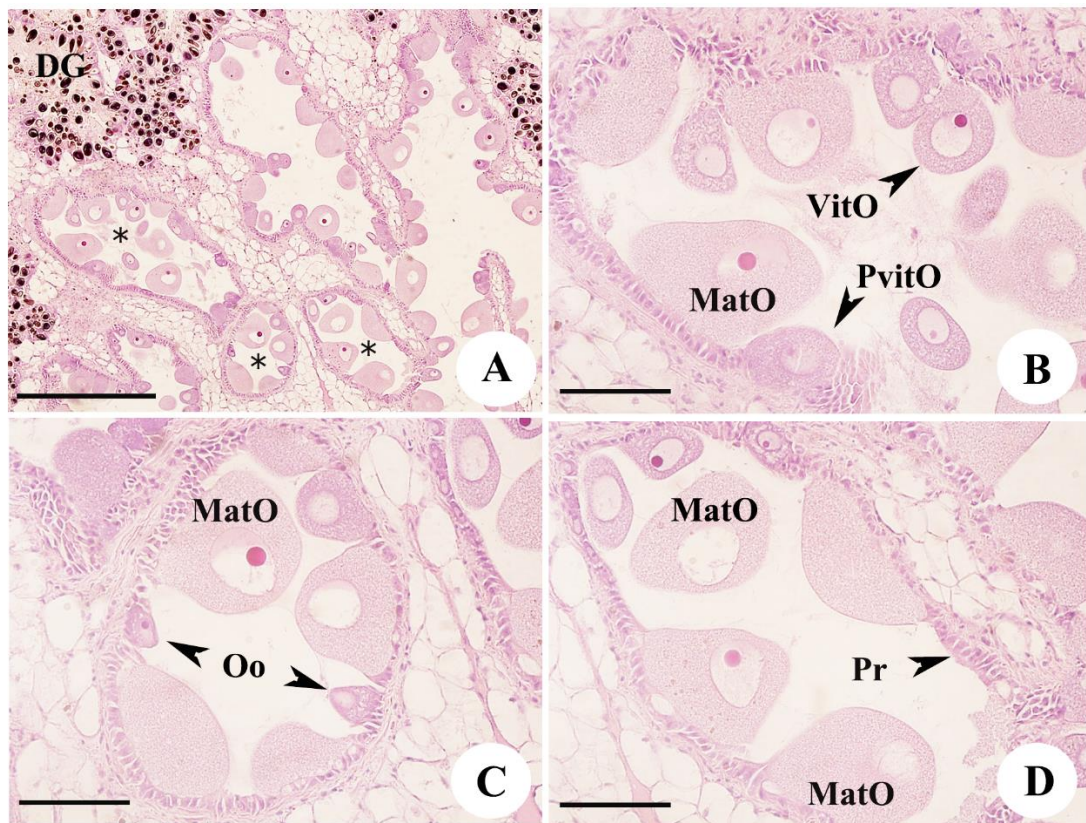


Figure 4.5 Photographs showing ovarian tubules containing difference oocyte stages surrounded by digestive gland (DG). (A-D) Ovarian tubule contained oogonia (Oo), protogonia, pre-vitellogenic oocytes (PvitO), vitellogenic oocytes (VitO) and mature oocytes (MatO). Scale bar, A = 1000 μm , B, C, D = 200 μm .

4.4 Light microscopic study of the oocytes

The gonadal tissue contained the ovarian tubule that surrounded by the connective tissue. The ovarian tubule contained all developmental stages of oocytes including protogonia, oogonia, pre-vitellogenic, vitellogenic and mature stages (Figure 4.6). In addition to an appearance of different stages of oogenesis, oocytes were found in different locations of the ovarian tubule. Protogonia and oogonia resided on the tubular wall, while vitellogenic oocytes were attached only by a stalk to the tubular wall. Mature oocytes were released into the lumen. Protogonia (germ cells) were located along the internal walls of the ovarian tubules. They were columnar in shape. Protogonia had large irregularly shaped nuclei. They were $9.38 \pm 2.13 \mu\text{m}$ in diameter. Oogonia were the smallest cells of the developmental stage of oocytes. Oogonia were presented in the wall of ovarian tubules and arranged in a single row. They were round or oval in shape and $15.12 \pm 2.67 \mu\text{m}$ in diameter. They had basophilic nuclei and lighter basophilic cytoplasm. Pre-vitellogenic oocytes were round or oval cells. The pre-vitellogenic oocytes were characterized by the increase in cell size and the decrease of nucleo-cytoplasmic ratio. Pre-vitellogenic oocytes could reach up to $28 \mu\text{m}$ in diameter with irregular edges. The long axis of the oocyte is generally oriented parallel to the tubular wall. These oocytes had basophilic nuclei and lightly eosinophilic cytoplasm. Their nuclei contained dispersed chromatins and prominent nucleoli. The cytoplasm became larger and no cytoplasmic granules were observed. Vitellogenic oocytes were larger and continued to grow by accumulation of yolk granules. Late vitellogenic oocytes were larger than early vitellogenic oocytes ($1.35 \pm 9.25 \mu\text{m}$) as they accumulated more yolk granules. Oocytes entering the vitellogenesis stage continued to grow while migrating into the acinar lumen by accumulating yolk granules in the

cytoplasm and could reach the diameter of 40 μm . They presented more enlarged cytoplasm which contained small cytoplasmic granules indicating the onset of yolk synthesis. The cytoplasm of vitellogenic oocytes were intensely eosinophilic staining. Vitellogenic oocytes were found in the lumen of acinus. The point of attachment to the acinal wall was visible and was referred as a stalk. Mature oocytes were located in the center of the acinus lumen, but still connected to the wall of acini by a stalk. The cytoplasm was extremely eosinophilic. Mature oocytes were characterized by a remarkable increase in cell size, more than three times compared to the pre-vitellogenic oocytes. Mature oocytes could reach up to 70 μm in diameter. They were the largest cells and were more elongated than vitellogenic oocytes (Table 1).

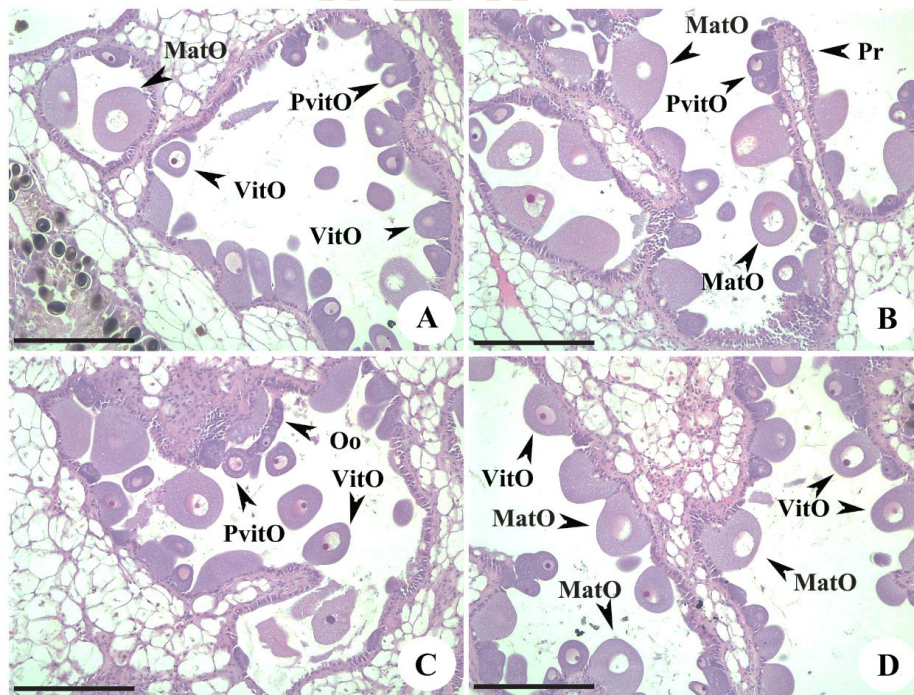


Figure 4.6 Photographs showing transverse sections through the ovarian tubules. (A-D) The ovarian tubules contained all developmental stages of oocyte including protogonia (Pr), oogonia (Oo), pre-vitellogenic (PvitO), vitellogenic (VitO) and mature oocyte stages (MatO). Scale bar = 500 μm .

Table 1 Sizes and shapes of oocytes of the golden apple snail.

Stages of oocyte	Shape of oocyte	Diameter of oocyte (μm)
Protogonia	Columnar	$9.38 \pm 2.13^{\text{a}}$
Oogonia	Round/Oval	$15.12 \pm 2.67^{\text{a}}$
Pre-vitellogenic oocyte	Oval	$28.87 \pm 4.39^{\text{a}}$
Vitellogenic oocyte	Oval	$51.35 \pm 9.25^{\text{b}}$
Mature oocyte	Oval	$70.34 \pm 9.92^{\text{c}}$

Values (mean \pm SD) with different superscripts are significantly different ($P < 0.05$).

4.5 Scanning electron microscopic study of oocytes

Stages of oogenesis *P. Canaliculata* have been investigated firstly by scanning electron microscope in the present study. According to external morphology analyses, the oocytes observed in ovarian tubules developed through five basic stages until the completion of oogenesis. These were the stages that developed during oogenesis (protogonia, oogonia, pre-vitellogenic, vitellogenic and mature oocytes). At the beginning of their development, protogonia and oogonia showed round in shape and smooth surface. The oocyte became progressively oval-shaped. They were found individually or a cluster on the tubular walls (Figure 4.7A). Pre-vitellogenic oocytes were small and oval in shape, commonly they occurred near an oogonium and vitellogenic oocyte (Figure 4.7B). At this time, in particular, follicular cells were attached to each pre-vitellogenic oocyte (Figure 4.7C). As the further development of pre-vitellogenic oocytes proceeded, the oocytes developed into vitellogenic oocytes. At

this stage, the oocytes continued to grow and differentiated. Vitellogenic oocytes were oval in shape and larger than pre-vitellogenic oocytes (Figure 4.7D). However, at this time, follicular cells that were attached to the oocytes gradually lost their intimate association with the surface of the oocytes where the follicular cells had withdrawn. In this stage of oogenesis, the follicular cells detached completely from the oocytes. Later, the oocytes detach from the tubular wall and as a result, the unbound oocytes become spherical. The present study did not find the post-vitellogenic oocytes, because mature oocytes were released into the lumen. So, they were washed away during tissue preparation.

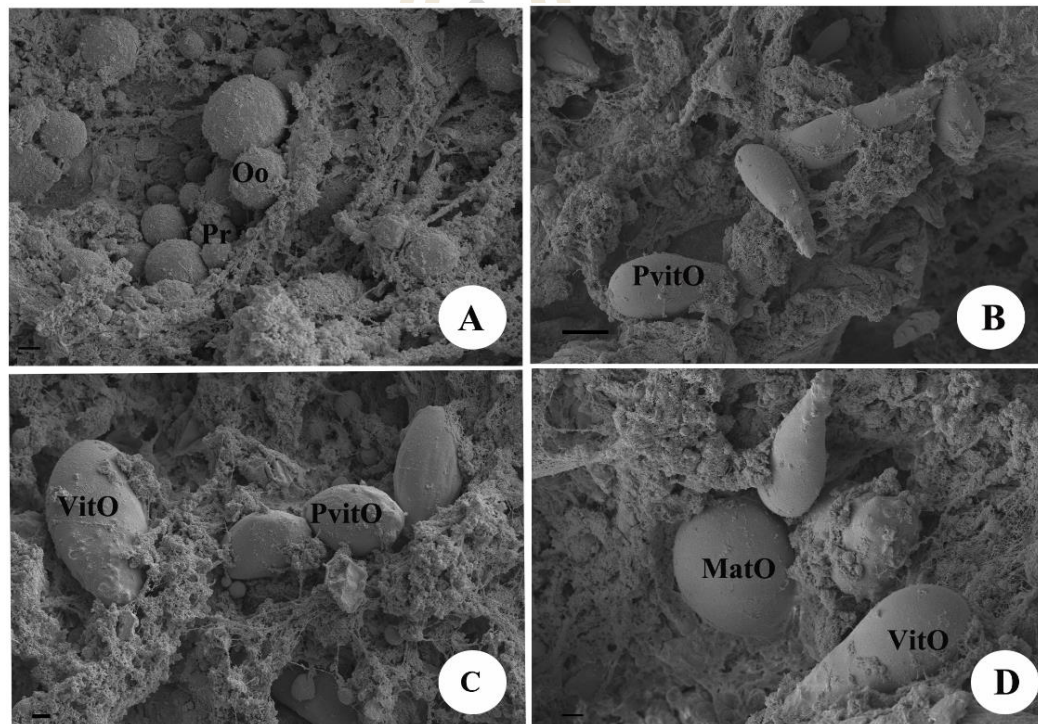


Figure 4.7 Photographs showing scanning electron microscopy of the various stages of development oocytes within ovarian tubules. (A-D) The ovarian tubules contained developmental difference stages including protogonia (Pr), oogonia (Oo), pre-vitellogenic (PvitO), vitellogenic (VitO) and mature stages (MatO). Scale bars: A = 1 μm ; B = 10 μm ; C = 2 μm ; D = 3 μm .

4.6 Transmission electron microscopic study of oocytes

In semithin sections, oogenesis of *P. Canaliculi* appeared to be asynchronous. Each ovarian tubule contained the difference stages of oocytes development. In addition, each ovarian tubule contained mostly early stage of oocytes and a few vitellogenic oocytes were observed. The smallest oocytes (oogonia) was round in shape and located within the wall of the tubular in the connective tissue space. They contained small nuclei and a single nucleolus within a nucleus. As oocyte volume increased, the nucleolus expanded and vitellogenesis began when the oocytes increased in diameter followed by the initial appearance of lipid droplets. Yolk granules were first appeared when a portion of the oocytes came into direct contact with the trabecular lumen following the partial withdrawal of follicular cells.

Protogonia

Protogonia were located along the internal walls of the ovarian tubules. They were columnar or low columnar in shape and $9.38 \pm 2.13 \mu\text{m}$ in diameter. (mean \pm SD). They were characterized by a high nucleocytoplasmic ratio (Figure 4.8F). The round nuclei were large. Lipid droplets were frequently presented in the cytoplasm. One or two nucleoli could be observed. The cytoplasm contained numerous small spherical mitochondria and Golgi apparatus. When protogonia entered mitosis, they were elongated and cytoplasmic organelles were the same as oogonia.

Oogonia

Oogonia were presented in the wall of ovarian tubules. They often had large nuclei in which chromatin were reticular and marginal. The same cytoplasmic organelles were identified as protogonia (Figure 4.8B). At the beginning of their development, oogonia were oval in shape and characterized by a high nucleocytoplasmic ratio. Because they contained only a small numbers of mitochondria and no microvilli, they could be easily distinguished from the oocytes in more advanced stages (Figure 4.8C). Oogonia diameters were $15.12 \pm 2.67 \mu\text{m}$ (mean \pm SD). Some membrane-bound cortical granules, mitochondria and Golgi body were visible. The nuclei of oogonia contained less condensed chromatin materials scattered in the nucleoplasm. Nucleoli were not conspicuous at any stage of oogonia. However, in this stage, the activity of vitellogenic characteristics in the pre-vitellogenic oocyte was weak, because yolk materials were not found in the cytoplasm.

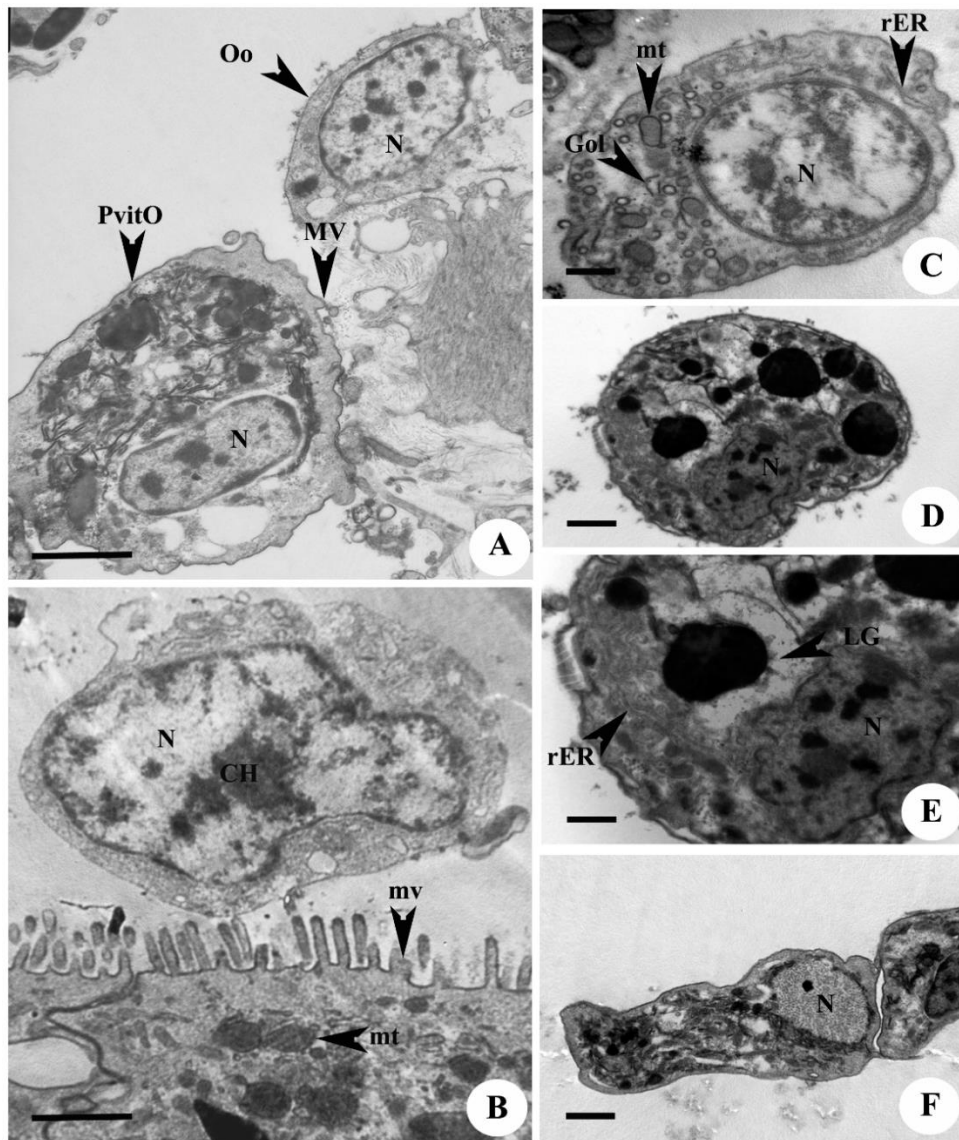


Figure 4.8 Photographs showing transmission electron micrograph of pre-vitellogenic oocytes (PvitO) and oogonia (Oo) of *P. Canaliculi*. (A and C) Ultrastructure of ovarian tubule lumen showing the arrangement of microvilli (MV) and oogonia cells along the connective tissue. (B and C) Fine structure of the oogonium with a well-defined nucleus (N) containing chromatin bodies (CH) and a nuclear membrane; cytoplasm contains numerous ribosomes, Golgi bodies (Gol), rough endoplasmic reticulum (rER) and mitochondria (mt). (D and E) Pre-vitellogenic oocyte with an enlarged nucleus, and lipid granule (LG) in the cytoplasm. Scale bar: A-E = 1 μ m; F= 2 μ m.

Pre-vitellogenic oocytes

Pre-vitellogenic oocytes were oval in shape. The diameter of the oocytes reached $28.87 \pm 4.39 \mu\text{m}$ (mean \pm SD). The nuclei elongated and the double nuclear membrane indented. The volume of cytoplasm increased, but it contained few organelles. Mitochondria were numerous and scattered in the cytoplasm. A prominent electron dense nucleoli were discernible in the nuclei of the oocytes at this stage. The nuclear membrane was well-defined and numerous mitochondria and rough endoplasmic reticulum were visible under TEM. The cytoplasm of developing oocytes contained many ribosomes, mitochondria, Golgi bodies, as well as rough endoplasmic reticulum (rER) indicating active synthesis of protein (Figure 4.8E).

Vitellogenic oocytes

Early vitellogenic oocytes contained lipid droplets and often circumscribed by rER cisternae. Golgi bodies appeared predominately in the cortical region of the ooplasm and secreted electron-dense, cortical granule-like organelles that gradually assume a dumbbell configuration. This stage indicated the onset of yolk synthesis (vitellogenesis). Less electron dense, round lipid droplets appeared in the cytoplasm of early vitellogenic oocytes. Several cell organelles presented in the cytoplasm of the oocytes, which might be associated with the formation of yolk components. The nuclei of early vitellogenic oocytes encompassed a clear round space. Large numbers of ribosome-studded, as well as smooth, membranebounded vesicles were also presented in the cytoplasm of early vitellogenic oocytes.

Late vitellogenic oocytes were larger ($51.35 \pm 9.25 \mu\text{m}$ in diameter) and continued to grow by an accumulation of yolk granules. At this stage, two types of yolk granules were distinguished, proteinaceous yolk granules and lipid yolk granules. The

first was membrane-bound granules, while the latter was membrane-lacking granules. As vitellogenesis proceeded, the oocytes bulged into the ovarian lumen and become laden with lipid droplets and yolk granules. Cytoplasm of late vitellogenic oocytes was uniformly filled with various quantities of darkly stained protein yolk granules and lipid droplets. Small granular materials were also seen in the cytoplasm. The nucleus occupied a very large volume of the cytoplasm and migrated to the free end of the oocyte. The nucleoli were a dark, round, electron-dense body in the nucleoplasm. Numerous mitochondria were also presents in the cytoplasm. As vitellogenesis progressed, these membrane specializations developed considerably, often encompassing several vesicles and yolk materials. An exogenous yolk precursor was produced through the process of heterosynthetic vitellogenesis. They were transferred into proteinaceous yolk granules. A number of yolk precursors, proteinaceous yolk granules, immature yolk granules lipid droplets, and yolk precursors appeared in the cytoplasm of the late vitellogenic oocyte. The ooplasm was largely devoid of organelles, except for lipid droplets and two types of nuage-like material, one resembling a nucleolus. Numerous lipid droplets and cortical granules were also seen, together with small mitochondria and rather large phagosomal vesicles containing partly-lysed material. A nucleolus-like body ('nuage') was seen in the cytoplasm (Figure 4.9B).

Mature oocytes

Mature oocytes of *P.canaliculata* were $70.34 \pm 9.92 \mu\text{m}$ in diameter. In this stage, the nucleolus appeared as a compact mass in close contact with the nuclear envelope, occasionally forming a nuclear ring. Then, it migrated towards a more central position in the germinal vesicle, and its associated chromatin scattered progressively. The nucleus was very large and less electron dense with a dark nucleolus (Figure 4.10 A). The nuclear envelope was very twisted and the nucleolus was homogeneous. It could be in close contact with the nuclear envelope which presented abundant pores identified in tangential section. The cytoplasm was extremely eosinophilic and TEM results showed that there were numerous yolk and lipid granules. Mitochondria and rough endoplasmic reticulum appeared through the ooplasm. Mature oocytes had highly dispersed chromatin and a large nucleolus, nuclear pores, cytoplasmic nucleolus-like bodies (nuages). Numerous lipid droplets and small oval or elongated mitochondria were also seen, as well as numerous membrane-bound, electron-dense granules. Some oval yolk bodies containing a single large protein crystalloid were also seen.

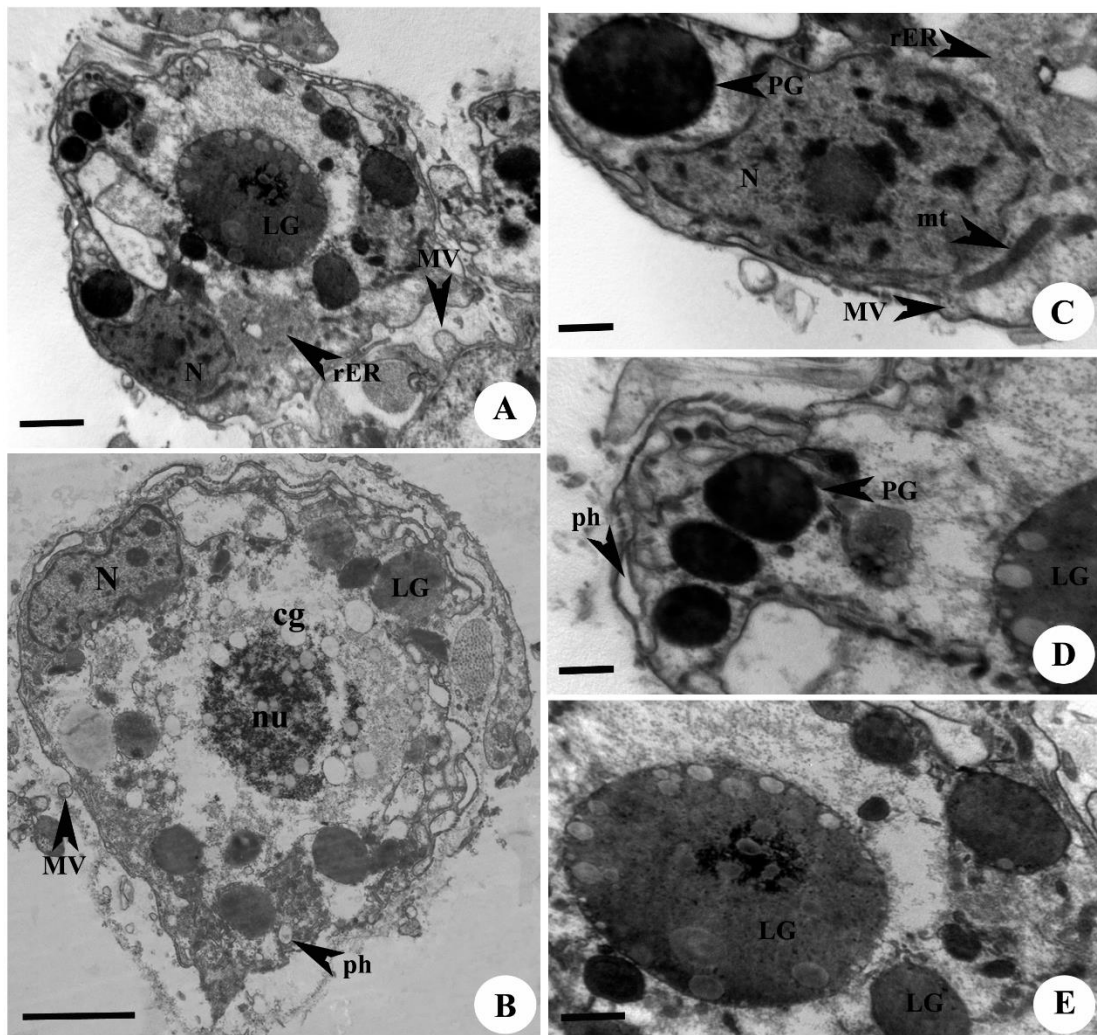


Figure 4.9 Transmission electron micrographs of difference stages oocytes. **(A)** Cytoplasm of Pre-vitellogenic oocyte initiating the synthesis of lipid granules (LG), numerous mitochondria (mt) and rough endoplasmic reticulum (rER) containing ribosomes. **(B)** Vitellogenic oocyte with both lipid granules (LG) and protein granules (PG), **(C)** Pre-vitellogenic oocyte encompassing lipid yolk components made up of rough endoplasmic reticulum (rER) containing ribosomes. **(D and E)** Cytoplasm of pre-vitellogenic oocyte oocyte with its fundamental components: lipid granules (LG), protein granules (PG) Scale bar: A = 2 μm ; B = 1 μm ; C, D = 0.5 μm ; V and E = 1 μm .

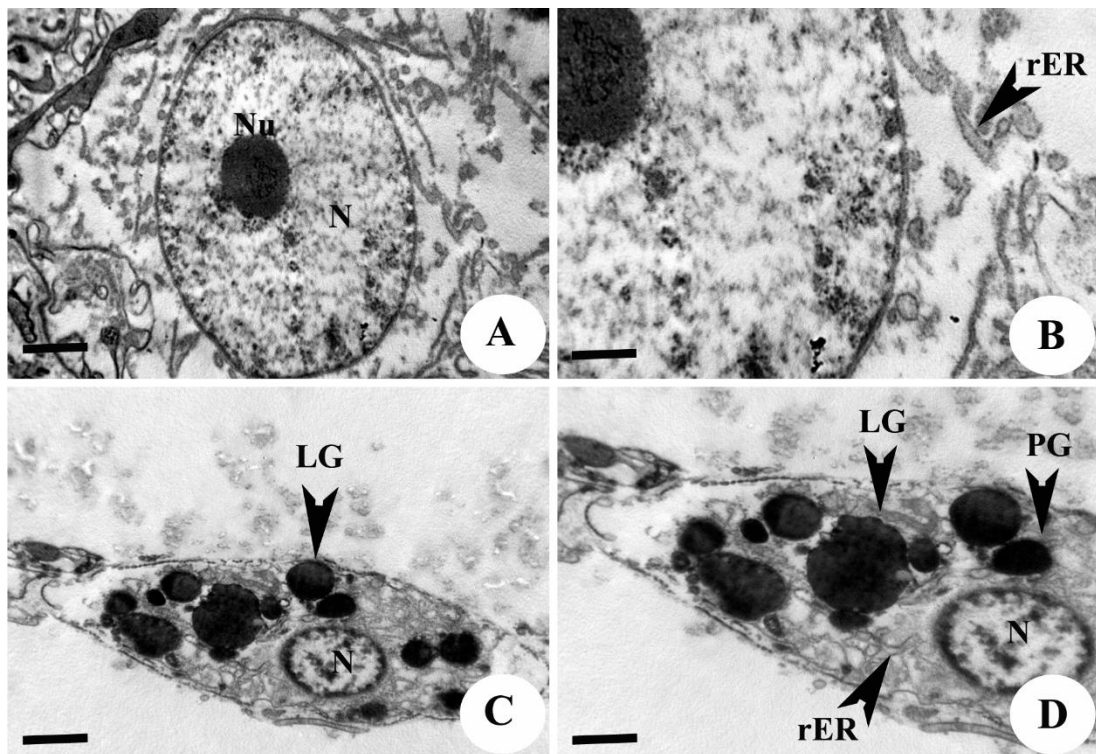


Figure 4.10 (A-B) Transmission electron micrograph of mature oocyte encompassing lipid granules components made up of rough endoplasmic reticulum (rER) containing ribosomes. (C-D) Cytoplasm of pre-vitellogenic oocyte with its fundamental components: lipid granules (LG), protein granules (PG), mitochondria and endoplasmic reticulum (rER). Abbreviation: NU, Nucleolus; N, Nucleus. Scale bar: A and C = 2 μm ; B and D = 100 μm .

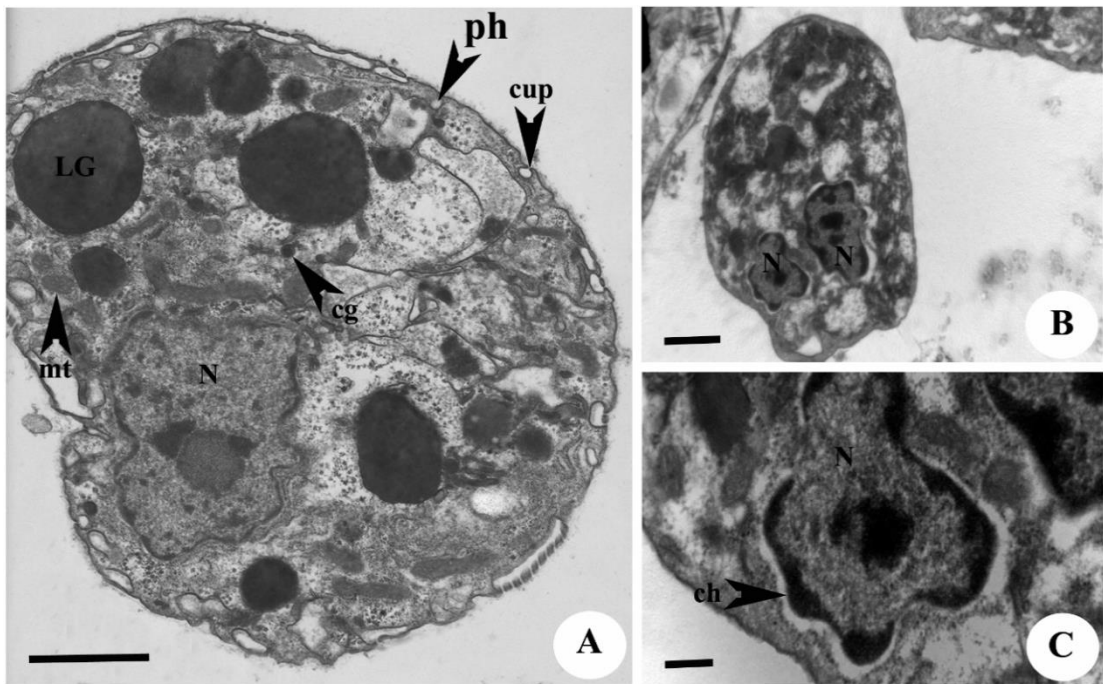
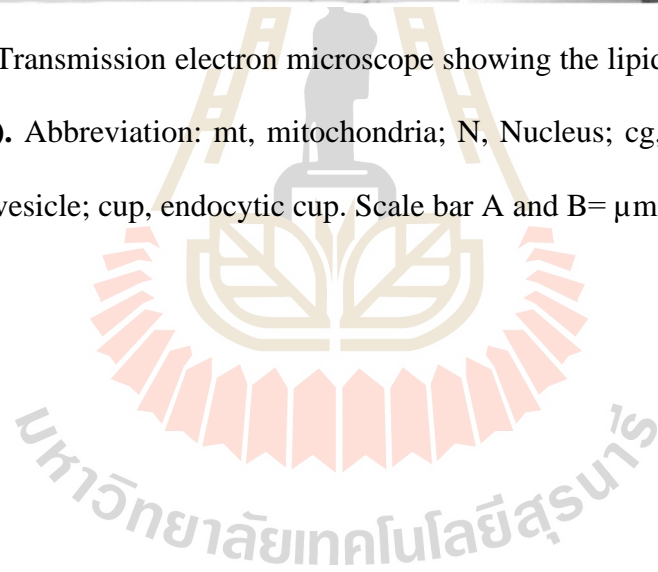


Figure 4.11 Transmission electron microscope showing the lipid granules (LG) in the oocyte (A-C). Abbreviation: mt, mitochondria; N, Nucleus; cg, cortical granule; ph, phagosomal vesicle; cup, endocytic cup. Scale bar A and B= μm ; C= 0.2 μm .



4.7 Presence of yolk granules in the oocytes

Staining with Sudan Black indicated the lipid accumulation in the cytoplasm of the oocyte. Lipid droplets were homogenously distributed throughout the cytoplasm of oocyte. The ovarian tubules presented signs of reactivation, as lipids showed an increasing tendency in respect to stages as well as numbers and sizes of oocytes. The accumulation of lipid increased from immature throughout mature oocytes. The pre-vitellogenic oocyte contained dense granules of different sizes which aggregated in the cytoplasm. The precursor yolk granules also arised at this stage. At the end of the pre-vitellogenic stage, the oocytes enter vitellogenesis. At the final stage of pre-vitellogenic oocyte, the cytoplasm contained numerous lipid droplets (Figure 4.12). They presented more volume of cytoplasm which contained small cytoplasmic granules indicating the onset of yolk synthesis. vitellogenic oocytes were larger than pre- vitellogenic oocytes as they accumulated more yolk granules. Mature oocytes were the largest cells and were more elongated than vitellogenic oocytes. They contained the most numerous yolk granules in the cytoplasm (Figure 4.12F). The number of large lipid granule were counted. Sizes of the lipid yolks ranged from 2.38 to 3.88 μm were counted and analyzed using a computerized image analysis program (Cell^D software). The large lipid granules were found in all stages of the oocytes, except the oogonia (Figure 4.13). The lowest number of the large lipid granules was found in pre-vitellogenic oocyte (15 ± 2.06). The cytoplasm also contained smaller lipid droplets, which were distributed randomly at the periphery of the cytoplasm. The numebers of the large lipid granules gradually increased in the vitellogenic oocyte (29.2 ± 11.20). The highest number of the large lipid granules was found in the cytoplasm of the mature oocyte 117.5 ± 19.98).

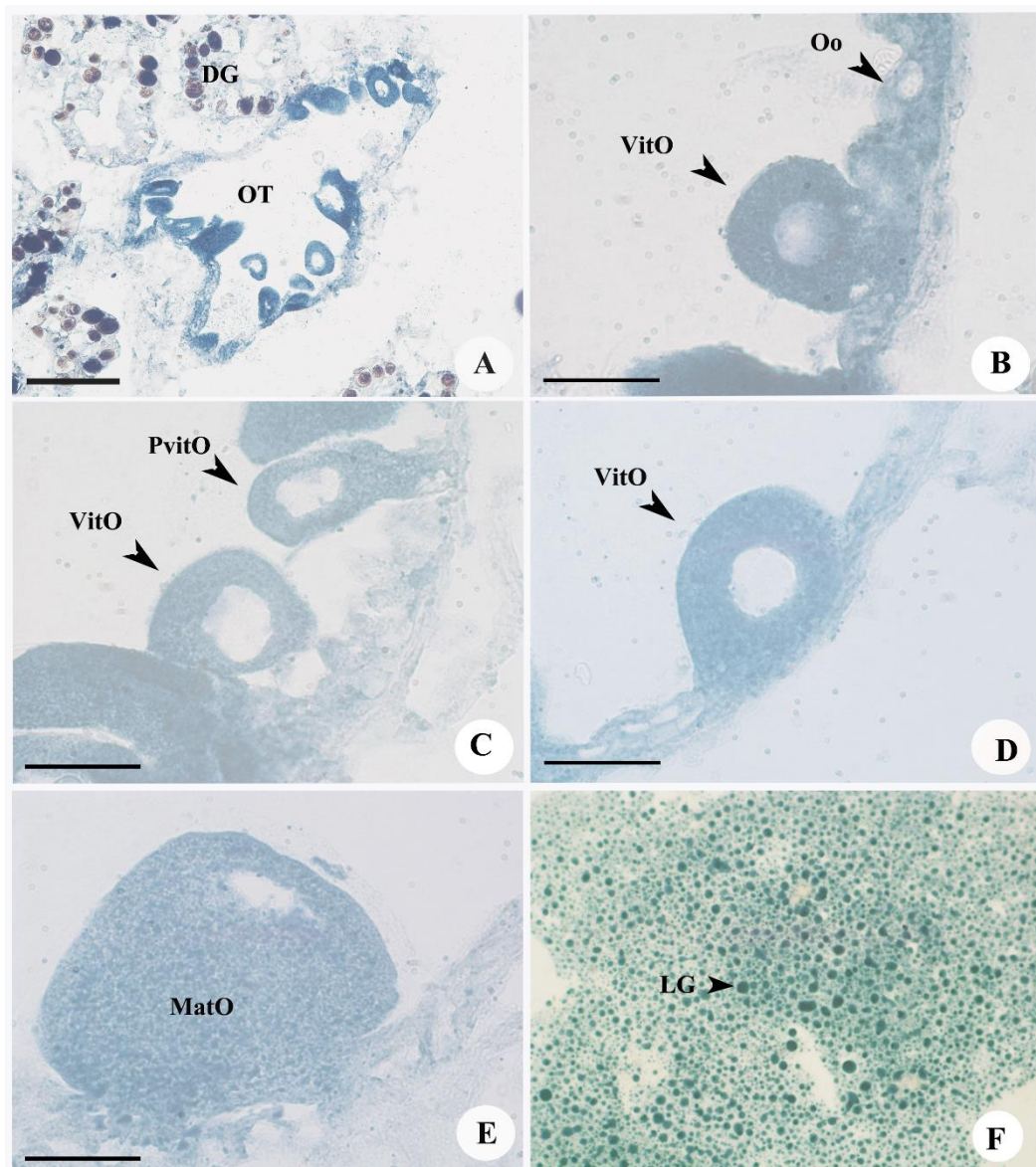


Figure 4.12 Light micrographs of Sudan black stained sections of ovarian tubules. (A) Ovarian tubule (OT) contained few difference oocytes. (B-E) Oogonia (Oo), pre-vitellogenic (PvitO), vitellogenic oocytes (VitO) and Mature oocytes (MatO). (F) Mature oocytes contained numerous lipid granules (LG). Scale bar, A=500 μm ; B- E =200 μm ; F= 500 μm .

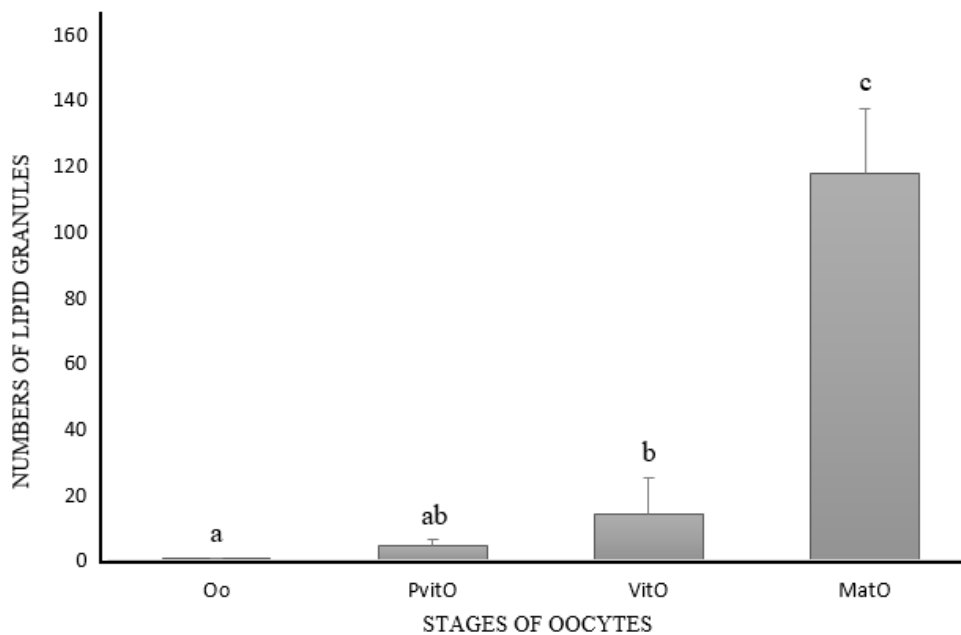


Figure 4.13 Numbers of lipid granules in different oocyte stages. Different letters indicate significant differences according to the one-way ANOVA followed by a Turkey post hoc range tests ($P < 0.05$).

4.8 Biochemistry analysis during oocyte development

In all oocyte stages, the strongest total absorbance was shown in the nuclei area (pink spectrum), followed by the ooplasm adjacent to the nuclei (red color) (Figure 4.14). The least total absorbance was observed at the periphery of the ooplasm (blue color). The major biochemical components in the oocytes were protein amide I and amide II, followed by nucleic acid and then carbohydrate (Figure 4.15). The average spectrum of the amide I showed a greater total absorbance when compared to the other components in all oocyte stages. The pre-vitellogenic oocytes contained the lowest spectral peaks of amide I and amide II (Figure 4.16). These peaks increased in the vitellogenic oocytes. The mature oocytes contained lower amide I and amide II spectral

peaks compared to the vitellogenic oocytes, but still higher than that of the pre-vitellogenic oocytes. The spectral peak of carbohydrate was highest in the pre-vitellogenic oocytes, but slightly decreased in the vitellogenic oocytes. The mature oocytes contained the lowest peak of carbohydrate. In contrast, spectral peak of nucleic acid was highest in the vitellogenic oocytes than in the pre-vitellogenic oocytes. However, the peak was lowest in the mature oocytes.

Second derivative spectra between 1,700-1620 cm^{-1} (amide I) was derived from each stage of oocytes (Figure 4.17). The 1656 and 1651 cm^{-1} spectra were assigned as α -helix protein structure and 1640 cm^{-1} spectrum was assigned as β -sheet protein structure. The band of α -helix protein structure in the pre-vitellogenic oocyte was at 1651 cm^{-1} which was different from those of the vitellogenic and mature oocytes (1656 cm^{-1}).

Curve-fitting on amide I spectrum showed that amide I structures were divided into 1) α -helix, 2) β -sheet, 3) β turn and 4) antiparallel structures (Figure 4.18). All oocyte stages contained the highest level of α -helix and the lowest level of antiparallel protein structures. During the process of the oocyte maturation, the absorbance ratio between α -helix and β -sheet bands gradually increased from the previtellogenic, vitellogenic, to mature oocytes. The previtellogenic oocytes exhibited stronger absorbance units of β -sheet protein than either the vitellogenic or mature oocytes.

PCA was analyzed from the spectral region between 1800-900 cm^{-1} of oocyte stages. The PCA showed distinctly separation into three clusters of oocyte stages. The

separation score plot observed in the PC1, PC2 and PC3 showed an accuracy of 58% (Figure 4.19). The score plots of the previtellogenic oocytes were clustered at the opposite side to the score plots of the mature oocytes. Score plots of the vitellogenic oocyte clustered between the previtellogenic and mature oocytes. Overlap score plots were identified in the clusters of the previtellogenic / vitellogenic oocytes and the vitellogenic/mature oocytes.

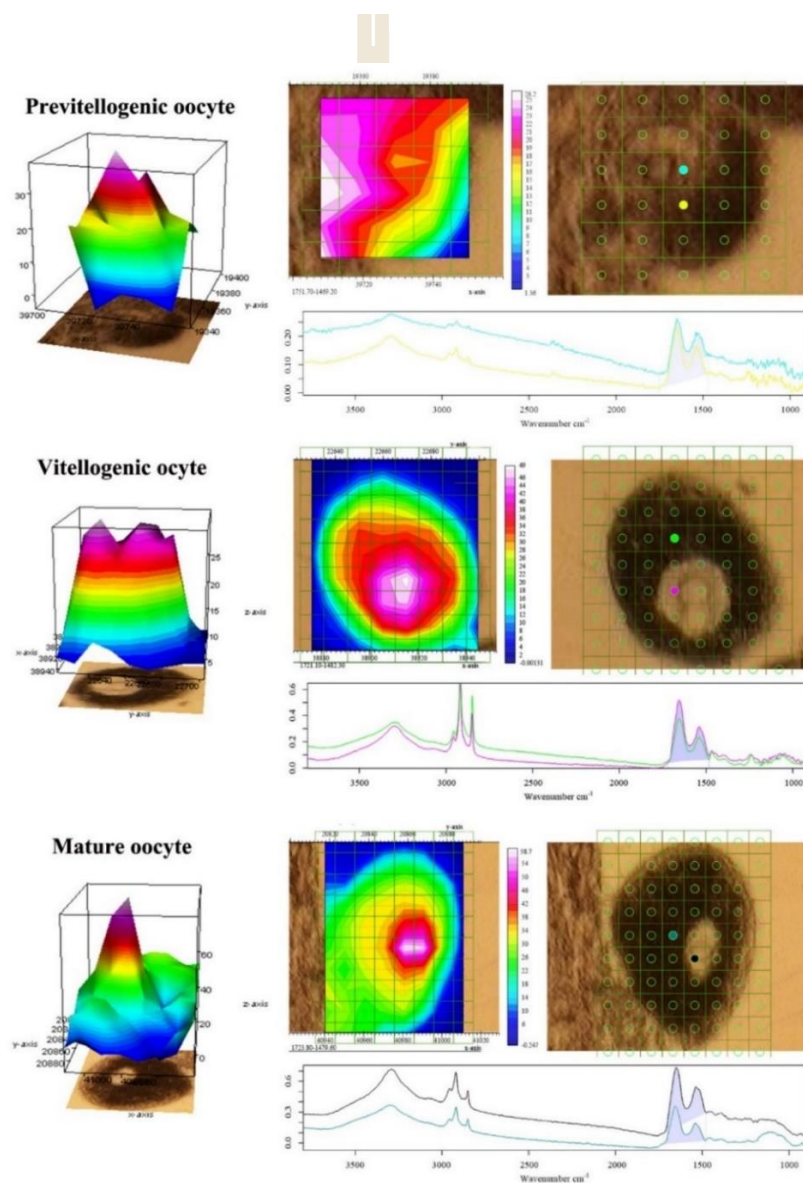


Figure 4.14 Functional group area maps obtained under the spectral regions ranged from 1,700-1,500 cm⁻¹ of pre-vitellogenic, vitellogenic, and mature oocytes.

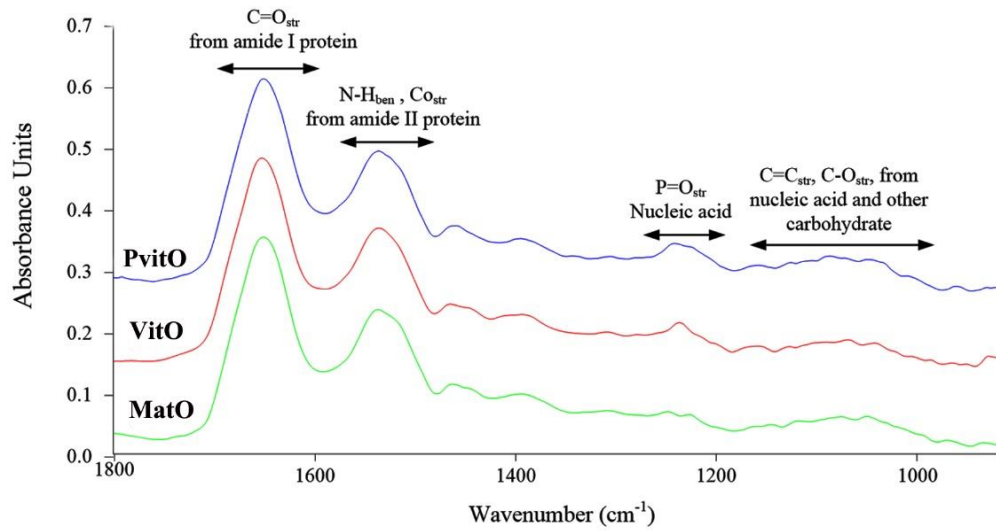


Figure 4.15 Infrared spectra from previtellogenic oocyte (PvitO), vitellogenic oocyte (VitO), and mature oocyte (MatO).

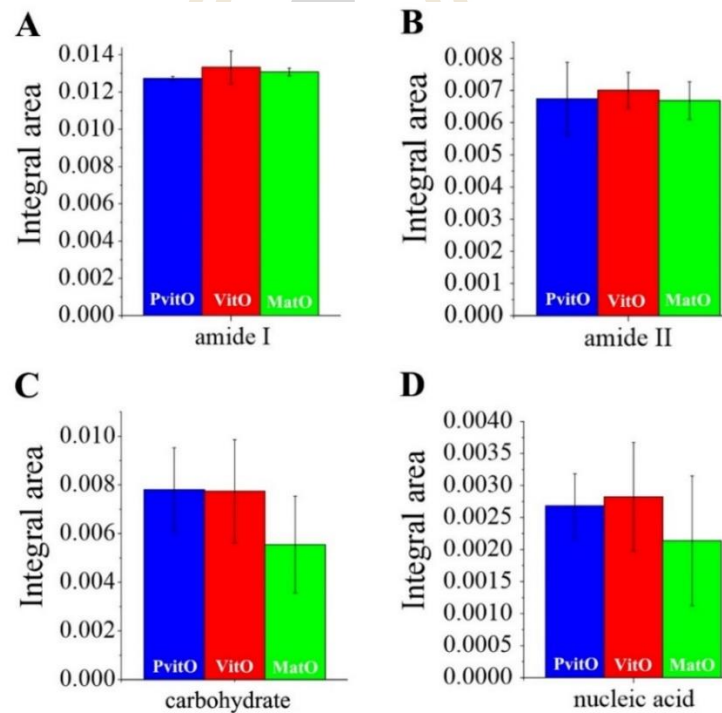


Figure 4.16 Average original infrared spectra of amide I, amide II, carbohydrate, and nucleic acid extracted from pre-vitellogenic oocyte (PvitO), vitellogenic oocyte (VitO), and mature oocyte (MatO).

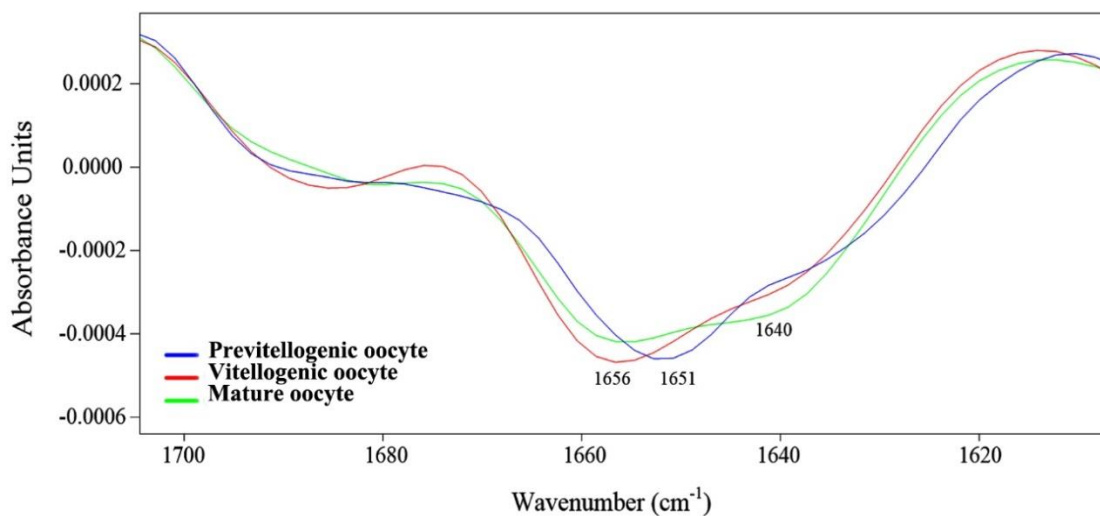


Figure 4.17 Second derivative spectra between 1,700-1620 cm^{-1} (amide I) from pre-vitellogenic oocyte (PvitO), vitellogenic oocyte (VitO), and mature oocyte (MatO).

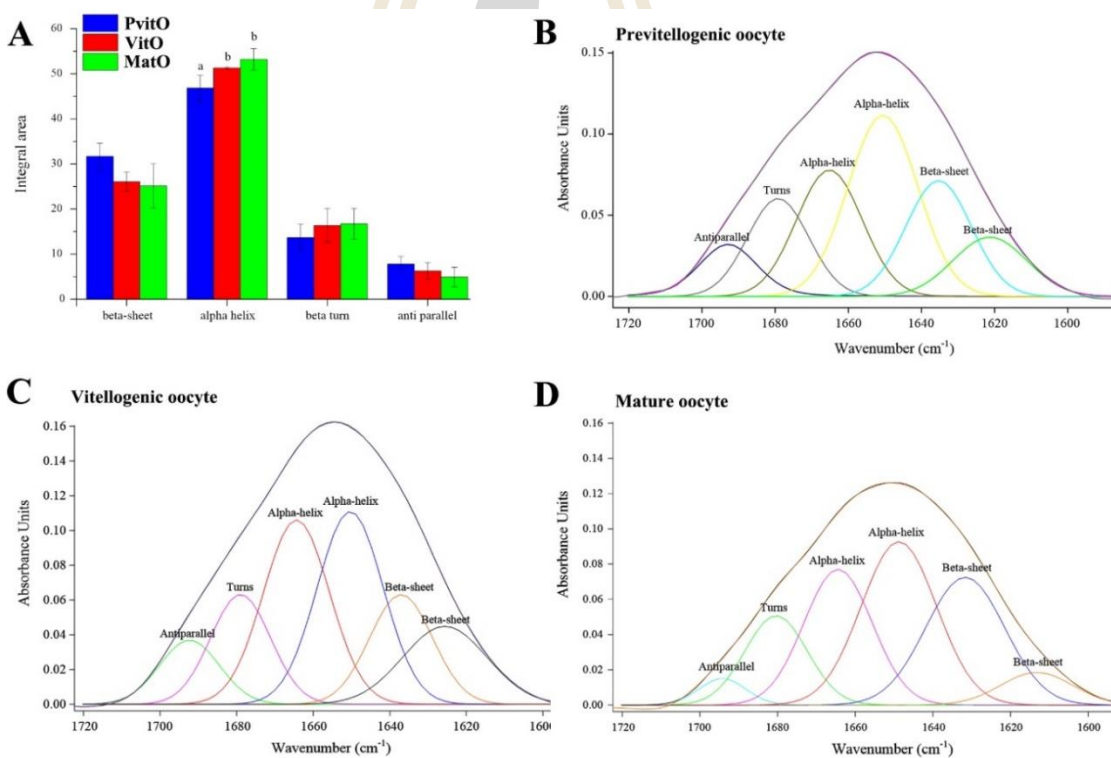


Figure 4.18 Curve-fitting on amide I from pre-vitellogenic oocyte (PvitO), vitellogenic oocyte (VitO), and mature oocyte (MatO).

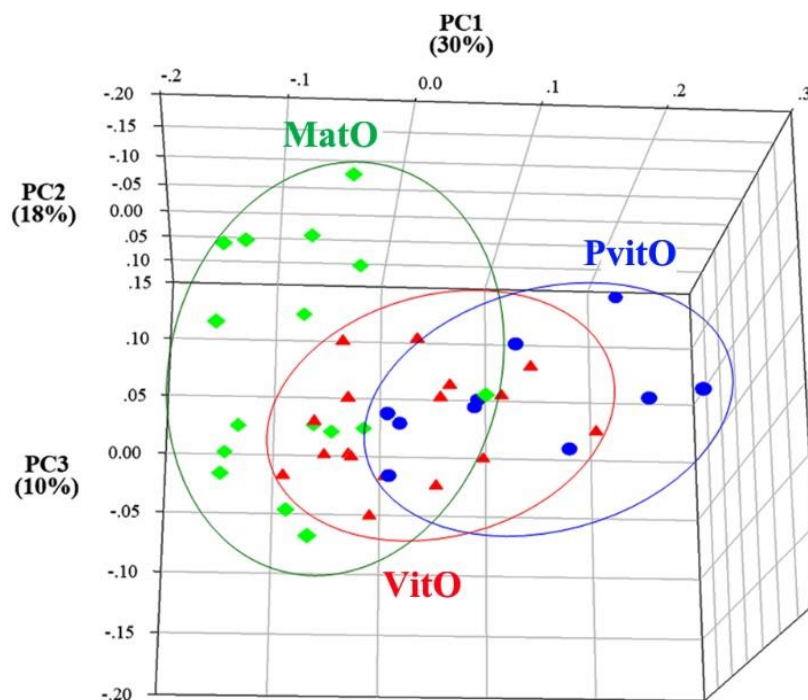


Figure 4.19 PCA analyzed from the spectra region between 1800-900 cm^{-1} of previtellogenic oocyte (PvitO), vitellogenic oocyte (VitO), and mature oocyte (MatO).

4.9 The relationship between ovarian tubule stages and oocyte stages

The ovarian tubules were classified into four continuous stages (stage I-IV) which occurred consecutively. The gonadal tissue was widely situated on the surface of the digestive gland located in the rear of the spiral meat part of the shell. As the gonadal maturation proceeded, the gonad was thickly distributed on the digestive gland. The mature gonadal tissue was dark yellow in color. However, after spawning, the gonadal tissue was pale yellow in color. Based on changing of the sizes and color of the gonadal tissue, the ovarian cycle was classified into four stages: stage I (spent), II (proliferative), III (premature) and IV (mature), respectively. Each part of ovarian tubule contained

various stages of oocytes, which indicating that the ovarian tubule developed asynchronously (Figure 4.20). After spawning, the ovarian cycle at day 0 was in stage I (spent stage). Histologically, the ovarian tubules contained mostly vitellogenic oocytes (67 ± 7.93) which were significantly higher than other oocyte stages. The ovarian cycle at day 5 was in stage II (proliferative stage) and still contained mostly vitellogenic oocytes (53 ± 7.34). However pre-vitellogenic oocytes (24.66 ± 6.84) occupied at the periphery of the ovarian tubules. The ovarian cycle at day 10 and 15 were in stage III (premature stage). In this stage, the ovarian tubules contained mostly pre-vitellogenic oocytes (51.66 ± 7.57 and 47.33 ± 4.93 at day 10 and 15, respectively) and vitellogenic oocytes (42 ± 2.64 and 43.33 ± 5.03 at day 10 and 15, respectively). No significant difference between the numbers of the pre-vitellogenic oocytes and the vitellogenic oocytes. In contrast, the numbers of these oocyte stages were significantly higher than that of oogonia (16 ± 3 and 25.66 ± 2.08 at day 10 and 15, respectively) and mature oocytes (24.33 ± 4.04 and 30.66 ± 3.38 at day 10 and 15, respectively). The ovarian cycle at day 20 was in stage IV (mature stage) and the ovarian tubules contained pre-vitellogenic oocytes (62 ± 15.87), vitellogenic oocytes (74.33 ± 10.00) and mature oocytes (17.33 ± 4.50). These oocytes were significantly higher in numbers more than that of oogonia (18.00 ± 1.00). Finally, the ovarian cycle at day 25 was also in stage IV (mature stage) and the ovarian tubules contained mostly pre-vitellogenic oocytes (67.66 ± 0.57) and vitellogenic oocytes (78.00 ± 7.54). Interestingly, mature oocytes decreased in number (10.66 ± 1.54) which was significantly lower when compared to other oocyte stages.

The percentages of oocyte stages housed in the ovarian tubules were shown in Figure 4.21. Stage I ovarian tubule (day 0) contained low percentages of the oogonia,

pre-vitellogenic and mature oocytes ($18.86\pm 11.44\%$, $20.33\pm 11.44\%$ and $18.65\pm 11.44\%$ respectively). However, the highest percentage was observed from the vitellogenic oocytes ($42.13\pm 11.44\%$) which was significantly higher than those of the oogonia, pre-vitellogenic, and mature oocytes. Stage II ovarian tubule (day 5) consisted mostly of the vitellogenic oocytes ($36.21\pm 8.64\%$) and the rest were oogonia ($19.72\pm 8.64\%$), pre-vitellogenic oocytes ($16.85\pm 8.64\%$), and mature oocytes ($27.10\pm 8.64\%$). The percentage of the vitellogenic oocytes was significantly higher than those of the oogonia, pre-vitellogenic and mature oocytes. Stage III ovarian tubule (day 10 and 15) contained high percentages of the pre-vitellogenic oocytes ($38.55\pm 12.12\%$ and $32.19\pm 6.97\%$ at to 10 and 15, respectively), and the vitellogenic oocytes ($31.31\pm 12.12\%$ and $29.47\pm 6.97\%$ at day 10 and 15, respectively). These percentages were significant higher than those of the oogonia ($11.94\pm 12.12\%$ and $17.46\pm 6.97\%$ at day 10 and 15, respectively), and mature oocytes ($18.15\pm 12.12\%$ and $20.86\pm 6.97\%$ at day 10 and 15, respectively). Stage IV ovarian tubule (day 20 and 25) composed of $10.48\pm 17.23\%$ and $9.10\pm 20.22\%$ of oogonia at day 20 and 25, respectively. The percentages of the pre-vitellogenic oocytes were $36.11\pm 17.23\%$ and $39.34\pm 20.22\%$ at day 20 and 25, respectively. The percentages of the vitellogenic oocytes were highest in this stage of the ovarian tubule ($43.30\pm 17.23\%$ and $45.34\pm 20.22\%$ at day 20 and day 25, respectively). However, the percentages of the mature oocytes dropped to $10.09\pm 17.23\%$ and $6.20\pm 20.22\%$ at day 20 and 25, respectively (Figure 4.21).

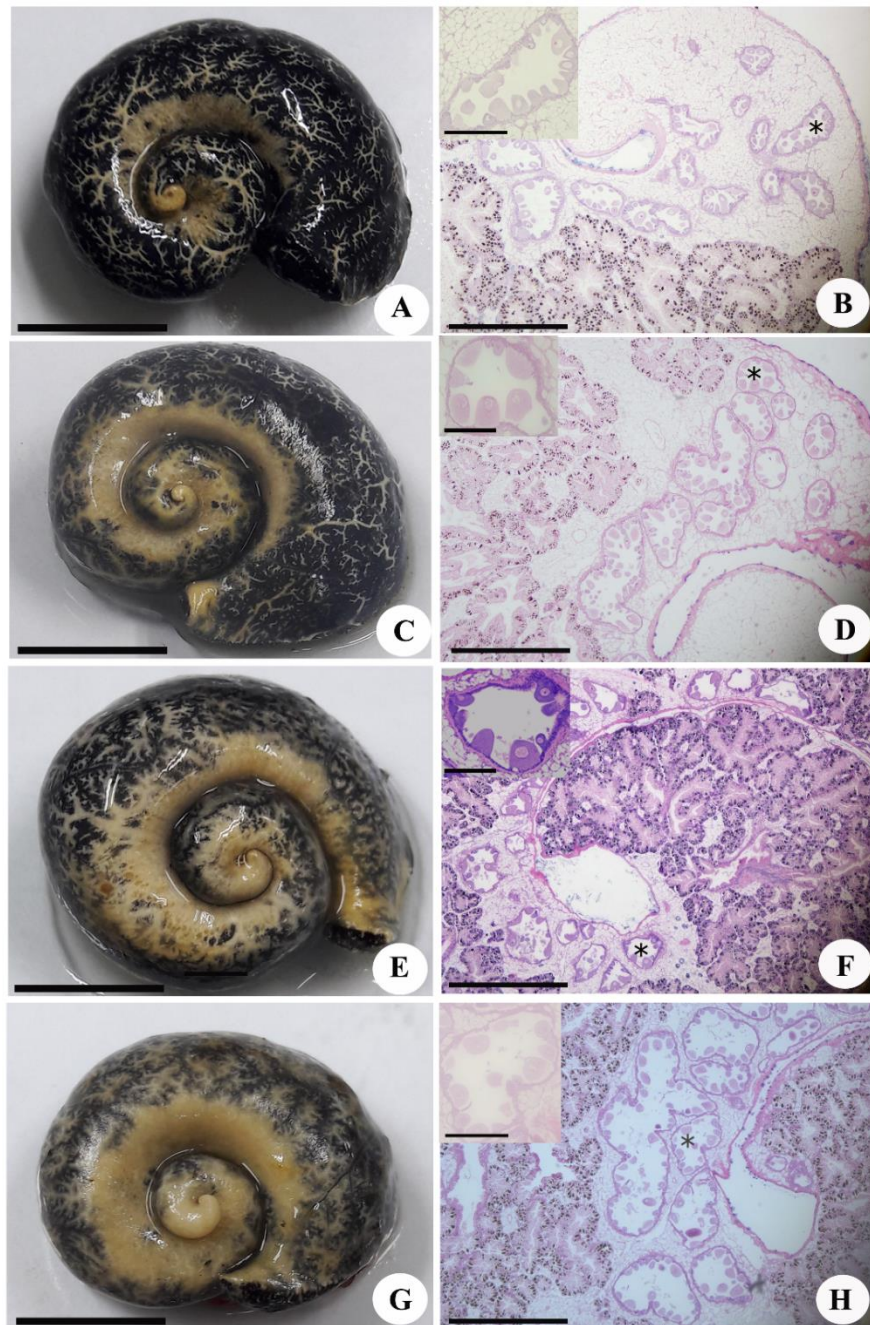


Figure 4.20 Photographs showing comparison between the histology of oocytes and external morphology of gonadal tissue. (A and B) Spent stage, (C and D) Proliferative stage, (E and F) Premature stage, and (G and H) Mature stage. Asterisk showing one ovarian tubule and a magnified view of ovarian tubules with many oocytes are shown in box. Scale bar, A, C, E, G = 1 cm; B, D, F, H =2000 μ m.

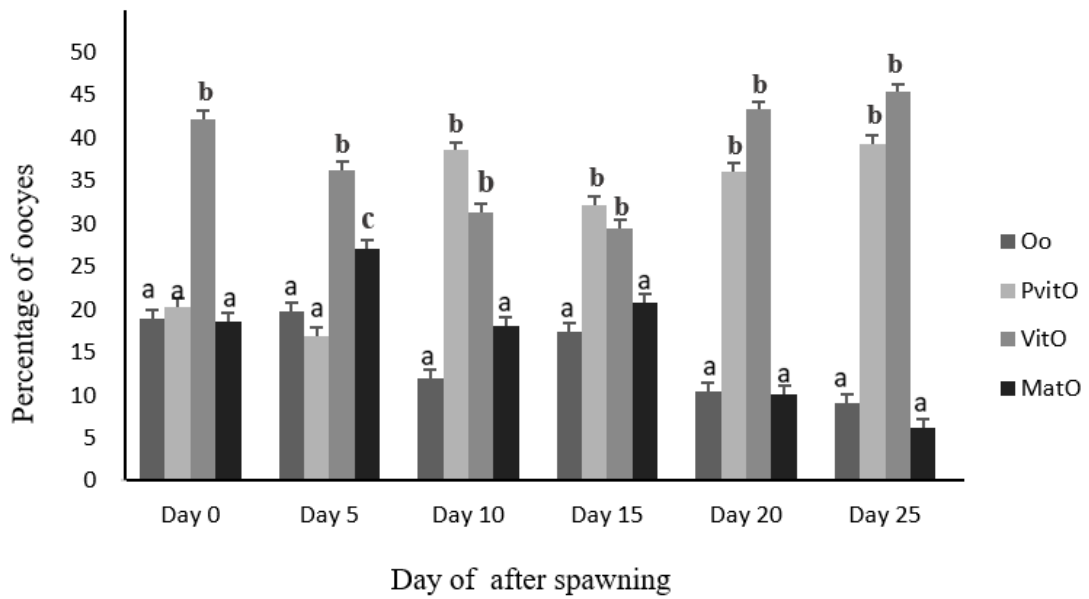
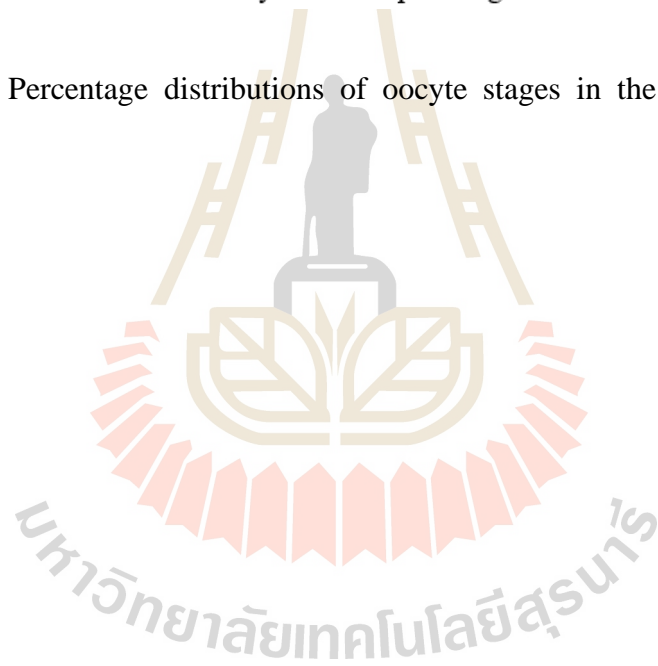


Figure 4.21 Percentage distributions of oocyte stages in the ovarian tubule after spawning.



CHAPTER V

DISCUSSION AND CONCLUSION

5.1 External morphology and histology of ovarian tubules

In the present study, the external morphology of the ovarian tubules appeared as a tubular branch structure, pale-dark yellow in color, and variable in size depending on the stage of maturity of the individual snail. The ovarian tubules were surrounded by white granules of the adipose tissue. Generally, vitellogenesis is the process that occurred during female reproduction in which the oocyte accumulates large quantities of yolk (Jasmani et al., 2004). The main yolk proteins are vitellogenin and vitellin (Tseng et al., 2001). Vitellogenin synthesis was reported to occur in the gonad as well as in extraovarian tissues, such as adipose tissue (Auttarat et al., 2006). In addition, vitellogenesis in molluscs was a complex process involving both autogenous and heterogenous pathways that contribute to the accumulation of more than one types of storage product (Eckelbarger and Young, 1997; Dreon et al., 2002; Pal and Hodgson, 2002; Matsumoto et al., 2003). There was strong evidence states the involvement of extraovarian components in vitellogenesis (Amor et al., 2004). Exogenous heterogenous vitellogenesis occurred through the incorporation of extraovarian precursors into oocytes by endocytosis. Vitellogenesis of *Scapharca subcrenata* occurred by way of autogenous and heterogenous synthesis (Kim, 2016). The process of endogenous autogenous synthesis involved the combined activity of the Golgi complex,

mitochondria and rough endoplasmic reticulum. The process of exogenous heterosynthesis involved endocytotic incorporation of extraovarian precursors at the basal region of the oolema of the early vitellogenic oocytes. Previous studies have described the processes of yolk formation by endogenous autosynthesis and exogenous heterosynthesis in *P. japonicus* are similar to those of *C. virginica* (Eckelbarger and Davis, 1996), *M. edulis* (Pipe, 1987), *P. yessoensis* (Chung et al., 2005), *farreri farreri* (Chung, 2008). Therefore, it was assumed that adipose tissue surrounded the gonadal tissue of *P. canaliculata* might be involved in the formation of lipid droplets through the process of exogenous heterosynthesis. Base on size and color of adipose tissue of *P. canaliculata*, the ovarian tubules were classified into four continuous stages including pre-vitellogenic, early vitellogenic, late vitellogenic and mature stages. The functions of adipose tissue could associated with the precursor of nutrients for vitellogenesis of oocyte development of this species. Exogenous yolk precursors were produced through the process of heterosynthetic vitellogenesis and transferred into proteinaceous yolk granules (Kim, 2016). Studies in *Mytilus edulis* (Pipe, 1987), *Crassostrea virginica* (Eckelbarger and Davis, 1996), *Macra veneriformis* (Chung and Ryou, 2000) and *Meretrix lusoria* (Chung, 2007) were related to heterosynthetic yolk formation in addition to autosynthetic vitellogenesis.

The general feature of the *P. canaliculata* gonadal tissue was similar to those of other mollusks. It consisted of tightly clustered, grape-like acini, each of which contained oocytes in all stages of oogenesis. The ovarian tubule of *P. canaliculata* consisted of several clusters of highly branched tubular surrounded by a thin muscular wall. Bivalve oocytes developed within acini that made up the female gonad. Each acinus was surrounded by connective tissue and intermittent myoepithelial cells (Pipe,

1987; Dorange and Le Pennec, 1989; Eckelbarger and Davis, 1996; Al-Mohanna et al., 2003). The ovarian tubules of *P. canaliculata* contained developmental stages of oocytes including protogonia, oogonia, previtellogenic oocyte, vitellogenic oocyte and mature oocyte. Similarly the gonad of Australian marine bivalve (*Neotrigonia margaritacea*) also consisted of protogonia, oogonia, pre-vitellogenesis, vitellogenesis and mature oocytes (Glavinic et al., 2012). The ovary of *Chamelea gallina* composed of vesicular connective tissue, and a small number of follicle cells surrounding the previtellogenic oocytes completely. The late vitellogenic stage move towards the stalk area. (Erkan, 2009).

5.2 Histology and ultrastructure of oocytes

The general process of oogenesis in *P. canaliculata* was similar to those of other mollusks which follicle cells were only associated with developing oocyte during the early stages of oogenesis. This is similar to those of *Atrina pectinata* (Fang and Qi, 1988), *Mytilus edulis* (Pipe, 1987), *Pecten maximus* (Dorange and Le Pennec, 1989), *Pecten maximus* (Dorange and Le Pennec, 1989), *Pinna nobilis* (De Gaulejac et al., 1995), *Amiantis umbonella* (Al-Mohanna et al., 2003), and *Elliptio complanata* (Won et al., 2005). Oogenesis in mollusk had been classified into solitary or follicular types. In the solitary oogenesis, the developing oocyte was not completely surrounded by follicle cells (Ituarte, 2009). Follicle cells of solitary oogenesis were only associated with developing oocyte during early stages of oogenesis (De Gaulejac et al., 1995). In the follicular oogenesis, the follicular cells completely surround the oocytes during all stages of oogenesis (Zelaya and Ituarte, 2004; Ituarte, 2009). This information suggested that oogenesis of *P. canaliculata* was the solitary type.

The ovarian tubules of *P. canaliculata* contained all developmental stages of oocytes including protogonia, oogonia, pre-vitellogenic, vitellogenic and post-vitellogenic (mature) oocytes. The solitary oogenesis in *Neotrigonia margaritacea* showed that the oogonia were derived from protogonia and then undergo three distinct stages of oogenesis: pre-vitellogenesis, vitellogenesis and post-vitellogenesis oocytes (Glavinic et al., 2012). Generally, oogenesis in mollusks can be divided into a generative (proliferative) and vegetative (growth) phase (Anderson, 1974). During the proliferative phase, the number of oogonial cells increases in the germinal zone by mitotic multiplication. In the vegetative phase of development, oocyte growth is very considerable, principally due to vitellogenesis, and requires substantial uptake and synthesis of nutritive materials (Pipe, 1987).

5.3 Development of oocytes

In the present study, changes of the biochemical components (proteins, nucleic acid and carbohydrate) were evaluated during the development of the oocytes. In order to evaluate the chemical map of the oocyte, the consistency infrared absorption spectrum between 1,700-1,500 cm^{-1} were found to be strongly related to the oocyte maturation. This is corresponded to dominant absorption spectra band around 1640-1654 cm^{-1} that indicated protein conformation of amide I which was found to be dominant in oocyte development (Giorgini et al., 2010).

In a previous study, resonance interactions of the amide I vibration had been considered for the pleated sheet with antiparallel- and parallel-chain packings and apparent dichroic ratios of the perpendicular amide I band (1630 cm^{-1}) of the pleated sheet and the perpendicular amide II band (1545 cm^{-1}) of the α -helix indicating the

degree of orientation of the fiber axes. The interpretations of the infrared spectra of several proteins had been revised (Miyazawa and Blout, 1960). The α -helix is one of the most widespread regular conformations in synthetic polypeptides and proteins. In the infrared spectra, the α -helix has a few strong amide bands. The calculated infrared spectra for the infinite helix was in good agreement with the spectra of synthetic polypeptides (Nevskaya and Chirgadze, 1976)

The present result also showed the difference in the second derivative of amide I between early stage of oocyte development (pre-vitellogenic oocyte) and late stage of oocyte development (vitellogenic and mature oocytes) suggesting that protein structure was changed by protein modification (phosphorylation and/or glycosylation) during oocyte development (Ami et al., 2011). Carbohydrate spectrum was found to decrease in late stage of oocyte development (Giorgini et al., 2010), stated that the infrared absorption spectrum of carbohydrate increased in corresponded to the increase of phosphorylation process. This suggested that modification of carbohydrate was gradually decreased during oocyte development.

β -sheet protein structure was found to be changed to α -helix protein structure during oocyte development. A study in biochemical architecture of bovine oocytes indicated that vitrification induced structural damages and the level of α -helix protein was decreased. This could be because of protein denaturation and/or transformation from α -helix to β -sheet of protein structure (Rusciano et al., 2017). In addition, the transformation of β -sheet protein to α -helix protein was observed during fertilization at the blastocyst stage. These revealed that protein modification occurred during oocyte development. The α -helix protein structure was believed to be the essentially protein structure used during the development of oocytes (Giorgini et al., 2010). The

consistency infrared absorption spectrum between 1,700-1,500 cm^{-1} were found to be strongly related to the oocyte maturation. The α -helix, the antiparallel-chain extended conformation and the parallel-chain extended conformation of polypeptides show both parallel and perpendicular dichroism in their amide I and II infrared absorption bands. The frequencies of the amide I and II bands of these conformations are characteristic and now have been shown to be explicable in terms of vibrational interactions between adjacent peptide groups in the chain and through hydrogen bonds (Miyazawa and Blout, 1960). Therefore, FTIR spectroscopy offers the possibility of identifying the most physiologically relevant conformation of a peptide or protein. Information on the secondary structure of proteins can be derived from analysis of the intensity of the amide I band.

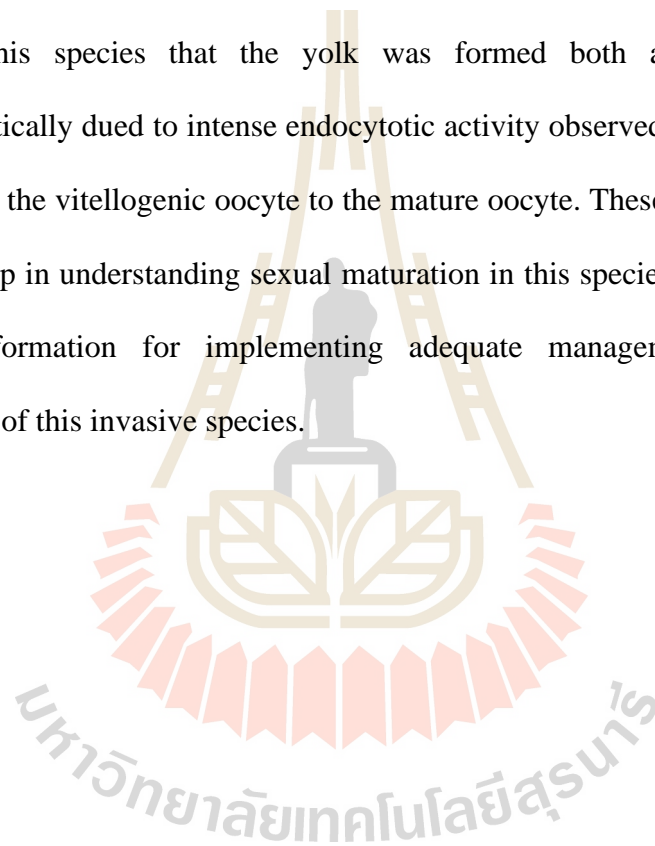
5.4 The relationship between ovarian tubule stages and oocyte stages

In this study, the undischarged mature oocyte in the gonads of *P. canaliculata* gradually degenerated. Therefore, it suggests that this species may have a mechanism to reabsorb the undischarged germ cells in order to provide the reproductive energy for the developing gametes. The mature post-vitellogenic in *N. margaritacea* oocytes were found throughout the reproductive cycle indicating that the oocytes were ready to spawn throughout the reproductive cycle. In the present study, the ovarian tubules contained various stages of oocytes, which indicated that the development of ovarian tubules was asynchronously. Similarly, asynchrony in development was also detected in gametogenic cycle of the trickle-spawning *Venus verrucosa* (Tirado et al., 2003). When bivalves release gametes over several months or seasons ensuring temporal

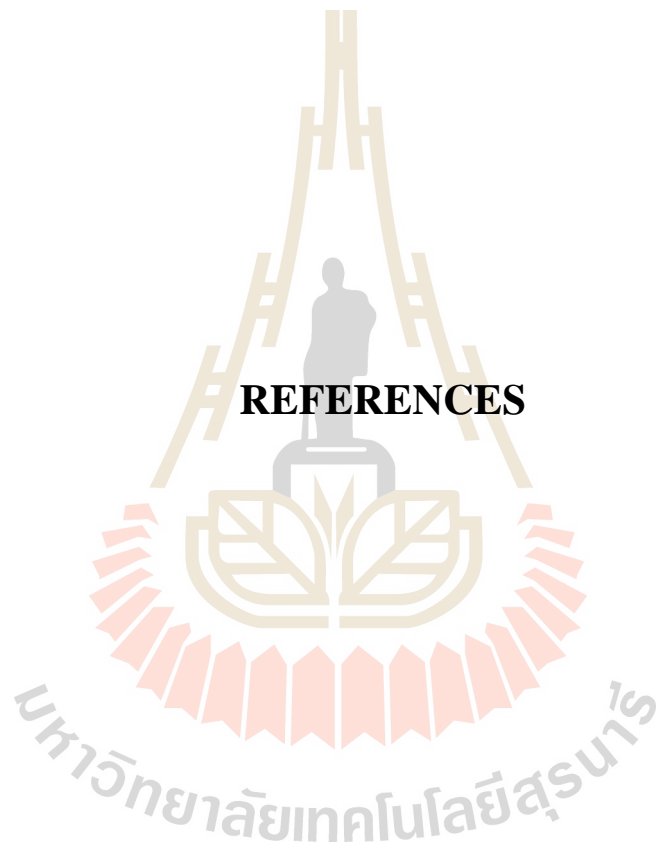
spreading of mortality risk. This strategy increases the chance of gametes experiencing favorable conditions and allows high rate of success fertilization (Chung, 1997; Chung et al., 1998), reported that after spawning, reabsorption of the undischarged germ cells was found in the oogenic of many bivalves (Dorange and Le Pennec, 1989; Xie and Burnell, 1994), stated that the atresia of the undischarged gametes in the follicles took place to reallocate the reproductive energies and other metabolic activities among developing gametes. After spawning, the undischarged germ cells in the gonads of *O. rusticus* gradually degenerated and were reabsorbed. Therefore, it suggested that *P. canaliculata* could have a mechanism to reabsorb the undischarged germ cells in order to provide the reproductive energy for the developing gametes. Oocyte degeneration and resorption in molluscs are brought about by a variety of natural environmental conditions, such temperature extremes, desiccation, or low levels of nutrition (Dorange and Le Pennec, 1989). In *Haliotis varia*, during oocyte degeneration, the oocytes became globular and the vitelline envelope was lifted off the oolemma. The yolk vesicles were surrounded by autophagic vacuoles. The number of lipid droplets and lysosomes increased sharply in the ovarian trabeculae. Oocyte degeneration occurs in different stages of oocyte development in different species (Najmudeen, 2008). In some gastropods like *Viviparous viviparous*, oocytes degenerated in all stages of development (Griffond, 1977), while in the freshwater snail, *Biomphalaria glabrata*, only ripe oocytes, i.e. the oocytes surrounded by a follicular cavity, degenerated. However, in *P. canaliculata*, oocyte degeneration and resorption was observed in vitellogenic and was found mostly in the mature oocytes.

In conclusions, the ovarian morphology of *P. canaliculata* and the stages of oogenesis have been investigated firstly in this study. The ultrastructural features of the

oocytes and the stages of oogenesis in *P. canaliculata* were similar, in terms of general features, to other mollusk. The ovarian tubule was a simple tubular structure containing only developing oocytes and associated follicular cells within a thin germinal epithelium. The main structure of the ovarian tubule was similar to those of other mollusk species. Germ cells at all stages of differentiation ranged from the protogonia to the mature stage were distributed along the inner wall of each ovarian tubule. It was shown in this species that the yolk was formed both autosynthetically and heterosynthetically due to intense endocytotic activity observed on the surface of the oocytes from the vitellogenic oocyte to the mature oocyte. These findings could be an important step in understanding sexual maturation in this species, and thus contribute essential information for implementing adequate management techniques for management of this invasive species.



REFERENCES



REFERENCES

- Albrecht, E. A., Carreno, N. B., and Castro-Vazquez, A. (1996). A quantitative study of copulation and spawning in the South American apple snail, *Pomacea canaliculata* (Prosobranchia: Ampullariidae). **Veliger**. 39: 142-147.
- Al-Mohanna, S. Y., Al-Rukhais, L. B., and Meakins, R. H. (2003). Oogenesis in *Amiantis umbonella* (Mollusca: Bivalvia) in Kuwait Bay, Kuwait. **Journal of the Marine Biological Association of the United Kingdom**. 83: 1065-1072.
- Amor, M. J., Ramon, M., and Durfort, M. (2004). Ultrastructural studies of oogenesis in *Bolinus brandaris* (Gastropoda: Muricidae). **Journal of Marine Science and Engineering**. 68: 343-353.
- Anderson, E. (1969). Oocyte-follicle cell differentiation in two species of Amphineurans (Mollusca), *Mopalia mucosa* and *Chaetopleura apiculata*. **Journal of Morphology**. 129(1): 89-125.
- Anderson, E. (1974). Comparative aspects of the ultrastructure of the female gamete. **International Review of Cytology**. 4: 1-70.
- Anderson, E. (2015). Oocyte-follicle cell differentiation in two species of Amphineurans (Mollusca). *Mopalia mucosa* and *Chaetopleura apiculata*. **Malacologia**. 59: 1-12.
- Andrews, E. (1964). The functional anatomy and histology of the reproductive system of some pilid gastropod molluscs. **Proceedings of the Malacological Society of London**. 36: 121-140.

- Auttarat, J., Phiriyangkul, P., and Utarabhand, P. (2006). Characterization of vitellin from the ovaries of the banana shrimp *litopenaeus merguensis*. **Comparative Biochemistry and Physiology**. 143: 27-36.
- Azevedo, C., Castilho, F., and Coimbra, A. (1969). Fine structure and cytochemistry of the oocyte nucleolus in the mollusk *Helcion pellucidus* (Prosobranchia). **Journal of Ultrastructure Research**. 89(1): 1-11.
- Beams, H. W. and Sekhon, S. S. (1966). Electron microscope studies on the oocyte of the fresh-water mussel (Anodonta), with special reference to the stalk and mechanism of yolk deposition. **Journal morphology Volume**. 119: 477-501.
- Bieler, R. (1992). Gastropod phylogeny and systematics. **Annual Review of Ecology and Systematics**. 23: 311-338.
- Bieler, R. and Mikkelsen, P. M. (1992). Handbook of Systematic Malacology. (*Loricata Polyplacophora; Gastropoda: Prosobranchia*). **Smithsonian Institution and National Science Foundation**. 625.
- Bolognari, A. and Licata, A. (1976). On the origin of the protein yolk in the oocytes of *Aplysia depilans* (Gastropoda, Opisthobranchia). **Experientia**. 32(7): 870-871.
- Branch, G. M. (1974). The ecology of *Patella Linnaeus* from the Cape Peninsula, South Africa. Reproductive cycles. **Transactions of the Royal Society of South Africa**. 41: 111-160.
- Burela, S. and Martin, P. R. (2009). Sequential pathways in the mating behavior of the apple snail *Pomacea canaliculata* (Caenogastropoda: Ampullariidae). **Malacologia**. 51: 157-164.

- Camacho-Mondragon, M. A., Ceballos-Vazquez, B. P., Uria-Galicia, E., Lopez-Villegas, E. O., Pipe, R., and Arellano-Martinez, M. (2010). Ultrastructural and histological study of oogenesis and oocyte degeneration in the *Penshell atrina maura* (Bivalvia: Pinnidae) **Animal Cells and Systems**. 14: 343-349.
- Camacho-Mondragon, M. A., Ceballos-Vazquez, B. P., and Uria-Galicia, E. (2015). Malacologia. **Journal of Morphology**. 129: 89-125.
- Catalan, N. N., Fernandez, S., and Winik, B. (2002). Oviductal structure and provision of egg envelopes in the apple snail *Pomacea canaliculata* (Gastropoda, Prosobranchia, Ampullariidae). **Biocell**. 26: 91-100.
- Cazzaniga, N. (1990). Sexual dimorphism in *Pomacea canaliculata* (Gastropoda: Ampullariidae). **Veliger**. 33: 384-388.
- Cazzaniga, N. J. (2002). Old species and new concepts in the taxonomy of *Pomacea canaliculata* (Gastropoda: Ampullariidae). **Biocell**. 26: 71-81.
- Cheng, E. Y. (1989). Control strategy for the introduced snail, *Pomacea lineata*, in rice paddy. In slugs and snails in World Agriculture. **British Crop Protection Council Monograph**. 41: 69-75.
- Chung, E. Y., Park, G. M., and Kim, B. S. (1998). Ultrastructure of germ cell development and sexual maturation of the short necked clam, *Ruditapes philippinarum* (Bivalvia: Veneridae), on the west coast of Korea. **The Yellow Sea**. 4: 17-29.
- Chung, E. Y. and Ryou, D. K. (2000). Gametogenesis and sexual maturation of the surf clam *Macra veneriformis* on the west coast of Korea. **Malacologia**. 42: 149-163.

- Chung, E. Y., Park, Y. J., Lee, J. Y., and Ryu, D. K. (2005). Germ cell differentiation and sexual maturation of the hanging cultured female scallop *Patinopecten yessoensis* on the east coast of Korea. **Journal of Shellfish Research**. 24: 913-921.
- Chung, E. Y. (2007). Oogenesis and sexual maturation in *Meretrix lusoria* (Roding, 1798) (Bivalvia: Veneridae) in western Korea. **Journal of Shellfish Research**. 26:1-10.
- Chung, E. Y. (2008). Ultrastructural Studies of Oogenesis and Sexual Maturation in Female *Chlamys (azumapecten) farreri farreri* (Jones & Preston, 1904) (Pteriomorphia: Pectinidae). **Malacologia**. 50(1): 279-292.
- Christeller, J. T. (2005). Evolutionary mechanisms acting on proteinase inhibitor variability. **Federation of European Biochemical Societies**. 272: 10-22.
- Curdia, J., Rodrigues, A. S., Martins, A. M. F., and Costa, M. J. (2005). The reproductive cycle of *Patella candei gomesii* Drouet, 1858 (Mollusca: Patellogastropoda), an Azorean endemic subspecies. **Invertebrate Reproduction and Development**. 48(1-3): 137-145.
- Cowie, R. H. (2002). Apple snails (Ampullariidae) as agricultural pests: their biology, impacts and management in Molluscs as Crop Pests. **The Association of International Research and Development Centers for Agriculture**. 11: 145-192.
- De Gaulejac, B., Henry, M., and Vicente, N. (1995). An ultrastructural study of gametogenesis of the marine bivalve *Pinna nobilis* (Linnaeus 1758) I. Oogenesis. **Journal of Molluscan Studies**. 61: 375-392.

- Dorange, G. and Le Pennec, M. (1989). Ultra-structural study of oogenesis and oocytic degeneration in *Pecten maximus* from the Bay of Saint-Brieuc. **Marine Biology**. 103: 339-348.
- Dreon, M. S., Lavarias, S., Garin, C. F., Heras, H., and Pollero, R. J. (2002). Synthesis, distribution, and levels of an egg lipoprotein from the apple snail *Pomacea canaliculata*. **Journal of Experimental Zoology**. (Mollusca: Gastropoda). 292(3): 323-330.
- Dreon, M. S., Heras, H., and Pollero, R. J. (2004). Characterization of the major egg lycolipoproteins from the perivitellin fluid of the apple snail *Pomacea canaliculata*. **Molecular Reproduction and Development**. 68: 359 -364.
- Dreon, M. S., Ituarte, S., and Heras, H. (2010). The role of the proteinase inhibitor ovorubin in apple snail eggs resembles plant embryo defense against predation. **Public Library of Science**. 5: e15059.
- Dreon, M. S., Gimeno, E. J., and Heras, H. (2014). Insights into embryo defenses of the invasive apple snail *Pomacea canaliculata*: egg mass ingestion affects rat intestine morphology and growth. **Public Library of Science**. 19: 6.
- Dyer, J .H. and Singh, H. (1998). The Relational View: Cooperative Strategy and Sources of Interorganizational Competitive Advantage. The Academy of **Management Review**. 23(4): 660-679.
- Eckelbarger, K. J. and Watling, L. (1995). Role of phylogenetic constraints in determining reproductive patterns in deepsea invertebrates. **Invertebrate Biology**. 114: 256-269.

- Eckelbarger, K. J. and Davis, C. V. (1996). Ultrastructure of the gonad and gametogenesis in the eastern oyster, *Crassostrea virginica*. I Ovary and oogenesis. **Marine Biology**. 127: 79-87.
- Eckelbarger, K. J. and Young, C. M. (1997). Ultrastructure of the ovary and oogenesis in the methane-seep mollusc *Bathynnerita naticoidea* (Gastropoda: Neritidae) from the Louisiana slope. **Invertebrate Biology**. 116: 299-312.
- Eckelbarger, K. J. and Young, C. M. (1999). Ultrastructure of gametogenesis in a chemosynthetic mytilid bivalve (*Bathymodiolus childressi*) from a bathyal, methane seep environment (northern Gulf of Mexico) **Marine Biology**. 135: 635-646.
- Enriquez-Diaz, C. C., Villalba, J. C., Pennec, G. L., and Pennec, M. L. (2003). Gametogenesis of *Atrina maura* (Bivalve: Pinnidae) under artificial conditions. **Invertebrate Reproduction and Development**. 43(2): 151-161.
- Erkan, M. (2009). Ultrastructure of ovary and oogenesis in *Chamelea gallina* (Linne, 1758) (Bivalvia, Veneridae). **Invertebrate Reproduction and Development**. 53(4): 201-209.
- Estebenet, A. L. and Cazzaniga, N. J. (1992). Growth and demography of *Pomacea canaliculata* (Gastropoda: Ampullariidae) under laboratory conditions. **Malacological Review**. 25.
- Estebenet, A. L. and Cazzaniga, N. J. (1993). Egg variability and the reproductive strategy of *Pomacea canaliculata* (Gastropoda: Ampullariidae). **Applied Physics Express**. 8: 129-138.

- Estebenet, A. L. and Cazzaniga, N. J. (1998). Sex-related differential growth in *Pomacea canaliculata* (Gastropoda: Ampullariidae). **Journal of Molluscan Studies**. 64: 119-123.
- Estoy, G.F., Yusa, Y., Wada, T., Sakurai, H., and Tsuchida, K. (2002). Size and age at first copulation and spawning of the apple snail, *Pomacea canaliculata* (Gastropoda: Ampullariidae). **Applied Entomology and Zoology**. 37: 199-205.
- Estoy, J., Gerardo, F., Yusa, Y., Wada, T., Sakurai, H., and Tsuchida, K. (2002). Effects of food availability and age on the reproductive effort of the apple snail, *Pomacea canaliculata* (Lamarck) (Gastropoda: Ampullariidae). **Journal of Entomology and Zoology**. 37: 543-550.
- Fang, K. T. and Fang, B. Q. (1988). Some families of multivariate symmetric distributions related to exponential distribution. **Journal of Multivariate Analysis**. 24(1): 09-122.
- Gamarra-Luques, C., Winik, B., Vega, I. A., Albrecht, E. A., Catalan, N. N., and Castro-Vazquez, A. (2006). An integrative view to structure, function, ontogeny and phylogenetical significance of the male genital system in *Pomacea canaliculata* (Caenogastropoda, Ampullariidae). **Biocell Technology**. 30: 345-357.
- Gamarra, L. C. D., Wempe, S. L., and Telleria, C. M. (2013). Synergistic lethality of mifepristone and LY294002 in ovarian cancer cells. **Cancer Growth Metastasis**. 6: 1-13.
- Gamarra-Luques, C., Giraud-Billoud, M., and Castro-Vazquez, A. (2013). Reproductive organogenesis in the apple snail *Pomacea canaliculata* (Lamarck,

- 1822), with reference to the effects of xenobiotics. **Journal of Molluscan Studies**. 79: 147-162.
- Gaulejac, B. D. (1995). Successive hermaphroditism with asynchronous maturation of *Pinna nobilis* (L.) (Bivalvia: Pterioidea). **Journal of Molluscan Studies**. 61(3): 393-403.
- Giraud-Billoud, M., Gamarra-Luques, C., and Castro-Vazquez, A. (2013). Functional anatomy of male copulatory organs of *Pomacea canaliculata* (Caenogastropoda, Ampullariidae). **Zoomorphology**. 132: 139-143.
- Gray, D. R. (1997). Studies on the biology and ecology of the high shore South African limpet *Helcion pectunculus* (Mollusca: Patellogastropoda). **Doctor of Philosophy Thesis, Rhodes University, South Africa**.
- Gilmanshin, R., Dyer, R. B., and Callender, R. H. (1997). Structural heterogeneity of the various forms of apomyoglobin: implications for protein folding. **Protein Science**. 6(10): 2134-2142.
- Glavinic, A., Benkendorff, K., and Rouse, G. W. (2012). Oogenesis and ultrastructure of the ovary in *Neotrigonia margaritacea* (Lamarck) (Bivalvia, Mollusca). **Invertebrate Reproduction and Development**. 56 (2): 111-123.
- Giorgini, E., Conti, C., Ferraris, P., Sabbatini, S., Tosi, G., and Rubini, C. (2010). Effects of *Lactobacillus rhamnosus* on zebrafish oocyte maturation: an FTIR imaging and biochemical analysis. **Analytical and Bioanalytical Chemistry**. 398: 3063-3072.
- Griond, B. and Bolzoni-Sungur, D. (1986). Stages of oogenesis in the snail, *Helix aspersa*: cytological, cytochemical and ultrastructural studies. **Reproduction Nutrition Development**. 26(2A): 461-474.

- Hayes, K. A., Joshi, R. C., Thiengo, S. C., and Cowie, R. H. (2008). Out of South America: multiple origins of non-native apple snails in Asia. **Divers.** 14: 701-712.
- Hayes, K. A., Cowie, R. H., Thiengo, S. C., and Strong, E. E. (2012). Comparing apples with apples: clarifying the identities of two highly invasive Neotropical Ampullariidae (Caenogastropoda). **Zoological Journal of the Linnean Society.** 166: 723-753.
- Heras, H., Garin, C. F., and Pollero, R. J. (1998). Biochemical composition and energy sources during embryo development and in early juveniles of the snail *Pomacea canaliculata* (Mollusca: Gastropoda). **Journal of Experimental Zoology.** 280: 375-383.
- Heras, H., Dreon, M. S., Ituarte, S., and Pollero, R. J. (2007). Egg carotenoproteins in neotropical Ampullariidae (Gastropoda: Arquitaenioglossa). **Comparative Biochemistry and Physiology.** 146: 158-167.
- Herrmann, M., Alfaya, J. E. F., Lepore, L. M., Penchaszadeh, P. E., and Laudien, J. (2009). Reproductive cycle and gonad development of the Northern Argentinean *Mesodesma mactroides* (Bivalvia: Mesodesmatidae). **Helgoland Marine Research.** 63: 207-218.
- Hodgson, A. N. (1999). The biology of siphonariid limpets (Gastropoda: Pulmonata). **Oceanography and Marine Biology: An Annual Review.** 37: 245-314.
- Hodgson, A. N. and Eckelbarger, K. J. (2000). Ultrastructure of the ovary and oogenesis in six species of *patellid limpets* (Gastropoda: Patellogastropoda) from South Africa. **Invertebrate Biology.** 119: 265-277.

- Ituarte, C. F., Cremonte, F., and Deferrari, G. (2001). Mantle-shell complex reactions elicited by digenean metacercariae in *Gaimardia trapesina* (Bivalvia: Gaimardiidae) from the Southwestern Atlantic Ocean and Magellan Strait. **Diseases of Aquatic Organisms**. 48: 47-56.
- Ituarte, C. F. (2009). Unusual modes of oogenesis and brooding in bivalves: The case of *Gaimardia trapesina* (Mollusca: Gaimardiidae). **Invertebrate Biology**. 128(3): 243 -251.
- Jasmani, S., Ohira, T., Jayasankar, V., Tsutsui, N., Aida, K., and Wilder, M. N. (2004). Localization of vitellogenin mRNA expression and vitellogenin uptake during ovarian maturation in the giant freshwater prawn *Macrobrachium rosenbergii*. **Journal of Experimental Zoology**. 301A: 334-43.
- Je- Cheon, J., Ee-Yung, C., Ki-Young, L., and Chang-Hoon, L. (2014). Gametogenic cycle and size at first sexual maturity in female *Chlamys (Azumapecten) farreri farreri* (Jones & Preston, 1904) (Bivalvia: Pectinidae) in western Korea. **Invertebrate Reproduction and Development**. 58(3): 235-244.
- Joshi, R. C. and Sebastian, L. S. (2006). Global advances in ecology and management of golden apple snails. **Philippine Rice Research Institute**. 27: 1-7.
- Kang, H. W., Choi, K. H., Email Author, Jun, J. C., Lee, K. Y., and Park, K. H. (2010). Ultrastructural studies of vitellogenesis in oocytes and follicle cells during oogenesis in female *prothaca (Notochione) jedoensis* (Bivalvia: Veneridae). **Animal Cells and Systems**. 14(4): 343-349.
- Kamler, E. (2005). Parent-egg ontogeny Relationships in Teleost Fishes: An Energetics Perspective. **Review Fish Biology Fisheries**. 15: 399-421.

- Kao, H. C., Chan, T. Y., and Yu, H. P. (1999). Ovary development of the deep-water shrimp *Aristaeomorpha foliacea* (Risso, 1826) (Crustacea: Decapoda: Aristeidae) from Taiwan. **Zoological Studies**. 38(4): 373-378.
- Katsuhisa, basa. (2004). Relationship between the vitellin concentration in the hemolymph and oocyte necroses during the annual reproduction cycle in the Japanese scallop, *Mizuhopecten yessoensis*. **Invertebrate Reproduction and Development**. 45(3): 175-184.
- Kim, S. K. (2016). Marine Glycobiology: Principles and Applications. **International standard book**. 13: 878-1-4987-0961-3.
- Kunduz, B. and Erkan, M. (2008). Seasonal Changes in the Histological Profile of the Ovary of *Mytilus galloprovincialis* (Bivalvia, Mytilidae) Lamarck, 1819. **Black Sea and Mediterranean** 14: 183-191.
- Lasiak, T. (1987). Observations on the reproductive cycles of *Cellana capensis* (Gmelin, 1791) and *Patella concolor* Krauss, 1848 (Gastropoda: Prosobranchia: Patellidae). **South African journal of Zoology Studies**. 22: 195-199.
- Litsinger, J. A. and Estano, D. B. (1993). Management of the golden apple snail *Pomacea canaliculata* (Lamarck) in rice. **Crop Protection**. 12(5): 363-370.
- Lowe, S., Browne, M., Boudjelas, S., and De Poorter, M. (2000). 100 of the World's Worst Invasive Alien Species. **Invasive Species Specialist Group**.
- Marian, A., Camacho-Mondragon., Bertha, P., Ceballos-Vazquez., Uria-Galicia, E., Edgar, O., Lopez-Villegas., Pipe, R., and Arellano-Martinez, M. (2015). Ultrastructural and histological study of oogenesis and oocyte degeneration in the penshell *atrina maura* (Bivalvia: Pinnidae). **Malacologia**. 59(1): 1-12.

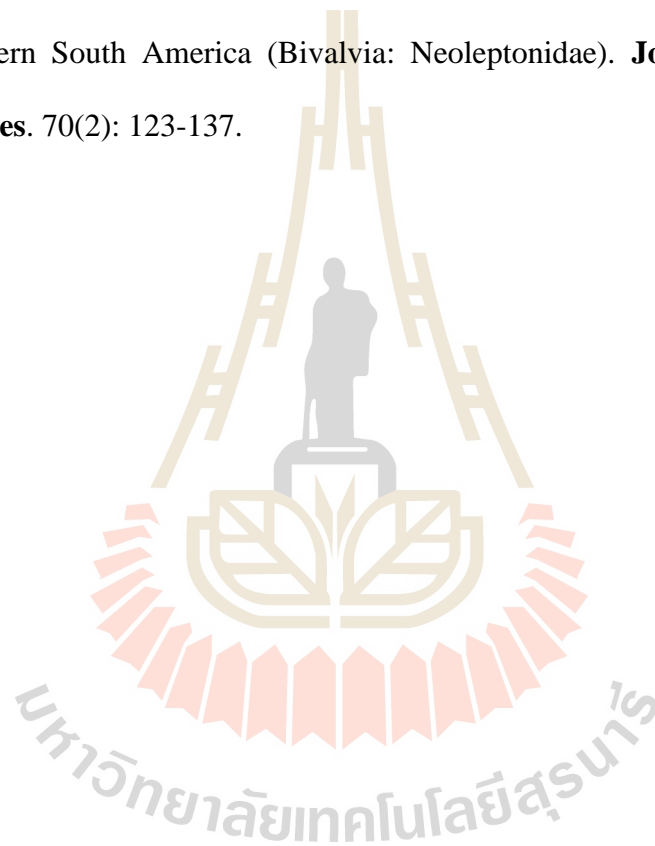
- Martin, G. G., Romero, K., and Miller-Walker, C. (1983). Fine structure of the ovary in the red abalone *Haliotis rufescens* (Mollusca:Gastropoda). **Zoomorphology**. 103: 89-102.
- Martin, P. R. and Estebenet, A. L. (2002). Interpopulation variation in life-history traits of *Pomacea canaliculata* (Gastropoda: Ampullariidae) in southwestern Buenos Aires Province, Argentina **Malacologia**. 44: 153-163.
- Mazzeo, D., Oliveti, G., and Arcuri, N. (2016). Influence of internal and external boundary conditions on the decrement factor and time lag heat flux of building walls in steady periodic regime. **Science Direct**. 164: 509-531.
- Melike, E. (2009). Ultrastructure of ovary and oogenesis in *Chamelea gallina* (Linne, 1758) (Bivalvia, Veneridae). **Invertebrate Reproduction and Development**. 53(4): 201-209.
- Miyazawa, T. and Blout, E. R. (1961). **Journal of the American Chemical Society**. 8(3): 712-719.
- Najmudeen, T. M. (2008). Ultrastructural studies of oogenesis in the variable abalone *Haliotis varia* (Vetigastropoda: Haliotidae). **Journal of Aquatic Biology**. 2: 143-151.
- Nantawan, S., Chaitip, W., Michael, J. S., Praphaporn, S., Prasert, M., Peter, J. H., and Prasert, S. (2012). Ultrastructure of Differentiating Oocytes and Vitellogenesis in the Giant Freshwater Prawn, *Macrobrachium rosenbergii* (de Man). **Microscopy Research and Technique**. 75: 1402-1415.
- Okumura, T. and Aida, K. (2000). Hemolymph vitellogenin levels and ovarian development during the reproductive and non-reproductive molt cycles in the giant freshwater prawn *Macrobrachium rosenbergii*. **Fish Science**. 66: 678-85.

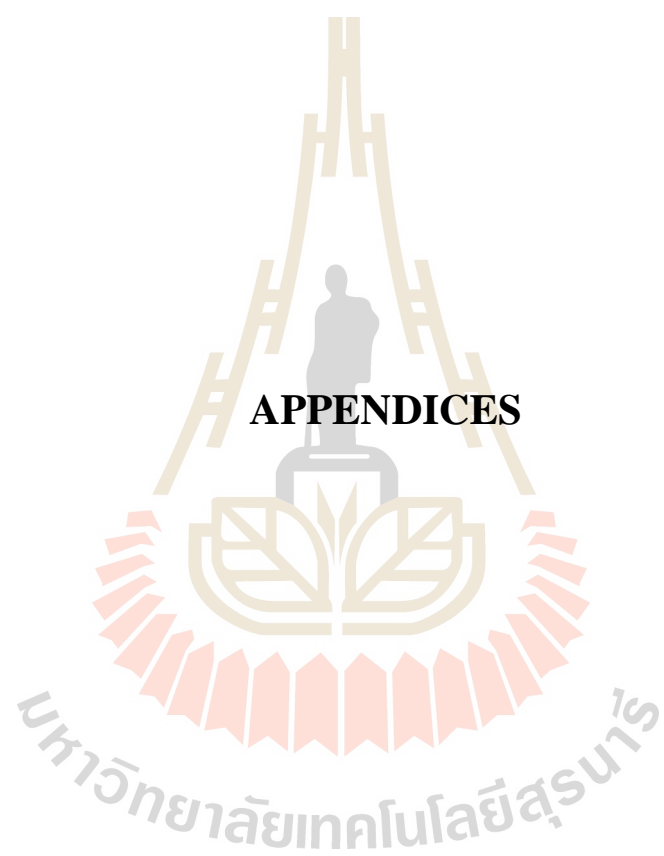
- Orton, J. H., Southward, A. J., and Dodd, J. M. (1956). Studies on the biology of II. The breeding of *Patella vulgata* L in Britain. **Journal of the Marine Biological Association of the United Kingdom**. 35: 149-176.
- Pal, P. and Hodgson, A. N. (2002). An ultrastructural study of oogenesis in a planktonic and a direct developing species of *Siphonaria* (Gastropoda: Pulmonata). **Journal of Molluscan Studies**. 68: 337-344.
- Palis, F. V., Macatula, R. F., and Browning, L. (1996). Niclosamide an effective molluscicide for the golden apple snail *Pornacea canaliculata* (Lamarck) control in Philippines rice production systems. In Slugs and Snail Pests in *Agriculture.British. Crop Protection Council Symposium Proceedings*. 66: 213-230.
- Pipe, R. K. (1987). Oogenesis in the marine mussel *Mytilus edulis*: an ultrastructural study. **Marine Biology**. 95: 405-414.
- Ponder, W. F. and Lindberg, D. R. (1996). Gastropod phylogeny challenges for the 90's. In: Origin and Evolutionary Radiation of the Mollusca. **The Malacological Society of London**. 135-154.
- Qiushi, X. and Burnell, M. (1994) Interference of Mg^{2+} and Ca^{2+} on protein determination with Lowry's method. *Comparative. Biochemistry and Physiology*. 107(4): 605-608.
- Rawlings, N. C., Bartlewski, P. M., Alexander, B. D., Barrett, D., and King, W. A. (2007). Ovarian responses, hormonal profiles and embryo yields in anoestrous ewes superovulated with Folltropin-V after pretreatment with medroxyprogesterone acetate-releasing vaginal sponges and a single dose of oestradiol-17beta. **Reproduction in Domestic Animals**. 43: 299-307.

- Rawlings, T. A., Hayes, K. A., Cowie, R. H., and Collins, T. M. (2007). The identity, distribution, and impacts of non-native apple snails in the continental United States. **BMC Evolutionary Biology**. 7: 97.
- Revathi, P., Iyapparaj, P., Munuswamy, N., and Krishnan, M. (2012). Vitellogenesis during the ovarian development in freshwater female prawn *Macrobrachium rosenbergii* (De Man). **International Journal of Aquatic Science**. 2008-8019.
- Rodrigues, A. S. and Medeiros, J. (2005). Reproductive cycle of *Leptaxis caldeirarum*, a locally endangered Azorean land snail. **Invertebrate Reproduction and Development**. 47: 191-195.
- Rusciano, G., De Canditiis, C., Zito, G., and Rubessa, M. (2017). Raman-microscopy investigation of vitrification-induced structural damages in mature bovine oocytes. **Public Library of Science**. 12(5): e0177677.
- Seung-Jae, W., Apolonia, N., Noemi, C., Melanie, T. R., Kelly, F., Makoto, O., and Ian, P. C. (2005). The Freshwater Mussel (*Elliptio complanata*) as a Sentinel Species: Vitellogenin and Steroid Receptors. **Integrative and Comparative Biology**. 45(1): 72-80.
- Sinclair, K. D. and Singh, R. (2007). Modelling the developmental origins of health and disease in the early embryo. **Theriogenology**. 67(1): 43-53.
- Singh, R. and Sinclair, K. D. (2007). Metabolomics: approaches to assessing oocyte and embryo quality. **Theriogenology**. 68(1):56-62.
- Sung, H. K. (2016). Ultrastructural Studies on Oocyte Development and Vitellogenesis associated with Follicle Cells in Female *Scapharca subcrenata* (Pelecypoda: Arcidae) in Western Korea. **Development & Reproduction**. 20(3): 227-235.

- Tamburi, N. E. and Martin, P. R. (2009). Reaction norms of size and age at maturity of *Pomacea canaliculata* (Gastropoda: Ampullariidae) under a gradient of food deprivation. **Journal of Molluscan Studies**. 75: 19-26.
- Tamburi, N. E. and Martin, P. R. (2011). Effects of food availability on reproductive output, offspring quality and reproductive efficiency in the apple snail *Pomacea canaliculata*. **Biological Invasions**. 13: 2351-2360.
- Thompson, F. G. (1997). *Pomacea canaliculata* (Lamarck, 1822) (Gastropoda, Prosobranchia, Pilidae): A freshwater snail introduced into Florida, U.S.A. **Malacological Review**. 30: 91.
- Tirado, C., Salas, C., and Marquez, I. (2003). Reproduction of *Venus verrucosa* L., 1758 (Bivalvia: Veneridae) in the littoral of Malaga (southern Spain). **Fisheries Research**. 63:437-445.
- Tseng, D. Y., Cheng, Y. N., Kou, G. H., Lo, C. F., and Kuo, C. M. (2001). Hepatopancreas is the extraovarian site of vitellogenin synthesis in black tiger shrimp, *Penaeus monodon*. **Comparative Biochemistry and Physiology**. 129: 909-917.
- Wood, B. R., Chiribogac, L., Yee, H., Quinnd, M. A., McNaughton, D., and Diema, M. (2004). Fourier transform infrared (FTIR) spectral mapping of the cervical transformation zone, and dysplastic squamous epithelium. **Gynecologic Oncology**. 93(1): 59-68.
- Wood, B. R., Chernenko, T., Matthaus, C., and Diem, C. (2008). Shedding New Light on the Molecular Architecture of Oocytes Using a Combination of Synchrotron Fourier Transform-Infrared and Raman Spectroscopic Mapping. **American Chemical Society** 80(23): 9065-9072.

- Yusa, Y. (2001). Predation on eggs of the apple snail *Pomacea canaliculata* by the fire ant *Solenopsis geminata*. **Journal of Molluscan Studies**. 67: 1-6.
- Yusa, Y. (2004). Inheritance of colour polymorphism and the pattern of sperm competition in the apple snail *Pomacea canaliculata* (Gastropoda: Ampullariidae). **Journal of Molluscan Studies**. 70: 43-48.
- Zelaya, D. G. and Ituarte, C. (2004). The genus *neolepton* monterosato, 1875 in southern South America (Bivalvia: Neoleptonidae). **Journal of Molluscan Studies**. 70(2): 123-137.





APPENDICES

APPENDIX A

THE PREPARATIONS OF REAGENTS

Phosphate Buffer saline pH 7.4

Chemicals

Sodium chloride (NaCl)	8 g
Potassium chloride (KCl)	0.2 g
Disodium hydrogen phosphate (Na_2HPO_4)	1.44 g
Potassium dihydrogen Phosphate (KH_2PO_4)	0.24 g
Distilled water	1 L

Preparation

Add chemical compounds one by one into 800 ml of distilled water. Adjust the pH to 7.4 with HCl. Add distilled water to a total volume of 1 liter. Sterilization by autoclaving (20 min, 121°C, liquid cycle). Store at room temperature.

Coating Buffer (carbonate buffer), 0.05 M pH 9.6

Chemicals

15 mM Sodium carbonate (Na_2CO_3)	1.59 g
35 mM Sodium bicarbonate (NaHCO_3)	2.93 g
Distilled water	1 L

Preparation

The total chemical compounds were mixed in distilled water pH was adjusted to 9.6. Sterilization by autoclaving (20 min, 121°C, liquid cycle).

Lysis Buffer

Chemicals

10 mM TRIS hydrochloride (Tris-HCl) pH 7.2	0.16 g
150 mM Sodium chloride (NaCl)	0.87 g
1 mM Ethylenediaminetetraacetic acid (EDTA)	0.04 g
0.5% Triton X-100	25 μl
1mM Phenylmethylsulfonyl fluoride (PMSF)	50 μl
Distilled water	100 ml

Periodic Acid Schiff (PAS)

Chemicals

Periodic acid	0.5 g.
Distilled water	50 ml.

Schiff reagent solution

Basic fuchsin	1 g.
Distilled water	100 ml.
Sodium metabisulfite ($\text{Na}_2\text{S}_2\text{O}_5$)	1.9 gm.
HCl (Concentrated)	0.3 ml

Alcian blue and nuclear fast red

Chemicals

Nuclear fast red solution

Aluminium sulfate ($\text{Al}_2(\text{SO}_4)_3 \cdot 18\text{H}_2\text{O}$)	5 g
Distilled water	100 ml.
Nuclear fast red	0.1 gm.

Alcian blue solution

Alcian blue 8 GX	1 g.
3% acetic acid	100 ml.

Ehrlich's Hematoxylin

Chemicals

Hematoxylin crystals	4 gm.
95% Alcohol	200 ml.
Ammonium or potassium alum	6 gm.
Distilled water	200 ml.
Glycerin	200 ml.
Glacial acetic acid	20 ml.

Sudan black B

Chemicals

Sudan black B	0.7 gm.
Propylene glycol	100 ml.

85% Propylene glycol

Propylene glycol	85 ml.
Distilled water	15 ml.

Eosin

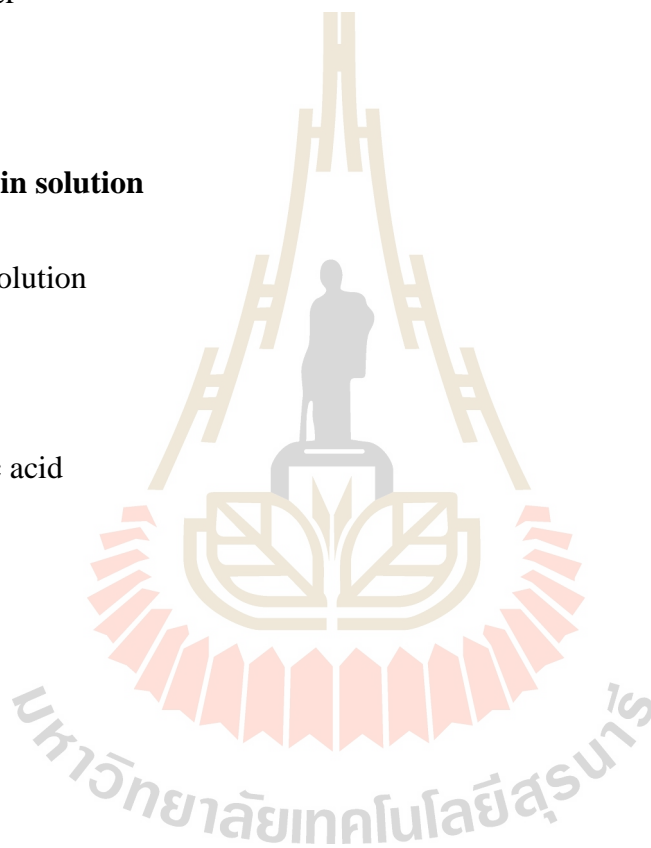
Chemicals

1% Stock alcoholic Eosin

Eosin Y water soluble	1 g.
Distilled water	20 ml.
95% Alcohol	80 ml.

Working eosin solution

Eosin stock solution	50 ml.
80% Alcohol	150 ml
Glacial acetic acid	7.5 ml.



APPENDIX B

PROCEEDING PRESENTATION

Proceedings of the APMC11 / MST33 / AAT39 Conference
May 23-27, 2016, Phuket, Thailand

PA31

Development of Oocytes in the Golden Apple Snail, *Pomacea Canaliculata*

Anucha Chomnonlao¹, Piyada Ngernsounnern², Apichart Ngernsounnern^{2*}

¹ School of Pharmacology, Institute of Science, Suranaree University of Technology, Nakhon Ratchasima, Thailand

² School of Anatomy, Institute of Science, Suranaree University of Technology, Nakhon Ratchasima, Thailand

*Corresponding author, e-mail: apichart@sut.ac.th

Abstract

The golden apple snail is an invasive mollusk. The snail has a short reproductive cycle and it can lay eggs throughout the year. In the present study, development of oocytes of the snail was observed. The oocytes were classified based on their diameters and morphologies into five stages; oogonia, previtellogenic oocyte (Oc1), early vitellogenic oocyte (Oc2), late vitellogenic oocyte (Oc3), and mature oocyte (Oc4). This study could be useful for understanding the reproductive biology of this snail species.

Keywords Golden apple snail, *Pomacea canaliculata*, oocyte, oogenesis

Background

The golden apple snail was initially found in South America. The snail was later brought to Asia for human food industry. Unfortunately, the snail escaped or was released from cultivation. The snail can consume varieties of food (rice seedlings, algae, leafy plants, and eggs of other snail species). In addition, it feeds more food than other species. This species has then become a pest for the food production (Hayes et al., 2008).

Reproductive cycle of the golden apple snail is short and it can reproduce throughout the year. The snail is able to reproduce approximately three generations per year (Liu et al., 2012). Some female snails are able to spawn up to 3.7 times by week on average during their whole life. Lifespan fecundities of the snail range from 1,316 to 10,869 eggs per female (mean, 4,506). Female snails can store sperm for 140 days and can spawn up to 3,000 eggs per a reproductive cycle. Eggs incubate from 1-2 weeks and become juveniles in 15-25 days after hatching. The juveniles develop to

sexually mature adults in 45-59 days later. The population of the golden apple snail has since then increased rapidly (Estebeinet and Martin, 2002; Wu et al., 2011).

At present, knowledge on the snail's reproduction is still limited. The reason why the snail can reproduce rapidly is still unclear. The main objective of the present study was thus to study oogenesis of this species.

Materials and Methods

Adult female snails were used. After euthanization of the snails, ovarian tubules were removed, fixed with Bouin's fixative, and then processed conventionally for embedding in paraffin wax. Subsequently, the tissue blocks were cut and the sections were stained with hematoxylin and eosin. The sections were then dehydrated, cleared, mounted, and finally observed under a light microscope.

Diameters of oocytes were measured using a computerized image analysis program (Cell^{AD} software). At least 20

oocytes from each stage were selected for the determination of their diameters.

Results, Discussion and Conclusion

Oocytes of the golden apple snail were classified into five stages; oogonia, previtellogenic oocyte (Oc1), early vitellogenic oocyte (Oc2), late vitellogenic oocyte (Oc3), and mature oocyte (Oc4) (Fig.1). Oogonia were the smallest cells and were low columnar or cuboid in shape. They arranged in a single row. Previtellogenic oocytes were round or oval cells. Their nuclei contained dispersed chromatin and prominent nucleoli. The cytoplasm was basophilic and no cytoplasmic granules were observed. Early vitellogenic oocytes were larger in size compared to previtellogenic oocytes. They presented more acidophilic cytoplasm which contained small cytoplasmic granules indicating the onset of yolk synthesis. Late vitellogenic oocytes were larger than early vitellogenic oocytes as they accumulated more yolk granules. Mature oocytes were the largest cells and were more elongated than late vitellogenic oocytes. They contained the most numerous yolk granules in the cytoplasm. The oogonia, previtellogenic, early vitellogenic, and late vitellogenic oocytes were attached to the germinal epithelium. Most of the mature oocytes were also adhered to the germinal epithelium, whereas some of them were detached from the epithelium and were floated in the lumens of the ovarian tubules.

Stages of the oocytes have been classified in mollusks. Oocytes of six patellid limpets and an abalone (*Haliotis varia*) were also classified into five stages as same as those stages of the golden apple snail (Hodgson et al., 2000; Najmudeen, 2008). However, it was reported in a bivalve mollusk (*Neotrigonia margaritacea*) that oocytes developed from oogonia and then underwent three stages of oogenesis; previtellogenesis, vitellogenesis, and postvitellogenesis with mature oocytes (Glavinic et al., 2012). In addition, developing oocytes of *Helix aspersa* were classified into six stages; oogonia, young oocyte, premeiotic oocyte, previtellogenic

oocyte, vitellogenesis I, and vitellogenesis II (Griffond and Bolzoni-Sungur, 1986).

Diameter of each oocyte stage of the golden apple snail was measured. Data is presented as mean \pm S.D. (Table 1). Diameters of the oogonia, previtellogenic, early vitellogenic, late vitellogenic, and mature oocytes were approximately 9, 15, 29, 51, and 70 μ m, respectively. It appears that the diameter of each stage of the oocyte is a bit different when compared among mollusks. A study in *Anodonta anatina* reported that diameters of the oogonia, early vitellogenic, and vitellogenic oocytes were 10-20, 25-35, and 55-80 μ m, respectively (Hinzmann et al., 2013). Diameters of early gametogenesis, growing, mature, and degenerating oocytes of *Crassostrea gigas* were 3.0-12.0, 12.1-30.0, 30.1-41.0, and 41.1-60.0, respectively (Lango-Reynoso et al., 2000). In addition, previtellogenic and vitellogenic oocytes of *Bathynnerita naticoidea* were 10-12 and 24 μ m in diameters, respectively. The largest mature oocytes of this species ranged from 135 to 145 μ m in diameter (Eckelbarger and Young, 1997).

Table 1 Mean diameters of oocyte stages of the golden apple snail

Stage of oocytes	Mean Diameter (μ m)
Oogonia	9.38 \pm 2.13
Previtellogenic oocyte (Oc1)	15.12 \pm 2.67
Early vitellogenic oocyte (Oc2)	28.87 \pm 4.39
Late vitellogenic oocyte (Oc3)	51.35 \pm 9.25
Mature oocyte (Oc4)	70.34 \pm 9.92

In conclusion, the oocytes of the golden apple snail were classified into five stages. This is similar to those of other mollusks. However, some differences in the classification were observed. Knowledge on reproductive biology of this invasive species could be important for effective management strategies which are going to be developed.

Acknowledgement

This work was supported by Suranaree University of Technology.

References

- 1 Eckelbarger KJ, Young CM. Ultrastructure of the ovary and oogenesis in the methane-seep mollusk *Bathynnerita naticoidea* (Gastropoda: Neritidae) from the Louisiana slope. *Invertebrate Biology* 1997; 116: 299-312.
- 2 Estebenet AL, Martin PR, *Pomacea canaliculata* (Gastropoda: Ampullariidae): life-history traits and their plasticity. *Biocell* 2002; 26: 83-9.
- 3 Glavinic A, Benkendorff K, Rouse G W. Oogenesis and ultrastructure of the ovary in *Neotrigonia margaritacea* (Lamarck) (Bivalvia, Mollusca). *Invertebrate Reproduction & Development* 2012; 56: 111-23.
- 4 Griffond B, Bolzoni-Sungur D. Stages of oogenesis in the snail, *Helix aspersa*: cytological, cytochemical and ultrastructural studies. *Reproduction Nutrition Développement* 1986; 26: 461-474.
- 5 Hayes KA, Joshi RC, Thiengo SC, Cowie RH. Out of South America: multiple origins of non-native apple snails in Asia. *Diversity and Distributions* 2008; 14: 701-12.
- 6 Hinzmann M, Lopez-Lima M, Teixeira A, Varandas S, Sousa R, Lopes A, Froufe E, Machado J. Reproductive cycle and strategy of *Anodonta anatine* (L., 1758): notes on hermaphroditism. *Journal of Experimental Zoology* 2013; 319A: 378-390.
- 7 Hodgson AN, Eckelbarger KJ. Ultrastructure of the ovary and oogenesis in six species of patellid limpets (Gastropoda: Patellogastropoda) from South Africa. *Invertebrate Biology* 2000; 119: 265-77.
- 8 Lango-Reynoso F, Chavez-Villalba J, Cochard JC, Pennec ML. Oocyte size, a means to evaluate the gametogenic development of the Pacific oyster, *Crassostrea gigas* (Thunberg). *Aquaculture* 2000; 190: 183-199.
- 9 Liu J, He YJ, Tan JC, Xu CX, Zhong L, Wang ZG, Liao QG. Characteristics of *Pomacea canaliculata* reproduction under natural conditions. *Ying Yong Sheng Tai Xue Bao* 2012; 23: 559-65.
- 10 Najmudeen TM. Ultrastructural studies of oogenesis in the variable abalone *Haliotis varia* (Vetigastropoda: Haliotidae). *Aquatic Biology* 2008; 2: 143-51.
- 11 Wu J-Y, Wu Y-T, Chiu Y-W, Liu M-Y, Liu LL. Reproduction and juvenile growth of the invasive apple snails *Pomacae canaliculata* and *P. scalaris* (Gastropoda: Ampullariidae) in Taiwan. *Zoological Studies* 2011; 50: 61-8.

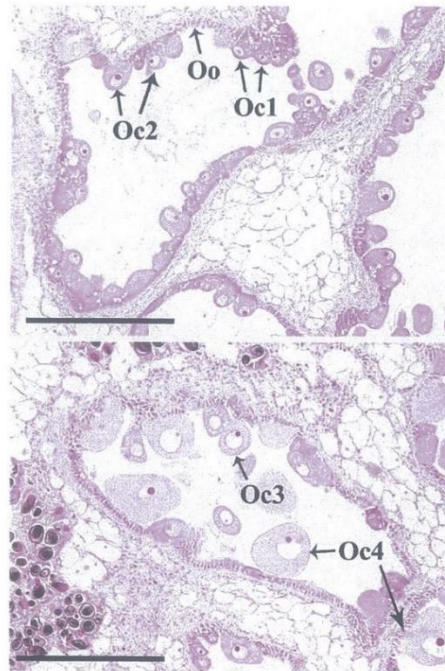


Fig.1 Morphology of the oocyte stages of the golden apple snail; oogonia (Oo), previtellogenic oocyte (Oc1), early vitellogenic oocyte (Oc2), late vitellogenic oocyte (Oc3) and mature oocyte (Oc4). Scale bars = 40 μ m.

CURRICULUM VITAE

NAME: Anucha Chomnonlao

DATENOF BIRTH: Jan 23, 1986

PLACE OF BIRTH: Nakhon Ratchasima, Thailand

EDUCATION: Nakhon Ratchasima Rajabhat University, 2004-2008:
Bachelor of Science (Applied biology)

HOME ADDRESS: 10 Moo 4, Chum Phuang, Nakhon Ratchasima, Thailand,
30270

PUBLICATION:
Chomnonlao, A., Ngernsoungnern, P., and Ngernsoungnern, A. Development of
Oocytes in the Golden Apple Snail, *Pomacea Canaliculata*. **Proceedings of the
APMC11/ MST33/ AAT39 Conference**. May 23-27, 2016, Phuket, Thailand.

มหาวิทยาลัยเทคโนโลยีสุรนารี